JOURNAL OF ADVANCES IN

ENGINEERING AND TECHNOLOGY

VOLUME 4, ISSUE 1
JANUARY 2026

ISSN 2961 - 5410

Civil Engineering | Electrical and Electronic Engineering | Materials Engineering | Mechanical Engineering | Mechatronics Engineering | Quantity Surveying

About the Journal of Advances in Engineering and Technology

The Journal of Advances in Engineering and Technology (JAET) is an international, open access, double blind peer-reviewed journal. It is published by the Faculty of Engineering of Sri Lanka Institute of Information Technology (SLIIT). The JAET aims at fostering research and development work in Engineering and Technology and bringing researchers on to a common platform. Furthermore, JAET will also accept review articles on appropriate subject areas including concept papers of academic opinions, book reviews, etc. for publication therein.

All copyrights reserved ©SLIIT Faculty of Engineering

The views and opinions expressed by the authors are their own and would not necessarily reflect the views of the Faculty of Engineering. The research articles submitted to JAET have not been nor envisaged to be published elsewhere and will not simultaneously be published elsewhere. It is also stated that at time of acceptance to publish an article submitted to JAET, the authors agree that the copyright for their accepted articles is transferred to JAET. The copyright covers the exclusive right to reproduce and distribute the article in any form by JAET without the permission of the author.

Notes for the authors: Please see page VI

All correspondence should be addressed to:

Editor-in-Chief
Journal of Advances in Engineering and Technology
Faculty of Engineering
SLIIT
Kandy Road, Malabe, 10115
Sri Lanka

Email: **jaet@sliit.lk**

Official website: **https://jaet.sliit.lk**

ISSN 2950-7138 (Printed)

ISSN 2961 - 5410 (Online)

Randhi Printers: No. 22 Sesatha Watta, Waduramulla, Panadura

Journal of Advances in Engineering and Technology (JAET)

Volume IV Issue (I)-2026

Sri Lanka Institute of Information Technology
Malabe, Sri Lanka

THE KNOWLEDGE UNIVERSITY

Journal of Advances in Engineering and Technology

Volume IV, Issue I, January 2026

Contents

JOURNAL PAPERS

Faculty of Engineering
Sri Lanka Institute of Information Technology (SLIIT)
Malabe, 10115, Sri Lanka

EDITORIAL TEAM

Editor-in-Chief

Professor Rahula Attalage

Editorial Committee

Dr. Nandika Miguntenna

Dr. Lakmini Malasinghe

Dr. Priyantha Bandara

Dr. Mudith Karunarathna

Ms. Priyanwada De Silva

Advisory Board

Prof. Dilanthi Amarathunga	University of Huddersfield, UK
Prof. Janaka Ekanayake	University of Peradeniya, Sri Lanka
Prof. Kyaw Thu	Kyushu University, Japan
Prof. Jagath Manatunge	University of Moratuwa, Sri Lanka
Prof. George Mann	Memorial University of Newfoundland, Canada
Prof. Srinath Perera	Western Sydney University, Australia
Prof. Ahmed Abu – Siada	Curtin University, Australia
Prof. R. Thevamaran	University of Wisconsin Madison, USA
Prof. S. C. Wirasinghe	University of Calgary, Canada

Editorial Assistant / Secretary of the Journal

Ms. Priyanwada De Silva

Notes to the Authors

Journal of Advances in Engineering and Technology (JAET) is a biannual peer review journal which aims at publishing original, theoretical and practice-oriented research papers related to Engineering and Technology. This journal provides a forum for researchers, scholars, academicians, and practitioners in the field of Engineering at international level to discuss and disseminate their findings in advanced and emerging technologies in Engineering.

Articles/ contributions should be sent to:

Editor-in-Chief
Journal of Advances in Engineering and Technology (JAET)
Faculty of Engineering
SLIIT , New Kandy Road, Malabe, Sri Lanka
E – mail: jaet@sliit.lkmailto:editors.sjhs@sliit.lk

- Your article will be subjected to a double-blind review process by two reviewers who are experts in their relevant field. In order to facilitate anonymous review process, you are requested to provide the title page separately.
- The title page should include the title of the article, your full name, affiliation, address, email and telephone/ mobile number.
- Recommendations of two reviewers are necessary for the publication of your article.
- The article should not exceed 6,000 words.
- Abstract should be between 150-200 words with 4-5 keywords.
- Article should include the following:
- Introduction to the research statement/ background to the research/ rationale
- Methods and Material
- Results and Discussion
- Conclusions and Recommendations
- References
- Footnotes can be numbered and given at the end of the article.
- Referencing should conform to the APA style.
- Tables/ graphs should be included in the appropriate places. Longer tables should be added at the end of the article as annexes.
- Use Times New Roman Fonts - Abstract 11pt; Article 11pt; Spacing Single

Machine Learning-Based Early Warning Systems for Urban Floods: A Case Study in Nilwala Basin

Abayapala A.I., Lindamulla L.M.L.K.B.
Department of Civil Engineering, Faculty of Engineering
Sri Lanka Institute of Information Technology, Malabe 10115, Sri Lanka.
abiruabayapala@gmail.com, lahiru.l@sliit.lk

ABSTRACT

This study pioneers the integration of Graph Neural Networks (GNNs) into flood forecasting systems, extending the predictive horizon from short-term forecasts to 7 days by effectively capturing spatial dependencies between rainfall stations. Focusing on the flood-prone regions of Matara and Galle districts within the Nilwala Basin, the research addresses the limitations of conventional forecasting methods by leveraging historical hydrological data, including daily rainfall records from six key stations and flow data from Pitabeddara. A hybrid machine learning framework combining Random Forest (RF) and K-Nearest Neighbors (KNN) models was developed to predict river discharge using rainfall data, overcoming challenges posed by limited water level data. The inclusion of GNNs introduces a novel approach to modeling complex spatial relationships, enabling improved accuracy in long-term flood prediction, particularly during extreme events. The proposed system demonstrates significant advancements in predictive reliability, offering a timely and accurate early warning tool to enhance disaster preparedness and risk management in the Nilwala Basin. This research underscores the transformative potential of data-driven methodologies in addressing the challenges of flood-prone regions.

KEYWORDS: *Floods, Flood Early Warning Systems, Nilwala Basin, Machine Learning*

1 INTRODUCTION

Flooding is one of the most severe natural disasters, significantly affecting human lives and economic activities. The Nilwala Basin, located in southern Sri Lanka, frequently experiences urban flooding due to its topography and seasonal rainfall patterns, especially during the Southwest monsoon. Traditional hydrological models for flood forecasting often fail to capture the complex non-linear relationships between rainfall and river discharge, leading to inaccurate predictions. Nilwala basin is located in southern region of Sri Lanka covering about 1032 km^2. This basin consists of flatlands, mountains and valleys. From the sea level the altitude varies from 0 to 925.m. Upper catchment receives about 3000 mm annual rainfall while the lower receives about 1900 mm annually. In the watershed the soil types include Red- Yellow podzolic soils, Alluvial soils and dune sands (Abeysiriwardana & Wijesekera, 2022). The Nilwala river basin experiences frequent flooding primarily during the Southwest monsoon (May-September) and the second intermonsoon periods, following the same monsoon patterns that affect other major Sri Lankan river basins including the Kelani basin (Dhanapala et al., 2022). Following Figure 1 shows the map of Nilwala river basin as per the study by Basnayake (2022).

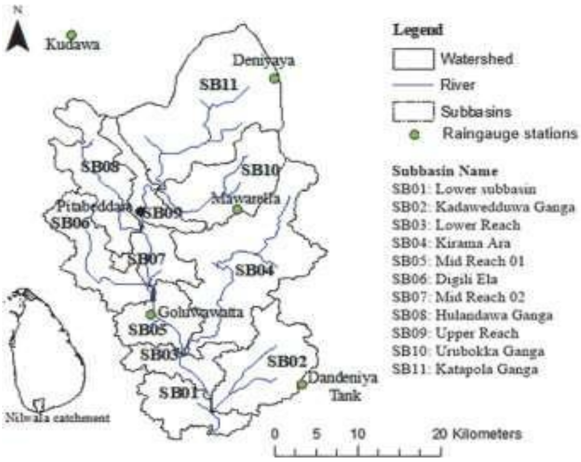

Figure 1. Location of Nilwala River, River Network, its Sub-basins, and Rain gauge Stations (Basnayake, 2022)

Flood forecasting has traditionally relied on hydrological and hydraulic models such as HEC- HMS and physically based numerical simulations (Ke et al., 2020). However, these models require extensive domain knowledge and computational resources, often lacking the flexibility to adapt to varying hydrological conditions (Samarasekara & Sooriyabandara, 2022). Following Figure 2 shows the locations of the rain gauge stations along with flood distribution in Nilwala basin (Kumara et al., 2018).

Figure 2. Matara District flood inundation region with water and rain gauge stations (Kumara et al., 2018)

Machine Learning in Flood Forecasting: Machine learning methods such as Artificial Neural Networks (ANN), Long Short-Term Memory (LSTM), and Support Vector Regression (SVR) have been successfully applied in hydrological modeling. These models outperform traditional statistical approaches by learning complex data patterns directly from historical records (Mosavi et al., 2018).

Hybrid and Advanced ML Models: The use of hybrid models combining multiple machine learning techniques have shown promising results in flood forecasting. For example, combining Random Forest with LSTM improves predictive accuracy by capturing both spatial and temporal patterns (Ganjirad & Delavar, 2023). Graph Neural Networks (GNN) is gaining popularity in hydrological forecasting due to their ability to model spatial dependencies. In the context of flood prediction, GNNs can capture the relationships between rainfall events across different parts of a river basin, improving the accuracy of runoff predictions (Zhao et al., 2024). A study by Shi et al. (2023) focused on computing water levels as a flood forecasting method using Graph Transformer Network (FloodGTN) for river systemsThe system is designed to incorporate external factors such as precipitation, tidal patterns, and the operational configurations of hydraulic infrastructure (eg: dam discharges, gate positions, and pump activity) along the river (Shi et al., 2023). The above study reported 70% accuracy improvement over HEC-RAS, however no raw MAE or root mean square error (RMSE) were reported.

This study aims to develop a Machine Learning (ML)-based early warning system for urban floods in the Nilwala Basin, leveraging historical hydrological data. To achieve this, the research focuses on the following objectives:

- To identify the required variables to understand the flood patterns in the Nilwala Basin.

- To build a relationship between rainfall in several stations and the flow variation at a specific station.
- To use combined machine learning techniques for accurate predictions.
- To train the machine learning models for one-week early predictions in flow.
- To enhance the accuracy of flow prediction in the machine learning models.

By employing a combination of Random Forest (RF), K-Nearest Neighbors (KNN), and Graph Neural Networks (GNN), this research seeks to provide a clear path for accurate short and long-term flood predictions, enhancing disaster preparedness and risk management.

2 METHODOLOGY

This study adopts a data-driven approach to develop an effective early warning system for flood prediction in the Nilwala Basin using a combination of machine learning techniques: Random Forest (RF), K-Nearest Neighbors (KNN), and Graph Neural Network (GNN). The methodology is divided into the following key components.

- Data collection and pre-processing
- Model development – several approaches
- Feature Engineering
- Model Evaluation and Validation
- Long-term predictions and enhancements

2.1 Data Collection and Preprocessing

Data Collection: The primary data used in this study consists of historical rainfall and river flow records from January 1, 2012, to December 31, 2022. Rainfall data were collected from six meteorological stations within the Nilwala Basin: Deniyaya, Kotapola, Athuela, Deegala, Goluwawatta, and Kekenadura. These stations were selected based on their geographical distribution and the availability of reliable data. The river flow data were obtained from the Pitabeddara station, located downstream, which is a critical point for monitoring flood risk in the basin.

The collected data required significant preprocessing due to issues such as missing values, inconsistent time intervals, and data quality. The daily rainfall data, , were merged with the hourly river flow data by converting the flow data to daily maximum values to match the rainfall dataset's time scale. Missing rainfall and flow records were identified and were adjusted using the data from neighboring stations to improve model accuracy (Subramanya, 2013). This method compares the provided data with the normal value for precipitation at a particular time period (e.g., hourly. daily, weekly, monthly). Due to the heavy variation of the normal precipitation following

$$P_x = \frac{N_x}{M}\left(\frac{P_1}{N_1} + \frac{P_1}{N_1} + \cdots + \frac{P_m}{N_m}\right) \qquad 01$$

Table 1 shows the data availability of the stations.

Table 1. Visual representation of the percentages of missing data in the selected stations

Station	Data Feature	Available Amount	% Available
Deniyaya	Rainfall	3196/4018	79.54%
Kotapola	Rainfall	2861/4018	71.20%
Athuela	Rainfall	2494/4018	62.07%
Deegala	Rainfall	2464/4018	61.32%
Goluwawatta	Rainfall	3376/4018	84.02%
Kekenadura	Rainfall	3987/4018	99.23%
Pitabeddara	Flow	4018/4018	100%

To ensure consistency across different input variables, MinMax Scaling was applied. This method normalized the data to the range 0 to 1, reducing the influence of variables with larger magnitudes and improving model convergence during training.

2.2 Model Development

The study implemented three machine learning models, each tailored to capture different aspects of the rainfall-flow relationship in the Nilwala Basin.

Random Forest (RF) Model

The Random Forest algorithm was chosen for its robustness in handling non-linear relationships and its ability to process large datasets effectively. RF is an ensemble learning method that builds multiple decision trees during training and averages their predictions, thereby reducing overfitting and increasing accuracy. Lagged rainfall data (1-day, 2-day, and 3-day lags) were included as input features to capture the delayed effect of rainfall on river flow. Additionally, rolling averages of rainfall were used to represent cumulative rainfall impacts.

These features become input predictors for each sample in the training dataset. The RF algorithm built an ensemble of decision trees using samples from the training data and selecting random features subjects (statistical metrics from different stations and times). The model objective was to build a nonlinear relationship between the statistical features and target flow values by averaging predictions.

The dataset was split into training (80%) and testing (20%) subsets. The model was trained on the training set, and its performance was evaluated on the test set using metrics such as Root Mean Square Error (RMSE) and R-squared (R^2) values.

K-Nearest Neighbors (KNN) Model

The KNN model was trained by constructing feature vectors from the same set of statistical rainfall and flow characteristics. The model was employed to capture localized patterns in the data, leveraging the similarity between recent rainfall and historical events. KNN is a non-parametric algorithm that identifies the k most similar data points (neighbors) and uses their outcomes to predict the target variable.

The input features for the KNN model included daily rainfall data from all six stations and the maximum daily flow value at Pitabeddara. A dynamic approach was used to determine the optimal value of k (number of neighbors) based on model performance during cross-validation.

KNN does not require an explicit training phase like other models; instead, it relies on the stored dataset to make predictions. The training phase involved storing these feature vectors along with observed flow values. The optimal number of neighbors k was determined via cross-validation by minimizing prediction error metrics on the validation set.

The KNN model's performance was assessed using RMSE to quantify prediction errors. Additionally, a confusion matrix was constructed to evaluate the model's ability to classify high-flow events, critical for flood warnings.

Long Short-Term Memory (LSTM) Model

The Long Short-Term Memory (LSTM) model used in this study follows a structured process to improve flood prediction in the Nilwala Basin. Initially, the model's development began with rigorous data collection and preprocessing, where historical daily rainfall data from six stations and hourly river discharge data (converted to daily maxima) were compiled.

Once gathered, the data underwent normalization to balance the input scales and reduce training biases. Subsequently, time-series sequences were created to capture temporal dependencies using a look-back window, enabling the model to learn from past rainfall patterns to influence future discharge. The LSTM architecture, featuring input, hidden memory cells, and output layers, was designed to effectively capture both short and long-term dependencies, which are crucial for understanding flood dynamics. The model was then trained using a training dataset and evaluated on separate validation data, utilizing optimization techniques and loss functions such as Root Mean Square Error (RMSE) to fine-tune performance. It was trained using mini-batch gradient descent, feeding batches of sequences. Model output was analyzed by comparing actual vs. predicted flows, with confusion matrices providing insight into classification accuracy.

Graph Neural Network (GNN) Model

The GNN model was implemented to address the complex spatial dependencies between the rainfall stations and the river flow at Pitabeddara. GNNs are well-suited for this task as they can effectively model relationships between nodes (stations) in a graph structure, capturing both spatial and temporal patterns. A graph was constructed where each node represented a rainfall station, and the edges represented the influence of rainfall on downstream flow. The edge weights were determined based on the correlation between rainfall at each station and the flow at Pitabeddara.

The GNN model consisted of three layers - An input layer to receive rainfall data, a hidden layer with Graph Convolutional Networks (GCN) for feature extraction, and an output layer that provided the predicted weekly maximum flow. The hidden layer applied convolutional operations across the graph to aggregate information from neighboring nodes, enhancing the model's ability to learn complex spatial relationships. The GNN was trained end-to-end using supervised learning, minimizing mean squared error between predicted and observed flows. The training process involved iterative message passing among nodes to aggregate spatial information. In addition to spatial features, the GNN model incorporated a temporal aggregation layer that processed a sequence of past rainfall data (up to 7 days) to capture long-term dependencies and delayed hydrological responses.

2.3 Feature Engineering

Feature engineering was critical to improve model performance. The following techniques were applied.

- Lagged rainfall data were included to account for the time it takes for rainfall to translate into increased river flow.
- Three-day rolling averages of rainfall were used to smooth out short-term fluctuations and emphasize the impact of sustained rainfall events.
- For time-series models like GNN, sliding window approach was used to create sequences of input data, allowing the model to learn from the temporal order of rainfall events.

2.4 Model Evaluation and Validation

The performance of each model was rigorously evaluated using both regression and classification metrics.

- Root Mean Square Error (RMSE) was used as the primary metric to quantify the prediction error, with lower values indicating better model performance.
- R-squared (R^2) provided a measure of the variance in the observed data explained by the model, indicating the goodness of fit.
- A confusion matrix was generated for each model's prediction accuracy in flow values.
- The Random Forest model served as a strong baseline, capturing non-linear relationships effectively but showing limitations in handling temporal dependencies. The KNN model performed well at localized flow predictions but struggled with sudden changes in flow rates. The GNN model outperformed both, demonstrating superior predictive capability by leveraging spatial and temporal dependencies, particularly during prolonged rainfall events.

2.5 Long-Term Prediction and Enhancements

To extend the predictive horizon to one week, the GNN model was tailored for long-term forecasting. The model provided maximum flow in 7 days' time as the output, which is critical for flood management and early warning systems.

3 RESULTS

The proposed framework demonstrated a marked improvement in flood prediction accuracy, with the GNN model outperforming conventional approaches such as Random Forests, achieving a 50% reduction in RMSE and a fivefold increase in R^2 compared to traditional models. Additionally, high- flow accuracy improved significantly, with GNN achieving 85%, representing a 15% enhancement over KNN and a 21% improvement over Random Forest, underscoring its superior performance in predicting extreme events. A time-series plot of predicted vs actual MaxFlow showed visibly closer peak alignment after the inclusion of elevation. Table 2 compares the models' performance using key metrics (RMSE and R^2), and their ability to classify high-flow events.

Table 2. The performance comparison of the four models

Metric	Random Forest	KNN	LSTM	GNN
RMSE (Testing)	61.44	45.21	34.89	30.57
R-squared (R^2)	0.14	0.31	0.59	0.68
High-Flow Accuracy	70%	78%	82%	85%

The Random Forest model captured non-linear relationships between rainfall and river flow but struggled with temporal dependencies, leading to reduced accuracy during peak flow events. In contrast, KNN performed better on short-term forecasts, yet its reliance on historical patterns made it less reliable during unusual weather conditions. LSTM excelled at capturing temporal patterns, adeptly handling the delayed impact of rainfall on river flow, but it was limited in modeling spatial dependencies between rainfall stations. The Graph Neural Network (GNN) outperformed all other models by effectively leveraging both spatial and temporal data. Its graph-based architecture captured the complex interactions between rainfall events and downstream flow, making it the most accurate and reliable model for flood forecasting in the study. The comparison of the predictions and actual values shown in Figure 3. Although the model did not capture the exact values similar to the actual values, it is noteworthy given the loss of data in the inputs, the model was able to capture the pattern of the variation. Furthermore, this can be integrated to predict water levels and predicting flood or non-flood scenario using a water level threshold.

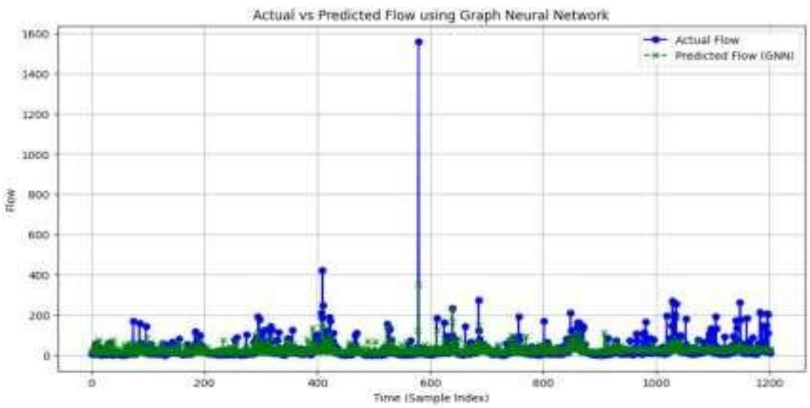

Figure 3. Actual vs. Predicted Flow at Pitabeddara Station using Graph Neural Network

4 CONCLUSION

This study presents a novel machine learning-based framework for flow prediction in the Nilwala Basin, integrating Random Forest, KNN, and GNN models. The GNN model, in particular, showed strong performance in capturing spatial and temporal patterns, making it a valuable tool for early warning systems. The results indicate that the proposed methodology significantly improves prediction accuracy compared to traditional hydrological models.

The following are the key findings of this project.

- Currently, the model predicts only flow values, but for it to be more useful in flood risk management, it needs to be updated to predict floods using a proper threshold. Defining and incorporating flood thresholds based on historical flood data or established flood levels will allow the model to classify high risk events more accurately.
- Integration of Graph Neural Network can provide a proper forecasting network, by treating time-series data as a graph.
- The combination of RF, KNN, and GNN models provides a comprehensive approach to handling the complexities of flood prediction.

- GNN's ability to model spatial relationships enhances the prediction of extreme flood events, offering a practical solution for disaster preparedness.
- Data quality and completeness remain critical to model performance, highlighting the need for improved data-collection infrastructure.
- The integration of elevation data helps address topographical variability in the basin, enabling more precise predictions of flow and flood hydrographs.

REFERENCES

Abeysiriwardana, H. D., & Wijesekera, N. T. S. (2022). Application of GIS and Logistic Regression for Flood Susceptibility Mapping in Nilwala River Basin, Sri Lanka. *Engineer: Journal of the Institution of Engineers, Sri Lanka*, *55*(2), 1. https://doi.org/10.4038/engineer.v55i2.7503

Basnayake, B. M. L. A. (2022). Prioritization of Sub-basins of Nilwala River Basin for Flood Exposure using Multi Criteria Decision Analysis. *Engineer: Journal of the Institution of Engineers, Sri Lanka*, *55*(1). https://doi.org/10.4038/engineer.v55i1.7483

Dhanapala, L., Gunarathna, M. H. J. P., Kumari, M. K. N., Ranagalage, M., Sakai, K., & Meegastenna, T. J. (2022). Towards Coupling of 1D and 2D Models for Flood Simulation—A Case Study of Nilwala River Basin, Sri Lanka. *Hydrology*, *9*(2), 17. https://doi.org/10.3390/hydrology9020017

Ganjirad, M., & Delavar, M. R. (2023). FLOOD RISK MAPPING USING RANDOM FOREST AND SUPPORT VECTOR MACHINE. *ISPRS Annals of the Photogrammetry, Remote Sensing and Spatial Information Sciences*, *X-4/W1-2022*, 201–208. https://doi.org/10.5194/isprs-annals-X- 4-W1-2022-201-2023

Ke, Q., Tian, X., Bricker, J., Tian, Z., Guan, G., Cai, H., Huang, X., Yang, H., & Liu, J. (2020). Urban pluvial flooding prediction by machine learning approaches – a case study of Shenzhen city, China. *Advances in Water Resources*, *145*, 103719. https://doi.org/10.1016/j.advwatres.2020.103719

Kumara, M. T., Madushanka, W. D. K., & Nandaseela, S. de S. (2018). *Spatial Distribution of Floods in Mathara District: With Special Focus on 2003 and 2017 Flood Events*. https://ir.kdu.ac.lk/handle/345/2460

Mosavi, A., Ozturk, P., & Chau, K. (2018). Flood Prediction Using Machine Learning Models: Literature Review. *Water*, *10*(11), 1536. https://doi.org/10.3390/w10111536

Shi, J., Stebliankin, V., Wang, Z., Wang, S., & Narasimhan, G. (2023). *Graph Transformer Network for Flood Forecasting with Heterogeneous Covariates* (Version 1). arXiv. https://doi.org/10.48550/ARXIV.2310.07631

Subramanya, K. (2013). *Engineering Hydrology* (Fourth Edition). https://www.goodreads.com/book/show/24967969-engineering-hydrology

Zhao, X., Wang, H., Bai, M., Xu, Y., Dong, S., Rao, H., & Ming, W. (2024). A Comprehensive Review of Methods for Hydrological Forecasting Based on Deep Learning. *Water*, *16*(10), 1407. https://doi.org/10.3390/w16101407

Synergistic Charge Dynamics and Light Harvesting in TiO_2/MgO Composites for Efficiency Enhancement in CdS Quantum Dot-Sensitized Solar Cells

N.F. Ajward*, J.V.P. Fernando and V.P.S. Perera
Department of Physics, The Open University of Sri Lanka, Nawala, Nugegoda
nf2010.ajward@gmail.com, jvfer@ou.ac.lk & vpper@ou.ac.lk

ABSTRACT

Quantum dot-sensitized solar cells (QDSSCs) represent a promising advancement in renewable energy technologies, with recent improvements achieving power conversion efficiencies close to 6%. Structurally similar to dye-sensitized solar cells (DSSCs), QDSSCs employ quantum dots (QDs) as sensitizers that absorb photons and inject excited electrons into the conduction band of a wide-bandgap semiconductor electrode, while the redox electrolyte removes the generated holes and completes the circuit through regeneration at the counter electrode. Quantum dots composed of materials such as CdS, CdSe, PbS, and InP are increasingly studied for use in QDSSCs, offering the advantage of tunable optical band gaps through particle size manipulation. This adaptability enhances QDSSCs' design potential, enabling the integration of third-generation solar cell configurations, including multiple exciton generation (MEG), to further improve energy conversion efficiency.

Despite these advancements, QDSSC performance is currently limited by issues such as reduced photovoltage and recombination losses at the TiO_2-QD-electrolyte interface. This study investigates the effect of MgO incorporation into TiO_2 photoanodes on the photovoltaic performance of CdS QDSSCs, with particular attention to the fill factor (FF) and overall cell efficiency. MgO is expected to act as an interfacial passivation layer suppressing combination and improving charge-selective transport. In addition, MgO may enhance light scattering within the photoanode, thereby improving light harvesting and short-circuit current density.

In this study, MgO powder was incorporated in specific mass ratios with TiO_2, followed by the application of CdS quantum dots (QDs) on the TiO_2/MgO composite layer using the SILAR method. Results indicated a significant improvement in the fill factor (FF) at an optimal MgO-to-TiO_2 ratio, attributed to synergistic effects of MgO on interface stabilization, reduced recombination, and enhanced charge transport. The optimized MgO-modified TiO_2 films achieved a current density of 1.95 mA cm-2, voltage of 437 mV, and power of 0.121 mW (active area = 0.49 cm^2), reaching an efficiency of 0.311 % (18.7% higher than TiO_2/CdS QDSCs), with improved interfacial impedance, Incident Photon to Current Efficiency (IPCE), and FF of 0.374.

KEYWORDS: *QDSCs, MgO, TiO_2, CdS, SILAR, efficiency, Fill factor.*

1 INTRODUCTION

Quantum dot-sensitized solar cells (QDSCs) represent a promising class of third-generation photovoltaic technologies, offering cost-effective fabrication, tunable optical properties, and potential for enhanced energy conversion via mechanisms such as multiple exciton generation. Structurally analogous to dye-sensitized solar cells (DSSCs), QDSCs replace organic dyes with semiconductor quantum dots (QDs), which absorb incident photons and inject excited electrons into the conduction band of a wide-bandgap semiconductor, typically TiO_2. The redox electrolyte simultaneously extracts holes and regenerates the QDs, completing the electrochemical circuit (Sambur & Parkinson, 2010).

The use of QDs such as CdS, CdSe, PbS, and InP has gained traction due to their size-dependent bandgap tunability and high extinction coefficients, enabling broader spectral absorption than conventional dyes (Sargent, 2005; Beard et al., 2007). Among them, CdS quantum dots are widely used owing to their favorable band alignment with TiO_2 and straightforward synthesis via methods such Successive Ionic Layer Adsorption and Reaction (SILAR). However, QDSCs still suffer from performance limitations caused by rapid charge recombination at the TiO_2–QD–electrolyte interfaces and low open-circuit voltages (Chen et al., 2012; Gao et al., 2017).

To address these challenges, recent studies have explored interfacial engineering strategies, including the introduction of wide-bandgap metal oxide layers such as MgO. MgO coatings have demonstrated an ability to suppress interfacial recombination, improve charge selectivity, and enhance light scattering within the photoanode structure, thereby boosting both the short-circuit current and fill factor (Wang et al., 2014; Chang et al., 2016). Furthermore, insulating nature of MgO can act as an electron-blocking layer, mitigating electron back-transfer and increasing the carrier lifetime in the system (Liu & Kamat, 1993).

Although MgO has previously been explored as a passivation or buffer layer in semiconductor-based solar cells, systematic optimization of the MgO–TiO_2 composition for CdS-based QDSSCs has received limited attention. In this work, MgO was incorporated into TiO_2 photoanodes at different mass ratios to identify the optimum composition for enhanced photovoltaic performance. CdS quantum dots were deposited by the SILAR method, and the resulting photoanodes were evaluated through photovoltaic, electrochemical, structural, and optical characterization to correlate MgO content with charge transport, recombination behavior, and light-harvesting properties.

2 EXPERIMENTAL DETAILS

2.1 Preparation of TiO2/MgO Films Varying Mass Ratio

MgO powder was measured according to the quantities specified in Table 1. For each sample, concentrated HNO_3 acid was added dropwise to the MgO powder which was then ground in a mortar and pestle. TiO_2 powder 0.25 g was subsequently mixed with one drop of Triton X-100, and 0.05 g of PEG 1000. The resulting paste was spread onto pre-cleaned conducting tin oxide (CTO) glass plates (1.0 cm × 2.0 cm) using the doctor blade method. The cleaning process involved ultrasonic bath treatment with detergent and distilled water. Finally, the TiO_2 coated films were dried on a hot plate and sintered in a furnace at 450 °C for 45 minutes

Table 1. Mass of MgO for each sample

Sample	**1**	**2**	**3**	**4**	**5**	**6**	**7**	**8**	**9**
Mass of MgO(g)	0.0025	0.0050	0.0075	0.0100	0.0125	0.0150	0.0175	0.0200	0.0225
Percentage	1%	2%	3%	4%	5%	6%	7%	8%	9%

2.2 Deposition of CdS using SILAR method.

To prepare solutions containing precise concentrations of Cd^{2+} and S^{2-} ions, 10.065 g of $CdCl_2$ and 3.902 g of Na_2S were weighed with an electronic balance (±0.001 g accuracy). These compounds were then dissolved in 100 ml of distilled water. To optimize the solubility of the relevant species and enhance the electrochemical behavior within the cell, the pH of the $CdCl_2$ solution was adjusted to 4.5. This was achieved by carefully adding 0.01 M NaOH or 0.01 M HCl solutions dropwise while closely monitoring the pH.

The SILAR method was employed to deposit CdS films on the TiO_2/MgO photoanodes. Each dipping step into the $CdCl_2$ and Na_2S solutions lasted for one minute. After each dip, the photoanodes were rinsed with distilled water to remove any excess reagents, then air-dried. To ensure uniform film formation, the photoanodes were then dipped in the complementary precursor solution (anionic or cationic), followed by a washing and drying cycle. This entire sequence of steps was repeated ten times to make a multilayered CdS film. Finally, the coated photoanodes were heated on a hot plate at 80 °C for 30 minutes to enhance the film's stability and adhesion to the substrate.

2.3 Preparation of Electrolyte

2ml of electrolyte solution was prepared by combining 0.1301g of Na_2S, 0.1283g of S, and 0.0301g of KCl mixed in Methanol (1.4ml) and distilled water (0.6ml) as solvents. The mixture was stirred for three (3) hours using a magnetic stirrer to ensure complete dissolution of the components and prevent sulfur precipitation of. The stirring time might require adjustment if sulfur precipitation is observed.

2.4 Fabrication of the cell

Conducting side of Pt counter electrode was placed face-to-face with the CdS coated TiO_2 or TiO_2/MgO film and secured with two clamps. The space between the electrodes was then filled with the electrolyte solution, completing the QDSSC assembly.

2.5 Characterization

The fabricated QDSSCs were rigorously characterized using a VK-PA-100 PV Power Analyzer to obtain J–V curves, from which key photovoltaic parameters including photo-conversion efficiency (PCE), short-circuit current density (Jsc), open-circuit voltage (Voc), and fill factor (FF) were extracted. To ensure reproducibility, a minimum of five devices per batch were evaluated. Electrochemical Impedance Spectroscopy (EIS), conducted with an Auto lab Nova 2.1 frequency response analyzer, was employed to investigate charge transport and recombination mechanisms over a frequency range of 0.1 Hz to 1 MHz under simulated solar illumination. This provided critical insight into interfacial resistance and electron lifetime within the photoanode. The Incident Photon-to-Current Efficiency (IPCE) was assessed using a VK-IPCE-10 system to determine the wavelength-dependent photo response and light-harvesting efficiency of the devices.

In addition to electrochemical and photovoltaic analyses, comprehensive structural and morphological characterizations were performed. X-ray Diffraction (XRD) was used to examine the crystallinity and phase composition of the composite materials, At the same time Fourier Transform Infrared Spectroscopy (FTIR) provided information on chemical bonding and surface modifications. Scanning Electron Microscopy (SEM) was utilized to observe the surface morphology and distribution of MgO within the TiO_2/CdS matrix, confirming uniform dispersion and structural refinement. These combined techniques enabled a holistic understanding of the material properties and their influence on the overall performance of the QDSSCs.

3 RESULTS AND DISCUSSION.

3.1 I–V characteristics of CdS QDSSCs

Figure 1(a) presents the current-voltage (I-V) and 1(b) power-voltage (P-V) characteristics of TiO_2/MgO/CdS thin films containing varying MgO mass content, ranging from 1% to 9%.

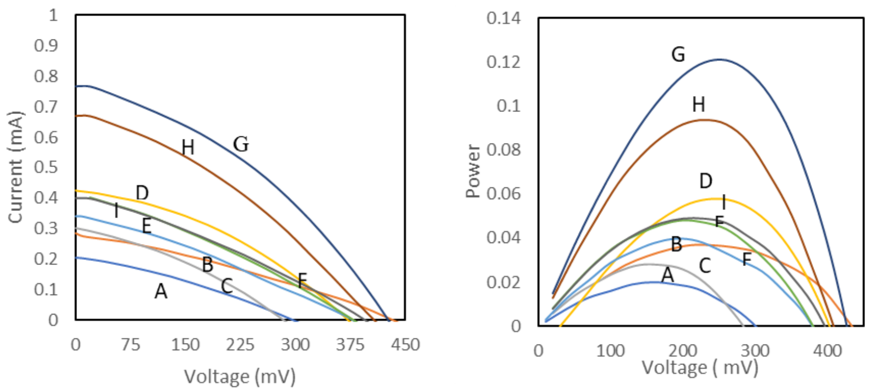

1(a) current-voltage (I-V) characteristics 1(b) power-voltage (P-V) characteristics

[A-MgO 1%, B-MgO 2%, C-MgO 3%, D-MgO 4%, E-MgO 5%, F-MgO 6%, G-MgO 7%, H-MgO 8% and I-MgO 9%,]

Figure 1(a) Current-voltage (I–V) plot for mass ratios ranging from 1% to 9%. (b) Power-voltage (P–V) plot for mass ratios from 1% to 9%.

Table 02: The photovoltaic data obtained for different mass ratio ranging from 1% to 9%

	1%	2%	3%	4%	5 %	6%	7%	8%	9%
V_{oc} (mV)	299.6	433.4	283.8	372	379.3	380.2	437	408.5	396.3
Jsc (mA $cm^{-2)}$	0.521	0.718	0.739	0.867	0.872	1.019	1.946	1.698	1.014

FF	0.323	0.307	0.346	0.369	0.307	0.316	0.374	0.349	0.316
η (%)	0.05	0.096	0.073	0.119	0.101	0.122	**0.311**	0.242	0.127
Power(mW)	0.02	0.037	0.028	0.058	0.04	0.048	**0.121**	0.094	0.049
V_{max} (mV)	160.1	239.9	170.1	210.0	190.1	200.0	260.2	229.9	229.9
I_{max} (mA)	0.123	0.155	0.166	0.278	0.208	0.239	0.466	0.410	0.215

The incorporation of MgO into TiO_2 photoanodes influenced the photovoltaic performance of the CdS QDSSCs, with the effect strongly dependent on MgO content. Among the investigated compositions, the 7 wt.% MgO sample exhibited the best performance, delivering a maximum efficiency of 0.311%, which is 18.7% higher than that of the unmodified TiO_2/CdS QDSC (0.262%). This improvement is attributed to an optimized balance between recombination suppression, charge transport, and light-harvesting enhancement at this composition.

The solar cell efficiency (η) is determined by the fundamental photovoltaic parameters and is given by

$$\eta = \frac{Voc\ X\ I\,sc\ X\ \ FF}{Pin\ X\ S}$$

Where P_{in} is the incident light power density and S= 0.49cm^2 is the illuminated area of the photoanode. The fill factor of the device was calculated based on the relation,

$$\mathrm{FF} = \frac{I\max\ X\ \ Vmax}{I\,sc\ X\ Voc}$$

The MgO coating acts as a buffer layer, blocking back electron transfer and thereby improving the fill factor. Figure 1 and Table 2 show that the MgO-coated TiO_2-based QDSC exhibited a higher fill factor (0.374) than the unmodified TiO_2/CdS QDSC (0.265). Therefore, the fill factor of MgO-coated TiO_2 based QDSCs is approximately 41.13% higher than that of TiO_2/CdS QDSCs.

Figure 1 and Table 2 show that the highest power output (0.121 mW) was obtained with a 7% variation in MgO mass. The performance enhancement observed at 7 wt.% MgO can be attributed to the formation of an effective passivation layer that suppresses interfacial recombination between TiO_2 and the electrolyte. Excessive MgO content, however, may hinder electron transport due to the insulating nature of MgO.

3.2 Electrochemical Impedance Spectroscopy of CdS QDSSCs

The Nyquist plot in Figure 2 illustrates the impedance behavior of the TiO_2/MgO/CdS composite material. EIS measurements were performed over the frequency range of 100 kHz to 0.1 Hz with an AC amplitude of 10 mV (rms) superimposed on the open-circuit potential at room temperature (25 ± 1 °C). As the MgO concentration increases, the semicircular arcs in the plot become more prominent, reflecting increased interfacial resistance. Moderate resistance improves recombination suppression, whereas excessive resistance (≥8 wt.% MgO) hinders charge transport (Chen et al., 2018). In contrast, lower MgO concentrations correspond to smaller arc diameters, suggesting reduced resistive and capacitive behavior. These frequency-dependent changes reveal the influence of MgO on conductivity and interfacial charge transfer within the photoanode structure (Wang et al., 2011; Zhang et al., 2020).

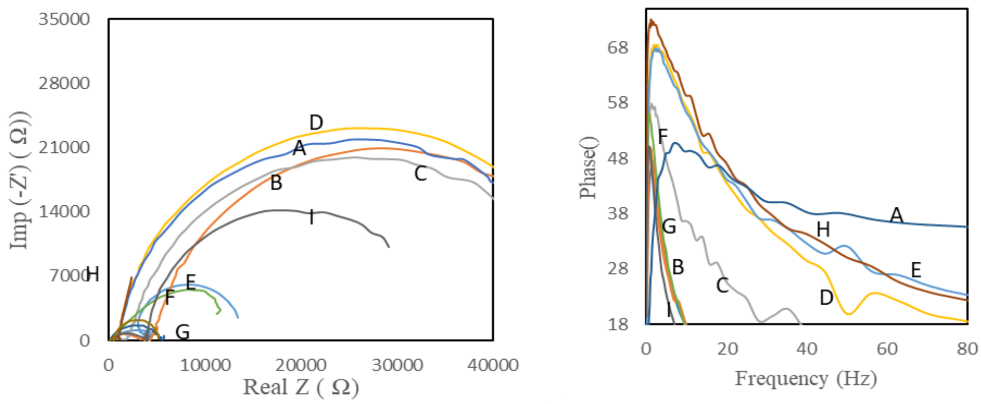

[A-MgO 1%, B-MgO 2%, C-MgO 3%, D-MgO 4%, E-MgO 5%, F-MgO 6%, G-MgO 7%, H-MgO 8% and I-MgO 9%,]

Figure 2(a) Impedance spectra characteristics of mass ratio MgO 1% to 9%

2(b) Phase-Frequency Plot for MgO Mass Ratios Ranging from 1% to 9%

According to the measured data, the TiO_2/CdS composite without MgO exhibited the lowest impedance, demonstrating superior charge transport properties. Upon MgO incorporation, a notable increase in impedance was observed, with the highest value recorded for the 8 wt.% MgO sample, indicative of excessive insulating behavior. The 7 wt.% MgO sample showed a decrease in impedance compared to 8 wt.%, highlighting its optimal composition for synergistic charge transport.

Figure 3 illustrates the series resistance (R_s) and polarization resistance (R_p) derived from circuit fitting, further supporting these observations. As shown in Table 3, the 7 wt.% MgO sample exhibits a very low Rs of 39 Ω, indicating enhanced bulk conductivity, and an Rp of 5.58 kΩ, reflecting a favorable balance between interfacial charge transfer and recombination suppression under the optimized MgO loading. (Roy-Mayhew et al., 2014; Villalva et al., 2009). A higher charge transfer resistance (Rp) indicates suppressed recombination at the semiconductor/electrolyte interface, thereby improving device performance. The optimized MgO composition exhibited the largest semicircle diameter, suggesting more efficient charge separation and reduced recombination losses.

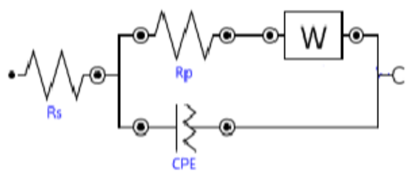

Figure 3: Equivalent Circuit Model for Nyquist Plot Fitting

Table 3. Parameters of equivalent circuit for different QDSC configuration EIS fitting parameters obtained from spectra measured at open-circuit under AM1.5G illumination (100 mW cm^{-2}). Device active area = 0.49 cm^2.

Parameters	1%	2%	3%	4%	5%	6%	7%	8%	9%
R_S (Ω)	2070	3130	1320	688	562	529	39	764	2710
R_P (kΩ)	120	51.6	48.6	49.6	48	41.7	5.58	134	32
CPE (n)	0.994	0.858	0.869	0.949	0.920	0.997	0.677	0.920	0.95
Phase (°) (Approx.)	49	50	68	69	49	48	30	48	44
Frequency at which phase peak observed.	10	9	5	4	10	10	100	10	10

Electrical parameters were reported with three significant figures, consistent with the measurement accuracy (~±3%). The TiO_2/MgO/CdS composite with 7% MgO exhibited notable deviation from ideal capacitive behavior, evidenced by its low CPE exponent of 0.677. A moderate phase angle (30°) near 10 Hz for the 7 wt.% MgO sample suggests a balanced system, effective charge transport combined with optimized interfacial capacitance and minimized recombination losses. Other MgO concentrations displaying either very high phase angles at low frequencies (indicating slow charge transfer or excessive capacitance) or very low phase angles at higher frequencies (reflecting resistive behavior or poor charge storage) are less optimal. This deviation likely results from increased interfacial roughness, composite inhomogeneities, or other structural factors introduced by MgO, impacting charge storage and transfer at the material interfaces.

3.3 Incident Photon-to-Current Efficiency (IPCE) of QDSSCS

Figure 4 illustrates the spectral response of the TiO_2/CdS/MgO composites at various MgO concentrations over the wavelength range of 500–600 nm. The plot indicates that the composite exhibits the highest response, particularly around 540 nm, with the 7% MgO concentration showing the highest peak, suggesting enhanced light absorption or photon-to-electron conversion in this region. However, at higher MgO concentrations, particularly beyond 7%, the response diminishes, indicating that excessive MgO may disrupt charge separation and transfer efficiency, thereby reducing the composite's ability to effectively absorb light. Overall, the findings suggest that an optimal MgO concentration exists maximize the light absorption capabilities of the $TiO_2/CdS/MgO$ composite, with the 7% MgO sample demonstrating a balance between absorption efficiency and material stability.

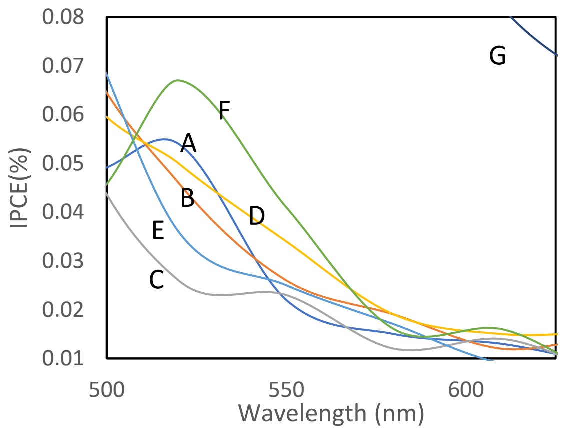

[A-MgO 2%, B-MgO 3%, C-MgO 4%, D-MgO 5%, E-MgO 6%, F-MgO 7%and G-MgO 8%]

Figure 4. Incident Photon-to-Current Efficiency (IPCE) of CdS Quantum Dot-Sensitized Solar Cells (QDSSCs) with various mass ratios of MgO, varying from 2% to 8%.

3.4 Scanning electron microscopy

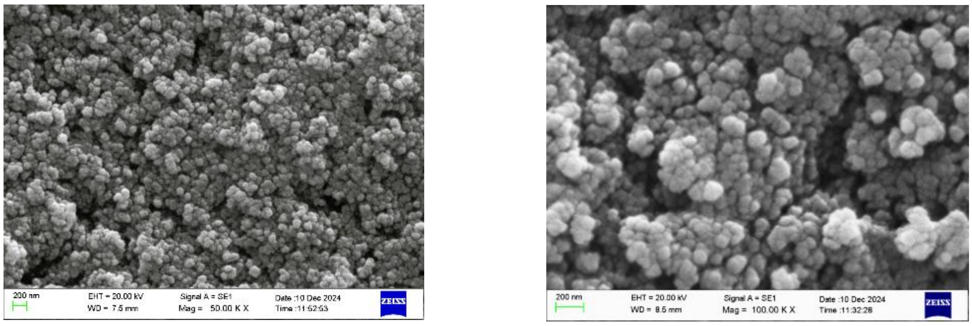

TiO_2 /CdS TiO_2 /CdS// MgO

Figure 5: SEM images of TiO_2/CdS and $TiO_2/MgO/CdS$ 7% films used in quantum dot-sensitized solar cells (QDSSCs).

Figure 5 shows SEM images that clearly illustrate the morphological differences between TiO_2/CdS and $TiO_2/MgO/CdS$ films used in quantum dot-sensitized solar cells (QDSSCs). In the TiO_2/CdS sample, the surface is composed of uniformly distributed, densely packed spherical nanoparticles with small diameters. This structure is advantageous for providing a large effective surface area, enhancing CdS quantum dot loading and light absorption (Wang et al., 2021). Surface roughness and nanoscale feature also facilitate strong interfacial contact for charge transfer.

Upon introducing 7 wt.% MgO, the $TiO_2/MgO/CdS$ sample exhibited a noticeable increase in particle size and surface granularity. This morphological evolution suggests the formation of a conformal MgO layer, which may lead to nanoparticle coalescence or growth. MgO has been reported to reduce surface trap states and suppress electron–hole recombination, leading to improved charge separation and device performance (Zhang et al., 2020). Although the surface area may decrease slightly, the passivation and improved charge- transport pathways outweigh this limitation.

3.5 XRD and FTIR spectra of TiO_2/CdS and $TiO_2/MgO/CdS$

Figure 6 (a) presents the X-ray diffraction (XRD) patterns of TiO_2/CdS and $TiO_2/MgO/CdS$ (7%) composite materials, revealing the crystalline characteristics of the synthesized samples. A prominent peak at $2\theta \approx 25.3°$ corresponds to the (101) plane of anatase TiO_2, in agreement with standard diffraction data (JCPDS No. 21-1272). Additional peaks in the 26°–38° range are assigned to CdS, which may include both hexagonal and cubic phases (JCPDS No. 80-0019 and 10-0454, respectively; Nazeeruddin et al., 2003). The incorporation of 7% MgO leads to a noticeable increase in peak intensity and sharpness, suggesting improved crystallinity and reduced structural defects, potentially due MgO's role in stabilizing the lattice and promoting domain growth (Zhang et al., 2014). The absence of clear MgO peaks is likely due to its low concentration and possible amorphous nature, as similarly reported in literature (Chen et al., 2017).

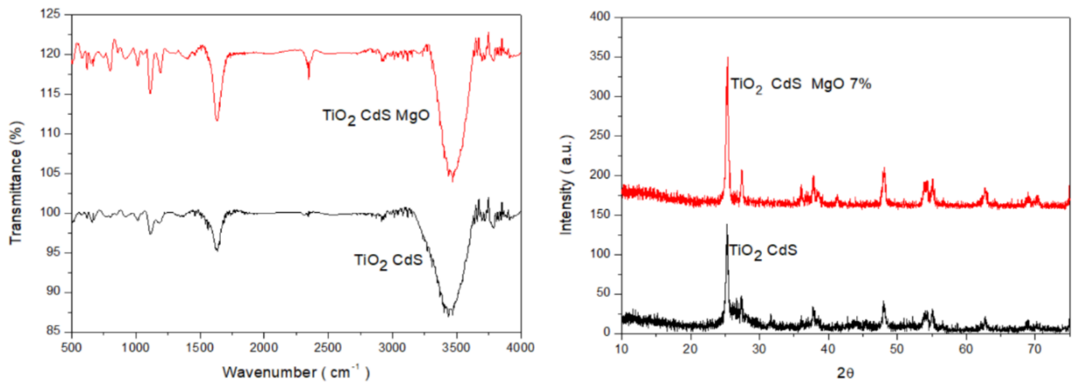

Figure 6: (a) X-ray Diffraction (XRD) patterns showing the crystalline structure of TiO_2, CdS, and the composite material TiO_2 CdS with 7% MgO.
(b) Fourier Transform Infrared (FTIR) spectra illustrating the vibrational modes of TiO_2 CdS and TiO_2 CdS with 7% MgO.

Figure 6(b) shows Fourier Transform Infrared (FTIR) spectra that illustrates vibrational changes upon MgO incorporation. A broad band around 3400 cm^{-1} in both spectra is attributed to O–H stretching vibrations from surface hydroxyl groups or adsorbed water (Nowak et al., 2010). In the MgO-modified sample, slight spectral shifts in this region may indicate the formation of Mg–OH bonds, thereby enhancing surface passivation. Ti–O–Ti and Cd–S stretching vibrations are observed below 800 cm^{-1}, although they may overlap in this range. The observed spectral changes in the TiO_2–CdS–MgO sample suggest alterations in bonding environments and successful MgO incorporation. Such modifications are expected to improve charge separation and reduce surface trap states, thereby enhancing the photovoltaic performance of quantum dot-sensitized solar cells (QDSCs) (Yu et al., 2015; Zhu et al., 2014).

4 CONCLUSION

The incorporation of MgO into TiO_2/CdS quantum dot-sensitized solar cells (QDSCs) enhances photovoltaic performance by modifying the photoanode's interfacial and optical properties. At an optimal loading of 7 wt.%, MgO achieves the highest efficiency (η = 0.311%), reflecting an 18.7% improvement over unmodified TiO_2/CdS systems. This enhancement is primarily attributed to MgO's passivation effect, which reduces interfacial charge recombination and promotes directional electron transport. X-ray diffraction (XRD) analysis confirms the preservation of crystalline phases in TiO_2 and CdS, while increased peak sharpness and intensity with MgO incorporation indicate enhanced crystallinity and structural order. Fourier transform infrared (FTIR) spectroscopy reveals shifts in O–H and metal–oxygen stretching bands, suggesting effective surface modification and reduced trap states.

Electrochemical impedance spectroscopy (EIS) supports these findings, showing reduced series resistance (R_s = 39 Ω), moderate polarization resistance (R_p = 5.58 kΩ), and a CPE exponent (n = 0.677) indicative of favorable interfacial heterogeneity. Scanning electron microscopy (SEM) reveals homogeneous distribution of MgO and improved surface morphology. Incident photon-to-current efficiency (IPCE) spectra demonstrate a significant enhancement around 540 nm for the 7 wt.% MgO sample, indicating improved light harvesting and photon-to-electron conversion. Furthermore, current–voltage (I–V) analysis confirms elevated short-circuit current density (J_{sc} = 1.946 mA/cm^2), open-circuit voltage (V_{oc} = 0.43 V), and fill factor (FF = 0.374).

Collectively, these findings underscore the role of MgO as a multifunctional additive that optimizes structural, optical, and electronic properties, thereby enabling a robust and efficient QDSC architecture. Overall, the results demonstrate that optimizing MgO content in TiO_2 photoanodes is an effective strategy for improving the structural, optical, and interfacial properties of CdS QDSSCs. Among the investigated compositions, 7 wt.% MgO provided the best overall performance, confirming the importance of composition control in interfacial engineering for enhanced quantum dot-sensitized solar cell efficiency.

REFERENCES

Sargent, E. H. (2005). Infrared photovoltaics made by solution processing. Nature Materials, 4, 377–378. https://doi.org/10.1038/nmat1375

Beard, M. C., Knutsen, K. P., Yu, P., Luther, J. M., Song, Q., Metzger, W. K., Ellingson, R. J., & Nozik, A. J. (2007). Multiple exciton generation in colloidal silicon nanocrystals. Nano Letters, 7(8), 2506–2512. https://doi.org/10.1021/nl071486l

Chen, H.-Y., Pan, C.-L., Lin, C.-L., & Lee, Y.-L. (2012). Effects of interface recombination on the performance of QDSSCs. The Journal of Physical Chemistry C, 116(12), 6974–6980. https://doi.org/10.1021/jp211337m

Gao, Y., Liu, C., Song, Y., Zhang, H., & Wang, W. (2017). Efficient quantum dot-sensitized solar cells using MgO interfacial layers. Solar Energy Materials and Solar Cells, 165, 145–153. https://doi.org/10.1016/j.solmat.2017.03.025

Wang, X., Wang, Y., Chen, H., & Ma, T. (2014). Surface passivation of MgO for efficient QDSSCs. Electrochimica Acta, 147, 186–192. https://doi.org/10.1016/j.electacta.2014.09.045

Chang, C.-H., Tseng, C.-H., & Su, C.-Y. (2016). Enhanced performance of CdS quantum dot-sensitized solar cells using TiO_2 photoelectrodes modified with a MgO buffer layer. ACS Applied Materials & Interfaces, 8(15), 9831–9838. https://doi.org/10.1021/acsami.5b12406

Liu, D., & Kamat, P. V. (1993). Photoelectrochemical behavior of thin ZnO films: Effects of sol–gel and electrodeposition methods. The Journal of Physical Chemistry, 97(46), 10769–10773. https://doi.org/10.1021/j100147a006

Chen, B., Yang, M., Priya, S., & Zhu, K. (2018). Origin of J–V hysteresis in perovskite solar cells. Journal of Physical Chemistry Letters, 9(22), 5561–5567. https://doi.org/10.1021/acs.jpclett.8b02171

Wang, P., Zakeeruddin, S. M., & Grätzel, M. (2011). Enhancement of charge transport in quantum dot-sensitized solar cells by interface engineering. Journal of Physical Chemistry C, 115(19), 9518–9525. https://doi.org/10.1021/jp202323s

Nowak, A. P., Rakoczy, R., & Kuśmierek, K. (2010). FTIR analysis of surface hydroxyl groups on metal oxide catalysts. Spectrochimica Acta Part A: Molecular and Biomolecular Spectroscopy, 76, 384–389. https://doi.org/10.1016/j.saa.2010.03.002

Roy-Mayhew, J. D., & Aksay, I. A. (2014). Graphene materials and their use in dye-sensitized solar cells. Chemical Reviews, 114(12), 6323–6348. https://doi.org/10.1021/cr400412a

Villalva, M. G., Gazoli, J. R., & Filho, E. R. (2009). Comprehensive Approach to Modeling and Simulation of Photovoltaic Arrays. IEEE Transactions on Power Electronics, 24(5), 1198–1208. https://doi.org/10.1109/TPEL.2009.201386

Zhang, J., Zhang, X., & Li, Y. (2020). MgO-modified photoanodes for enhanced quantum dot-sensitized solar cell performance. Solar Energy Materials and Solar Cells, 210, 110484. https://doi.org/10.1016/j.solmat.2020.110484

Nazeeruddin, M. K., Kay, A., Rodicio, I., Humphry-Baker, R., Müller, E., Liska, P., Vlachopoulos, N., & Grätzel, M. (2003). Conversion of light to electricity by cis-X_2bis(2,2'-bipyridyl-4,4'-dicarboxylate) ruthenium (II) charge-transfer sensitizers on nanocrystalline TiO_2 electrodes. Journal of Photochemistry and Photobiology A: Chemistry, 159(1), 131–138. https://doi.org/10.1016/S1010-6030(03)00164-4

Zhang, Y., Wang, L., Zhao, Y., & Li, H. (2014). Enhanced photocatalytic activity of MgO-doped TiO_2 nanocomposites. Materials Chemistry and Physics, 148, 371–377. https://doi.org/10.1016/j.matchemphys.2014.07.041

Zhu, R., Zhang, Q., Cao, G., & Wang, Y. (2014). Interface modification strategies for high-efficiency quantum dot-sensitized solar cells. Nano Energy, 4, 138–145. https://doi.org/10.1016/j.nanoen.2014.02.008

Chen, S., Li, D., Zhang, S., Liu, Y., & Yang, H. (2017). Structural and optical properties of MgO-modified nanocomposites. Journal of Alloys and Compounds, 703, 153–160. https://doi.org/10.1016/j.jallcom.2017.01.073

Mobile Applications Usage and Awareness Among Sri Lankan Small Business Owners

Vidana Pathirana Y.K. [a], Munasinghe B.[a]
[a]Department of Computing and Information Systems, Faculty of Applied Sciences, Wayamba University of Sri Lanka, Kuliyapitiya, 60200, Sri Lanka
yashodakawindi@gmail.com, bhagya@wyb.ac.lk

ABSTRACT

Many Sri Lankan small business owners (SBO) today use mobile applications to manage their businesses. The relatedness of the purpose of the mobile applications that the SBO communities commonly use to the objectives and nature of their business (i.e. specifically designed for small businesses), the awareness among the SBOs in finding applications that can serve their business purposes, or their awareness of the importance of using dedicated applications for small business' purposes is an area that has not been investigated. This paper presents the findings of a pilot study on current trends and the nature of mobile application usage among Sri Lankan small business owners to understand the level of awareness they have on choosing mobile applications tailored for small businesses, and their expectations for features in such applications . It also investigates SBO demand for integrated, SBO-specific mobile solutions. The findings show that the Sri Lankan SBO community has either not considered these facts in their mobile applications usage or has found it difficult to manage their businesses using existing mobile applications because those applications are not designed to cater to their specific needs. This paper also summarizes the nature of mobile application usage among SBOs from several perspectives, providing meaningful insights for mobile application developers about this competitive community of users.

KEYWORDS: *Mobile Applications, Small Business Owners (SBO), Small Business Management, User Experience (UX) Enhancement, User-centric mobile applications*

1 INTRODUCTION

Mobile applications have become essential tools for modern business operations, offering convenience, automation, and accessibility in a fast-paced digital environment. In Sri Lanka, small business owners (SBOs) play a vital role in the local economy, accounting for a significant share of the business landscape. As smartphones and internet connectivity become increasingly widespread (Bandara & Jayawardena, 2022), many SBOs have turned to mobile applications to manage various aspects of their businesses, including inventory and sales tracking, communication, and financial management.

While mobile application usage is on the rise among Sri Lankan SBOs, it is evident that most applications in use are general-purpose or designed for larger enterprises in mind. These mobile applications may not adequately address the unique operational needs, budgetary constraints, and growth goals of small businesses. The challenges include customers' unfamiliarity, employees' limited knowledge of mobile payment systems, inadequate management focus, and customers' low computer literacy (Jayarathne et al., 2023). Additionally, there is a noticeable gap in user awareness regarding the importance and availability of mobile applications specifically designed for small-scale enterprises.

Despite the growing adoption of mobile applications by Sri Lankan SBOs, many may be unaware of mobile applications specifically designed for their business scale, or they may face challenges using existing mobile applications that lack features tailored to their workflows. This disconnects results in underutilization of digital tools or reliance on inefficient workarounds. To date, little research has been conducted to explore the nature of mobile application usage among SBOs in Sri Lanka and their level of awareness about purpose-built mobile solutions. This paper presents the findings of a pilot study that aimed to address this research gap by analysing current application usage patterns, assessing awareness levels, and identifying the demand for more targeted mobile applications among this user group.

2 RELATED WORK

The impact of literacy challenges on usability is a well-studied area in mobile application usage research. However, finding applicable results on the objective use of mobile applications among Sri Lankan communities, particularly small business owners, is challenging because of the lack of studies and possibly inconsistent terminology . As such, we reviewed studies where researchers employed various terms like 'low literates' and 'semi-literates' preamble by 'Sri Lankan' to describe users, as all these terms commonly refer to individuals who encounter difficulties in areas requiring literacy for full societal participation.

Raveendran and Rajeshwaran (2016) have highlighted the need to implement a quick, yet strategic approach that matches the pace of internet adoption and mobile device usage in the growing Sri Lankan online market. Sahina and Sachithra (2021) found a significant relationship between mobile marketing initiatives such as mobile application marketing and SMS marketing, highlighting the importance for the marketers to understand the influence of these initiatives on consumer buying attitudes and behaviors whether they are positive or negative.

Silva and Kariyapperuma (2021) showed that Sri Lankan managers engage in conspicuous consumption of mobile phones to maintain or enhance their wealth and social status, influenced by psychological factors such as personal achievement, personality traits, attitudes, and the development of self-concept. Although they have identified that brand-related elements, interpersonal influences, a drive to stay current with technological trends, and market demand shape their intentions, no evidence has been presented regarding the use of mobile applications in particular. However, these researches are focused on the perspective of digital marketing, with the main attention given to customers and how they behave on electronic market platforms, rather than on how the business owners thrive in their businesses using digital media and/or mobile applications.

3 METHODOLOGY

The SBOs referred to in this study are self-managed enterprises with small operational scales, such as grocery shops, beauty salons, private medical practices, and local retail stores, which typically employ fewer than 10 personnel and rely on owner-led management. We used a descriptive study design to:

1. Explore how mobile applications are currently used by SBOs in Sri Lanka, including understanding the commonly used types of mobile applications and how they help manage business operations such as sales, inventory, customer service, or finance.
2. Identify the limitations and challenges faced by SBOs when using existing mobile applications, with a specific focus on the feature availability gaps between available mobile applications and SBOs specific needs (e.g. lack of customization, unnecessary complexity, missing key features, etc.).
3. Explore whether there is demand or preference among SBOs for mobile applications tailored to their needs. This will help determine the perspective of Sri Lankan SBOs on whether the current mobile applications are satisfactory, and/or whether they would benefit from solutions designed specifically for small-scale business environments.

3.1 User Grouping

Based on their responses, the respondents were grouped into three categories based on their current usage namely: 1) SBOs who do not use any mobile applications, 2) SBOs who use multiple separate mobile applications for different tasks, and 3) SBOs interested in adopting an integrated, single mobile application. Preliminary investigations indicated that a vast majority of those who use mobile applications in their business use more than one application to meet their needs. Table 1 summarises the respondents numbers to each category. Surveys with questions focused on deriving answers to the above were designed and used. The 100 participants comprised a range of small businesses including beauty salons, private medical practices, teachers, and local shops, etc.

Table 1. No of respondents from each category

Categories	No of Participants
Business owners not using any mobile application	37
Business owners using multiple separate mobile applications for different tasks	58
Business owners interested in adopting an integrated, single mobile application	5

3.2 Data Collection

A structured questionnaire was developed and shared through social media platforms, WhatsApp business groups, and direct email outreach to reach a wide and diverse sample of self-managed small business owners across sectors. Responses were collected over a defined period. The survey was focused on key areas, namely the nature of current mobile application usage, awareness of small business-specific mobile applications, common business challenges in using mobile technology, and feature preferences in a customizable small business-oriented application. To strengthen the analysis, the geographical scope was also considered, eight participants classified as urban or rural areas. The questions were both multiple-choice and open-ended, targeting both quantitative and qualitative insights.

3.3 Data Analysis

The data analysis was categorized into two: Challenge Identification, and Feature Expectation Study. The Challenges Identification involved identifying the main operational challenges faced by SBOs, particularly those not using mobile applications and/or using various/mismatched mobile applications. Common pain points identified included difficulties in managing appointments, tracking customers, organizing staff schedules, maintaining financial records, and monitoring inventory. The Feature Requirements Analysis was used to understand which features SBOs desire most in an SBO-focused mobile application. The survey included questions on functionalities SBOs consider essential in a business management tool. The most frequently requested features such as inventory control, financial tracking, customer relationship management, appointment booking, and sales tracking were highlighted and ranked based on frequency of mention and user priority.

Collected data were processed and visualized to present user preferences, awareness levels, and application usage patterns. Graphical trends helped identify behaviour patterns across user groups and provided key insights into the need for more tailored mobile solutions for SBOs.

4 RESULTS

4.1 Mobile Application Usage Among Small Business Owners

Sixty-three percent (63%) of participants responded positively to using some form of mobile application in their small businesses, indicating a general awareness of the use of mobile technologies for business operations. However, over 30% of participants indicated to have not been using any mobile application for business purposes is significant, highlighting a gap in digital adoption among SBOs. This suggests a need for greater awareness and/or availability of more suitable application solutions for small businesses. The question "Do you use multiple mobile applications in your business?" was used to determine whether SBOs use multiple separate mobile applications for different business functions (e.g. different mobile applications for accounting, communication, reservation, etc.), manage their operations using a single application or are merely using one application without much consideration. Of those who use mobile applications, 92.1% reported using to use multiple applications for business purposes. This indicates both the lack of available mobile applications that can be customized to different business needs and/or the SBOs lack of awareness of such mobile applications.

Participants were asked whether the different mobile applications they use in their business for different purposes are easy and/or user friendly. Figure 1 shows the ratings they provided in the four application categories they have experienced, namely: Human Resource Management, (HRM) Finance Management, Inventory Management and Scheduling and Appointments.

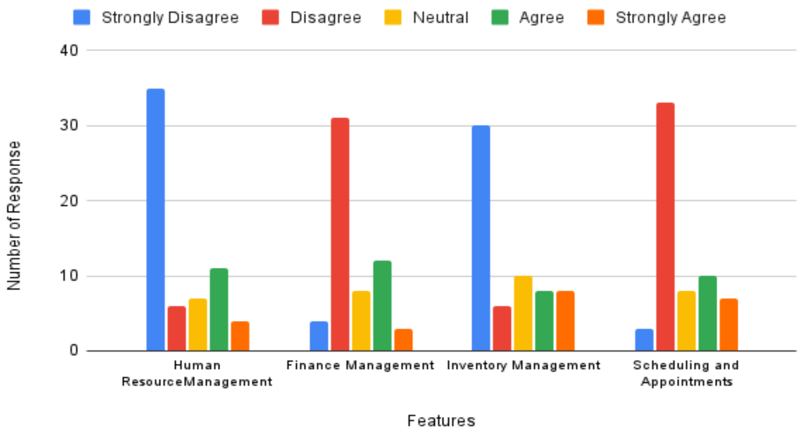

Figure 1: User Ratings on the Ease of Use Across Business App Categories

This rating reflects the combined responses from multiple users for each application category. Rather than evaluating a single application, users rated different mobile applications they personally use under each category. Therefore, the results represent a broader perception across various mobile applications commonly used for these business functions.

The participants have indicated that the HRM and inventory control systems as least user friendly, with most respondents (over 30%) opting to 'Strongly Disagree'. This indicates significant usability challenges in with mobile applications for staff scheduling and payroll functions in HRM with stock-tracking and restocking alert features that do not meet user expectations in inventory control. Interestingly, only a limited number of participants have 'strongly agreed' that any of the mobile applications are easy to use. The reason for this could be either the unavailability of destined mobile applications or unawareness for user-friendlier mobile applications. Finance Management mobile applications and scheduling mobile applications have received the largest negative responses (around 30%) selecting 'Disagree' and only a small percentage 'Strongly Agree'. This indicates that invoicing and expense-tracking mobile applications may be too complex or not sufficiently intuitive for SBOs. Inventory Management mobile applications also had a high number of 'Strongly Disagree' responses, indicating that stock tracking and restocking alert features are not meeting user expectations in terms of ease of use. Scheduling and Appointments mobile applications saw a similar trend to finance mobile applications, with most users (around 30%) disagreeing on ease of use, and relatively low agreement levels. This shows that calendar management and booking systems may also need improvements.

Overall, this data highlights that ease of use varies widely across application types, and many small business owners struggle with the usability of essential mobile tools. These findings emphasize the need for simplified and user-focused mobile application design across functional areas to improve adoption and satisfaction among Sri Lankan small business owners.

4.2 Specific Features Users Find Difficult to Use

The individual respondents were asked about the features they find difficult to use in the applications they use. This question aimed to gather insights into aspects of mobile applications that would create difficulties for users in their real-world, authentic scenarios. Unlike previous aggregated responses across application categories, this question reflects the direct experiences of individual users with specific features they personally interact with.

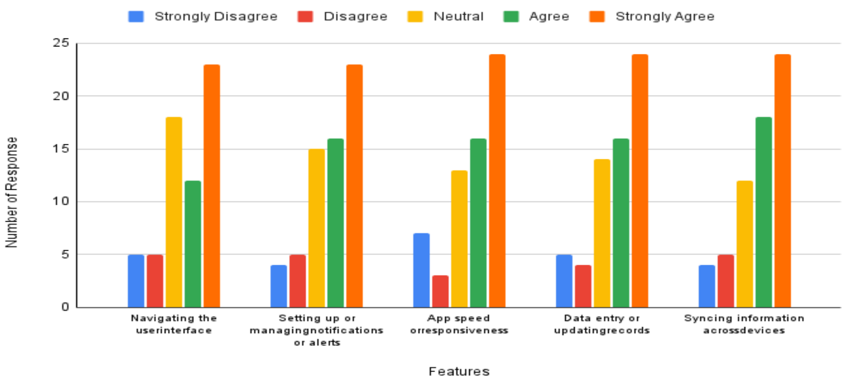

Figure 2: User difficulty ratings for specific applications features

As shown in Figure 2, 63% of respondents reported facing difficulties with certain applications features. The most frequently mentioned issues were navigating the user interface, setting up or managing notifications or alerts, application speed or responsiveness, data entry or record updates, and syncing information across devices/mobile applications. These results suggest that even basic application functions can pose barriers to effective use, especially for SBOs who may lack advanced technical skills. This user feedback highlights the importance of simplifying key features, improving performance, and ensuring that critical functions such as syncing and data entry are intuitive and reliable. These findings reinforce the need for user-centered design in mobile applications tailored for Sri Lankan SBOs, with special attention to usability, accessibility, and feature relevance.

4.3 Reasons for Not Using Mobile Applications

Participants who indicated they had not used any mobile applications for their small businesses were surveyed to understand the barriers to mobile application adoption. When asked for the main reasons as to why they have not been using any mobile applications to support their business, 67.6% indicated that they do not find mobile applications sufficiently suited to their business purposes. Figure 3 shows the main reasons the SBOs have indicated for not using mobile applications in their businesses namely: the cost of dedicated mobile applications, lack of knowledge and awareness of the availability and/or use of such applications, and reluctance to trust third party mobile applications.

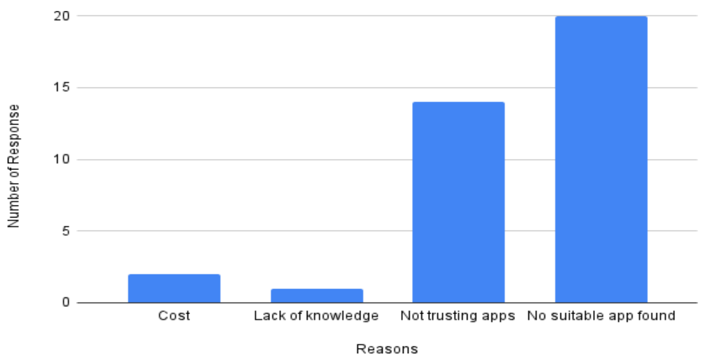

Figure 3: Reasons for Not Using Mobile Applications

Nevertheless, when the participants were asked if they would be interested in a common mobile application that integrates all necessary business features into one platform, a strong majority (92%) expressed interest, indicating a clear demand for a centralized mobile solution for small business operations. These findings highlight a key area of opportunity for developers and service providers: there is a pressing need for affordable, trustworthy, and customizable mobile applications destined for SBOs along with a need for increasing awareness for less tech-savvy users.

4.4 Desired Features for Improvement in Mobile Application

In order to further understand user expectations, respondents were asked about the features they would like to add or remove from the mobile applications that they already use for their business purposes. The results highlight the features users find most important for business functionality (Figure 4) and most commonly requested improvements as: Financial records and expense tracking, customer notifications and alerts, and business performance tracking in finance mobile applications and bookings and appointment management, and staff scheduling in human resource management applications.

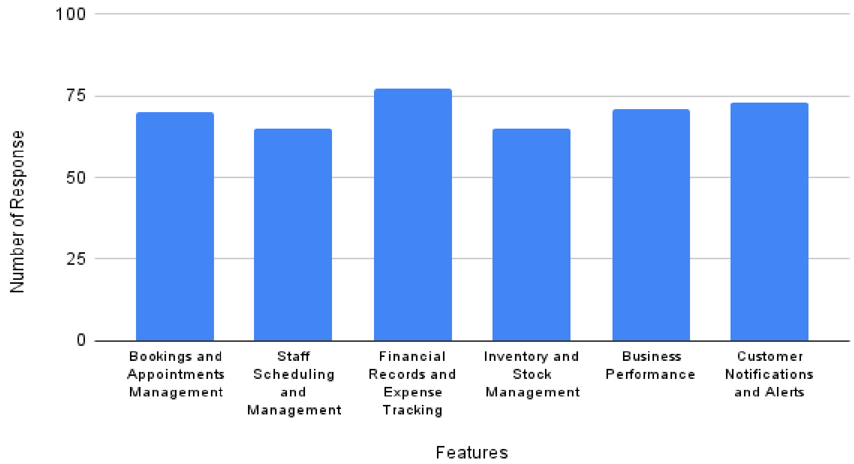

Figure 4: Features to added to or improved in commonly used business mobile applications

5 DISCUSSION AND CONCLUSION

This study highlights the current state of mobile applications usage among Sri Lankan SBOs and reveals key gaps in both awareness and functionality. It shows that although many Sri Lankan SBOs use mobile applications for their business, a significant portion still do not. The main reasons they cited were the complexity of the existing mobile applications, poor usability, and a lack of suitable/customizable mobile applications to suit their specific business needs, highlining a gap in the mobile applications development market for tools designed specifically for small businesses. Among current users, many rely on multiple mobile applications for different tasks, which create confusion and inefficiency. the most commonly used mobile applications among Sri Lankan SBOs were for human resource management, finance, inventory control, and scheduling. However, they indicate that the mobile applications they already use are difficult to use, especially when for data entry, application speed, and synchronization since they are individual applications. A vast majority of the participants showed an interest in a single application that combines all essential business features, with key features requested including finance tracking, customer alerts, performance reports, appointment and schedules management, and inventory control. These findings suggest a strong need for well-designed, all-in-one mobile applications made for SBOs in Sri Lanka. Developers should focus on simplicity, affordability, and essential features to better support this community.

The findings clearly show a strong demand for a user-friendly, all-in-one mobile application that supports essential business operations such as finance, inventory, customer management, appointments, and staff scheduling, presented in a less-complex, small business friendly manner. The participants' strong interest in such a solution suggests a significant opportunity for developers to create purpose-built tools that are affordable, easy to use, and specifically designed to meet the authentic needs of Sri Lankan small businesses. Addressing these needs through thoughtful application design can enhance digital adoption, improve operational efficiency, and empower SBOs to manage their businesses more effectively in the digital age.

REFERENCES

Rajapakse, R., & Gunasekara, T. (2024). *Usage of mobile devices related to sleep among Sri Lankan doctors*. ResearchGate. https://www.researchgate.net/publication/378262906

Bandara, A.M.A.S.M. and Jayawardena, L.N.A.C. (2022) '*Mobile phone-enabled internet services and the technology readiness of the users'*, Sri Lanka Journal of Social Sciences, 45(2), p. 199-212. Available at: https://doi.org/10.4038/sljss.v45i2.8063.

Jayarathne, P.G.S.A., Chathuranga, B.T.K., Dewasiri, N.J. and Rana, S. (2023), "Motives of mobile payment adoption during COVID-19 pandemic in Sri Lanka: a holistic approach of both customers' and retailers' perspectives", *South Asian Journal of Marketing*, Vol. 4 No. 1, pp. 51-73. https://doi.org/10.1108/SAJM-03-2022-0013

Raveendran, N. and Rajesvaran, A. (2016), Are Businesses Succeeding In Sri Lanka Through Online Marketing? in proceedings of International Conference on Contemporary Management (ICCM-2015), University of Jaffna, Sri Lanka.

Shahina, Fathima, and Vilani, Sachitra. (2021). "Mobile Marketing Initiatives on Consumer Attitudes and Buying Behaviour of Young Consumers in Sri-Lanka". *Asian Journal of Advanced Research and Reports* 15 (1):54-67. https://doi.org/10.9734/ajarr/2021/v15i130358.

Silva, A.A.S.D. and Kariyapperuma, S. (2021), Conspicuous Consumption of Mobile Phones among Sri Lankan Managers, in Proceedings of International Conference on Business Management, Faculty of Management Sciences, University of Sri Jayewardenepura, Nugegoda, Sri Lanka, Vol. 18 (2021). https://doi.org/10.31357/icbm.v18

ADOPTION OF A CIRCULAR ECONOMY FRAMEWORK IN THE DESIGN PHASE OF THE REFURBISHMENT PROJECT

S Abilash[1], K A N Gunarathna[2], C. Kalugala[3]
Liverpool John Moores University, UK[1]
Sri Lanka Institute of information Technology, SL[2]
Skills College of Technology, SL[3]

ABSTRACT

Sustainable development in the built environment depends on minimizing environmental impact and conserving resources. In refurbishment projects, integrating circular economy (CE) principles during the design stage can significantly reduce waste and enhance resource efficiency. This study presents a tailored CE framework based on the 2D3R model, which emphasizes Design for Disassembly, Design for Adaptability, and Reduce, Reuse, and Recycle strategies. The framework was developed through a combination of literature review, expert interviews, and survey analysis to identify drivers and barriers to CE adoption in refurbishment. Key findings highlight the role of digital technologies particularly Building Information Modelling (BIM) in improving material traceability and facilitating lifecycle assessments. These tools support the implementation of circular strategies by enabling better planning and design decisions early in the project. The study concludes that applying the 2D3R approach in initial design phases enhances sustainability, reduces costs, and improves the adaptability and longevity of refurbished buildings.

KEYWORDS: *Circular Economy, 2D3R method, Sustainable construction, Building Information Modelling, Resource efficiency*

1 INTRODUCTION

The circular economy (CE) is an evolving model of sustainable development that aims to decouple economic growth from resource consumption and environmental degradation. Unlike the traditional linear model of “take, make, use, dispose,” CE emphasizes restorative and regenerative design by prioritizing resource efficiency, renewable energy use, and minimizing the use of hazardous substances (Ekins et al., 2019). The phrase "circular economy" originated in 1990 while creating a new economic model based on the law of thermodynamics by Mr. Pears and Mr. Turner (Ghisellini et al., 2016). The foundation of contemporary CE emerged through interconnected models such as environmental economy, the green economy, and industrial ecology (Tambovceva & Titko, 2022). Earlier concepts, including Boulding’s “Spaceship Earth” model and Stahel’s “cradle-to-cradle” principle, further established CE's theoretical foundations (Milovic et al., 2024).

As the construction sector remains one of the largest contributors to global environmental degradation, the application of CE in this domain has garnered increasing attention. The industry accounts for approximately 40% of global raw materials consumption generates 30% to 40% of all solid waste (Wijesinghe et al., 2024). Construction processes also account for 39% of carbon dioxide emissions, with 11% attributed to embodied carbon in materials and products (Desilva et al., 2023). Moreover, construction-related activities consume significant quantities of energy, fresh water, and other natural resources, exacerbating ecological pressures (Osobajo et al., 2022). These statistics underscore the urgent need for systemic change, prompting the integration of CE principles into the construction and refurbishment sectors.

Refurbishment, defined as the process of modifying, upgrading, or extending existing structures, has emerged as a sustainable alternative to demolition and new construction. Given the escalating costs of infrastructure and environmental concerns in developing nations such as Sri Lanka, refurbishment offers a cost-effective and environmentally viable solution (De Silva et al., 2023a). It enables the preservation of building assets while addressing issues of deterioration, obsolescence, and changing functional requirements (Ekanayake et al., 2018). When aligned with CE principles such as design for disassembly (DfD), material reuse, and regenerative practices refurbishment can substantially mitigate waste generation, reduce reliance on virgin resources, and support carbon-reduction goals (Bimsara et al., 2024).

The design phase of refurbishment projects presents a critical opportunity for CE integration. Design decisions made at this early stage influence material selection, construction techniques, and lifecycle performance, directly affecting sustainability outcomes (Wijewansha et al., 2021). For instance, DfD facilitates deconstruction, promotes component reuse, and minimizes waste at end-of-life stages (AlJaber, Alasmari, et al., 2023). Digital tools such as Building Information Modelling (BIM) and material passports support these objectives by enhancing traceability, enabling lifecycle assessment, and informing sustainable design strategies (Leindecker et al., 2024). The deployment of such tools during the design stage allows for comprehensive resource planning and optimization.

Numerous CE frameworks and models have been proposed to guide implementation across various scales of the built environment. At the micro level (materials), meso level (buildings), and macro level (cities), frameworks like REVERT (Resource, Envisagement, Validation, Entity, Regulation, and Technology) and RESOLVE (Regenerate, Share, Optimize, Loop, Virtualize, Exchange) facilitate multi-scale stakeholder engagement and circular transformation (Bostancı et al., 2025; Csete & Esses, 2022). The 3R (Reduce, Reuse, Recycle) and extended 9R models (including Refuse, Rethink, Repair, Refurbish, Remanufacture, and Repurpose) further provide structured approaches to resource efficiency and waste minimization (Rahla et al., 2021). Together, these frameworks support regenerative practices that preserve the value of materials and infrastructure, contributing to long-term environmental and economic sustainability.

Nonetheless, the integration of CE principles in refurbishment design remains limited, particularly in developing countries. Significant barriers persist, including regulatory ambiguities, inadequate policy enforcement, limited financial incentives, and low stakeholder awareness (AlJaber, Martinez-Vazquez, et al., 2023; Fernandes & Ferrão, 2023b). The absence of standardized documentation, weak construction demolition waste policies, and insufficient training further hinder CE adoption (Metinal & Gumusburun Ayalp, 2025). In the Sri Lankan context, outdated regulations, a limited technological infrastructure, and minimal institutional support pose additional challenges (Athapaththu et al., 2016; Weerakoon & Thayaparan, 2023). These systemic issues result in inconsistent practices and limit practical application, even where awareness of CE benefits exists.

Despite these challenges, global and local case studies demonstrate the practical viability and advantages of CE implementation. The Grensen 9b office project in Norway, for example, achieved a 93% reduction in CO_2 emissions by integrating reused materials into its refurbishment process (Baarnes & Liang, 2025). Similarly, in Sri Lanka, The University of Ruhuna, Matara, and the Ocean University Galle demonstrate how refurbishment projects have successfully applied DfD and design for adaptability (DfA) principles, achieving material circularity rates exceeding 85% through lifecycle assessment tools (De Silva et al., 2023b). These examples underscore the transformative potential of CE when incorporated at the design phase.

While existing CE frameworks offer a robust theoretical foundation, they are largely oriented towards new construction rather than refurbishment, which presents distinct constraints and opportunities (Fernandes & Ferrão, 2023a). Refurbishment projects often involve existing structural limitations, non-standardized material documentation, and diverse stakeholder requirements. As such, a specialized framework is needed to facilitate systematic CE integration from the design stage in refurbishment contexts (Charef et al., 2021). Doing so can enable better resource planning, material recovery, and carbon management, ultimately contributing to a more sustainable built environment (Wijewansha et al., 2021). This study plans to develop a custom approach to applying circular economy standards in the design phase of refurbishment projects, primarily to make them more sustainable, unique, and less wasteful in places like Sri Lanka and similar areas.

2. RESEARCH METHODOLOGY

This research aims to develop a framework for applying circular economy (CE) principles during the design phase of refurbishment projects. A qualitative literature review was conducted to explore CE's impact on sustainability, resource use, and waste management in construction. A mixed-methods approach was adopted, combining quantitative survey data with qualitative insights from stakeholders to assess environmental impacts and identify sustainable strategies. Purposive sampling was used to select 5–7 experienced professionals, including architects, quantity surveyors, and project managers. Structured interviews provided in-depth data. Ethical approval was secured, ensuring confidentiality and anonymity throughout the research process, in alignment with core ethical standards.

3. DATA COLLECTION AND ANALYSIS

3.1 Structured Interview Respondent's Profile

Interviews with construction stakeholders, including architects, quantity surveyors, and project managers, provided valuable insights into the practical challenges, opportunities, and strategies for applying CE principles in refurbishment design. Six structured interviews were carried out for data collection. The respondents' details were gathered through the first section of the semi-structured interview guideline. The summarized composition of respondents is presented in Table 1.

Table 1: The composition of the respondents

Interviewee	Profession	Industry Experience (Years)
Respondent 1 (R1)	Civil Engineer	10 years
Respondent 2 (R2)	Quantity Surveyor	4 years
Respondent 3 (R3)	Senior Cost Manager	12 years
Respondent 4 (R4)	Chartered Quantity Surveyor	30 plus years
Respondent 5 (R5)	Client Cost Consultant and Estimator	11 years
Respondent 6 (R6)	Chartered Quantity Surveyor	30 years

3.2 Thematic Analysis

The thematic analysis method is used to analyze the data gathered from structured interviews. The selected interviewees had experience in refurbishment and were familiar with sustainable approaches, particularly CE principles. This target group includes leading quantity surveyors, cost managers and project managers working on construction projects in Sri Lanka, providing the study with a diverse set of perspectives. Selecting these variables in this way ensured that the collected data was rich, specific to the context and aligned with the aims of the study.

3.2.1 Theme 1 - Explore CE principles relevant to refurbishment projects

Expert interviews revealed both shared and unique views on the importance of CE principles in refurbishment projects. Respondents R1, R4, and R6 emphasized materials reuse, highlighting examples such as rubber dust in road pavements, reused AC ducts and sanitary fittings, and steel, aluminium, and bricks. They stressed that reuse saves costs and benefits the environment, making it a practical approach in Sri Lanka. Other participants highlighted different CE aspects: R2 focused on designing out waste and pollution, reusing furniture, and using durable materials; R3 emphasized adapting structures to minimize material use; and R5 emphasized design for disassembly with modular parts to reduce waste. These diverse perspectives show that circular refurbishment depends on multiple factors reuse, adaptability, waste reduction, and disassembly. This diversity indicates the need for flexible, combined CE training models to address various principles suited to each project effectively. Recognizing the diversity among professionals shows that a flexible and combined model of CE training is needed to address several principles that fit each case.

All professionals in this study agreed that CE significantly enhances the sustainability of refurbishment projects. Respondents R2, R3, R5, and R6 emphasized CE's environmental benefits, including reduced use of fresh raw material, lower carbon emissions, and minimized demolition waste. They highlighted the importance of material reuse, repurpose, and life cycle thinking in improving sustainability. For instance, R2 and R3 noted CE's role in reducing embodied carbon and extending building lifespans, while R5 shared that using similar materials in hotel renovations benefited both the environment and the budget. R6 mentioned the use of renewable timber and bamboo supporting green energy.

Respondents R1 and R4 added economic, social, and procedural perspectives. R1 stressed CE's economic value in Sri Lanka, offering sustainable opportunities for young workers. R4 highlighted how well-organized planning and communication, such as use of variation orders, influence material reuse and demolition decisions. Overall, experts agreed on CE's positive sustainability impact but emphasized different aspects including materials, carbon reduction, management, and local relevance.

3.2.2 Theme 2 – Analyse opportunities and issues of implementing a CE in the design stage

The interviewees identify important opportunities, challenge specialists with various problems, and examine how regulations play a role in this area. The study reveals the truth about CE, illustrating how sustainable construction is practiced in real life including its various hurdles and rewards for people working in industry. Six industry experts shared common and distinct views on integrating CE principles in refurbishment design. R2, R3, and R4 emphasized material assessment and reuse, highlighting early project decisions to reduce waste and costs. They noted that involving contractors and clients early supports sustainability efforts. Meanwhile, R1 focused on financial benefits for clients and contractors, linking CE adoption to economic viability. R5 stressed the importance of designing adaptable retail and interior spaces to minimize waste during layout changes. R6 highlighted environmental priorities, advocating Life Cycle Assessment and local sourcing to lower carbon footprints and supporting regional economies. Overall, CE integration in refurbishment design balances economic, environmental, and functional considerations, with material reuse complemented by adaptability and sustainability strategies tailored to project needs.

Interviews revealed several challenges professionals face when applying CE principles in refurbishment projects. Respondents R1, R2, R3, and R6 highlighted a widespread lack of CE knowledge within companies, with both experienced leaders and younger engineers being unfamiliar with, or hesitant to adopt it. R2 noted that contractors and clients often do not understand CE's importance, while R3 pointed to outdated systems and missing guidelines that limit design flexibility. R6 emphasized skill gaps blocking successful implementation. Financial and technical barriers were also significant, as R4 observed clients' reluctance to consider higher upfront costs and Life Cycle Costing. R3 mentioned budget constraints prevent refurbishing many buildings, and R5 noted insufficient documentation complicates reuse. R6 stressed the poor material traceability of material due to regulations and data gaps. Overall, awareness, funding, expertise, and systemic limitations challenge CE adoption in refurbishment projects.

Experts widely agree that regulatory and policy frameworks play a crucial role in supporting or hindering CE adoption in refurbishment design. R1, R3, and R4 emphasized that clear regulations and support from design bodies guide sustainable decisions early in projects. R3 highlighted rules on sustainability and waste reduction, encouraging early CE integration, while R4 noted resources from the UDA promote green practices. R1 urged authorities like CIDA and ICTAD to establish consistent, strict CE policies. Conversely, R2, R5, and R6 felt that current policies are insufficient, citing limited industry awareness and challenges in implementing standards such as BS 8001:2017. They suggested certification programs could help but stressed the need for clearer guidelines, wider dissemination, and stronger enforcement to drive meaningful CE adoption in design processes. Table 2 below shows the expert opinion on policy influences.

Table 2: Summary of Expert responses on policy influence

Respondent	Main Viewpoint	Similar to	Key Comments
R1	Strongly supports regulatory role	R3,R4	Emphasized that professional bodies (CIDA, IESL, IQSSL) must set CE standards, particularly for quality assurance.
R2	Limited awareness, suggests certification	R5,R6	Not very aware of current CE policies; proposed that certifications (like sustainability) could help spread CE adoption.
R3	Favors mandatory CE policies	R1,R4	Stated that clear legislation and sustainability mandates push stakeholders to adopt CE from design stage.
R4	Recognizes UDA's green policy influence	R1,R3	Noted that UDA requires green practices at planning stage, making stakeholders comply early on.
R5	Policies are evolving, but not compulsory	R2,R6	Believes CE regulations in Bahrain are still informal; acknowledged green encouragement but no mandates.
R6	Weak regulatory impact in Sri Lanka	R2,R5	Highlighted limited effect of CE regulations; BS 8001 is rarely used; called for better support and collaboration.

Source: Data: Analysis of the Expert Interviews

3.2.3 Theme 3 – Summarize current knowledge regarding the implementation of CE

Interviews with experts revealed key strengths and challenges of current CE frameworks in refurbishment projects. Most respondents agreed that CE principles promote environmental care and reduce costs by minimizing resource use, waste, and lifecycle expenses. R4 emphasized life-cycle cost analysis, while R6 highlighted benefits such as lower emissions, local job creation, and use of nearby resources. R3 noted CE encourages sustainable design and innovation, and R1 mentioned longer-lasting, repairable products reduce waste. However, a major weakness is limited guidance and awareness. R1, R2, and R6 pointed to inadequate knowledge, weak training, and unclear risk-taking, leading to poor implementation. R5 stressed the difficulties of adding CE features due to a lack of data on older buildings, while R6 noted that the absence of a centralized material database hinders reuse. These findings suggest CE's environmental and economic benefits are clear, but improvements in policy, education, and digital systems are necessary for effective adoption in South Asia's refurbishment sector.

Expert interviews reveal common and differing views on CE adoption in refurbishment projects. Respondents R1, R3, and R6 agree that CE use is limited and not fully established, with client willingness and awareness being key factors. R6 noted ongoing reliance on virgin materials and weak policy enforcement in Sri Lanka. R2 and R4 highlighted cost concerns, lack of knowledge, and adherence to traditional methods as barriers, often prioritizing time and budget over sustainability. R4 recommended better training to overcome reluctance and low oversight. R5 noted faster CE adoption in regions such as Bahrain, driven by lifecycle costing and green supply chains. These findings suggest that targeted efforts, stakeholder collaboration, and institutional support are essential to expand CE implementation in refurbishment design across different contexts. Table 3 below shows the Professionals' views on CE adoption.

Table 3: Professionals' view on CE adoption

Respondent	View on CE Adoption	Key Points	Similar to
R1	Supportive, conditional	Willing clients and consultants essential; CE leads to savings and reduces waste	R3, R6
R2	Skeptical, limited adoption	CE often ignored due to cost and time pressures; reuse happens rarely; more awareness needed	R4
R3	Optimistic, slow progress	Adoption seen in high-profile/government projects; relies on client motivation	R1, R6
R4	Critical, minimal adoption	Few CE projects; traditional mindset; workers not trained for reuse	R2
R5	Positive (International context - Bahrain)	CE adoption growing; lifecycle costing and sustainable procurement practiced	Unique perspective
R6	Partially aligned, systemic gaps	Some progress via case studies; over-reliance on virgin materials; weak enforcement	R1, R3

Interviews revealed key opportunities to strengthen CE frameworks for refurbishment. R1, R2, and R3 emphasized the need to increase awareness among contractors, clients, and designers, noting this as a major barrier to CE adoption. They also suggested creating clear, separate standards to improve implementation. R4 recommended starting projects with surveys to assess recycling potential and apply CE principles early. R5 highlighted improving designers' CE knowledge at the project's outset, while R6 advocated for consistent data, training, stronger regulations, and incentives. They also noted that reusing existing buildings is more challenging than new construction, requiring careful planning. Overall, findings show that alongside awareness and guidelines, effective CE design demands tools, education, and supportive policies for sustainable refurbishment.

Role of Digital Tools in Supporting CE Integration

Interviewees widely recognized BIM as essential for supporting CE in building renovations. Respondents R2, R3, R5, and R6 highlighted BIM's role in material tracking, lifecycle assessment, sustainable design, and collaboration. R2 noted its use for mapping materials and simulating environmental impact, while R5 applied BIM for reuse identification and facility planning. R3 praised its support for digital twins and audits, and R6 emphasized material control and greener choices. However, R1 and R4 had limited BIM knowledge, seeing potential benefits but lacking expertise. This gap may hinder full CE adoption. Overall, BIM is seen as a valuable tool for circular refurbishment, but advanced training is needed for construction professionals to maximize its sustainability potential.

3.3 Questionnaire Survey Respondent's Profile

We conducted a survey to see how well those in the construction industry are familiar with, recognize and make use of CE principles in their work. The survey sought to find what various stakeholders in the construction industry thought about using CE at the design stage by combining the literature review with interviews. Table 4 shows the number of respondents received from the industry professionals through the questionnaire survey.

Table 4: Number of Respondents

Professionals	Number of Participant	
	Percentage	No
Project Manager	8.70%	4
Site Engineer	10.90%	5
Civil/Structural Engineer	8.70%	4
Architect	10.90%	5
Quantity Surveyors	50%	23
Others	10.90%	5

Figure 1 shows that 82.6% of survey participants are early-career professionals with less than five years of experience. Only 14% have 6–10 years, while 2.2% each have 11–15 years and over 15 years of experience. This suggests that the survey results on CE awareness, training, and application in refurbishments may lack input from highly experienced professionals.

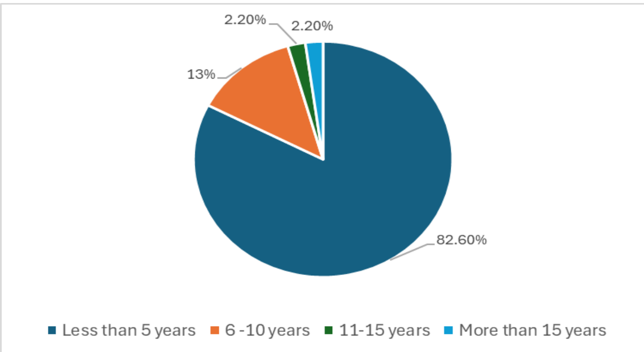

Figure 1: Experience of the Respondent
Source: Data Analysis of the Questionnaire Survey

3.3.1 Awareness and Understanding of CE Principles

Figure 2 shows the level of familiarity with CE concepts in construction.

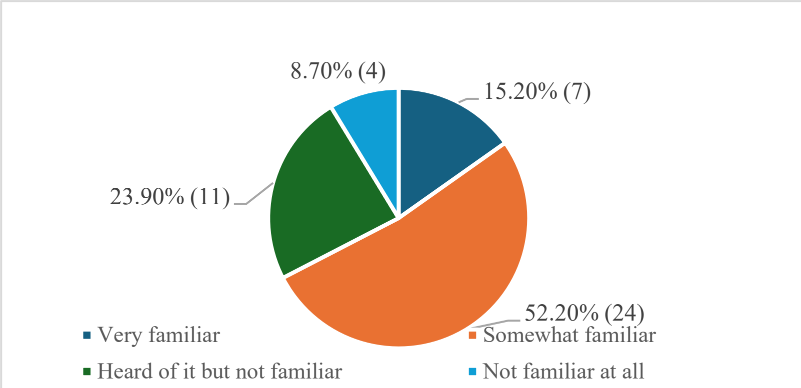

Figure 2: Awareness among Participants

Figure 3 shows the significance of integrating CE principles at the design stage.

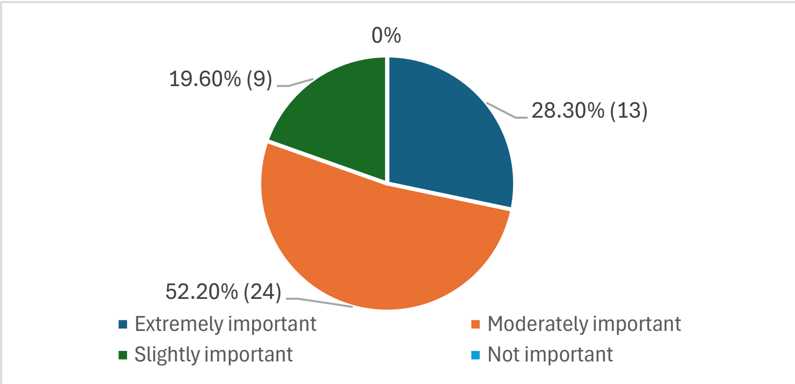

Source: Data Analysis of the Questionnaire Survey

Figure 4 shows the identification of the most relevant CE principles.

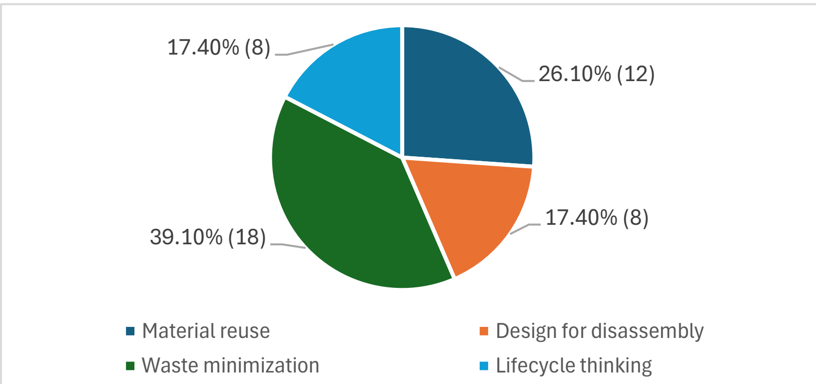

Figure 4: Identification of the most relevant CE principle
Source: Data Analysis of the Questionnaire Survey

Figure 5 shows the current level of CE integration in the design phase.

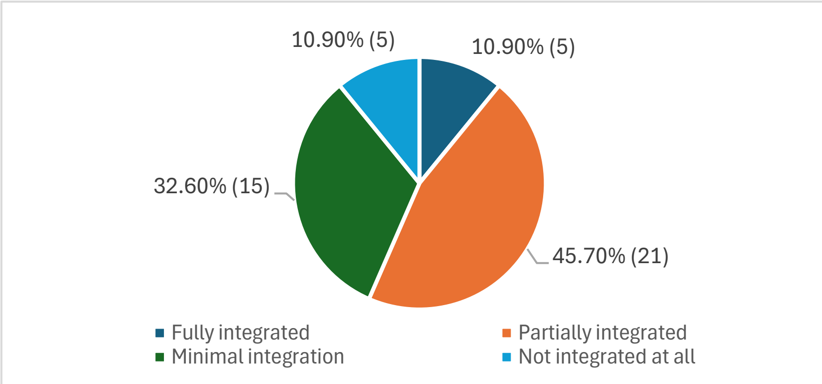

Figure 5: Current level of CE integration in the design phase
Source: Data Analysis of the Questionnaire Survey

Figure 6 shows the frequency with which DfD strategies are considered.

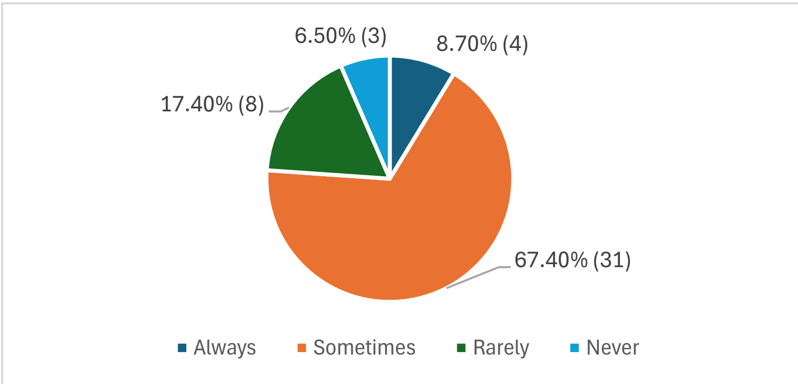

Figure 6: Frequency of considering DfD strategies
Source: Data Analysis of the Questionnaire Survey

Figure 7 shows the key barriers to CE implementation.

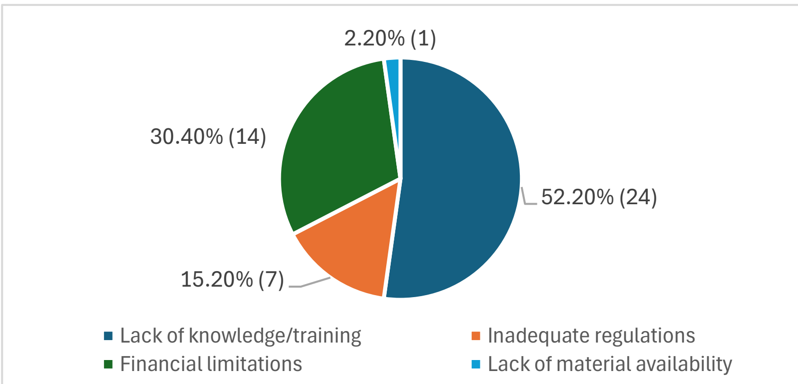

Figure 7: Key barriers to CE implementation
Source: Data Analysis of the Questionnaire Survey

Figure 8 shows the greatest opportunity for CE in design.

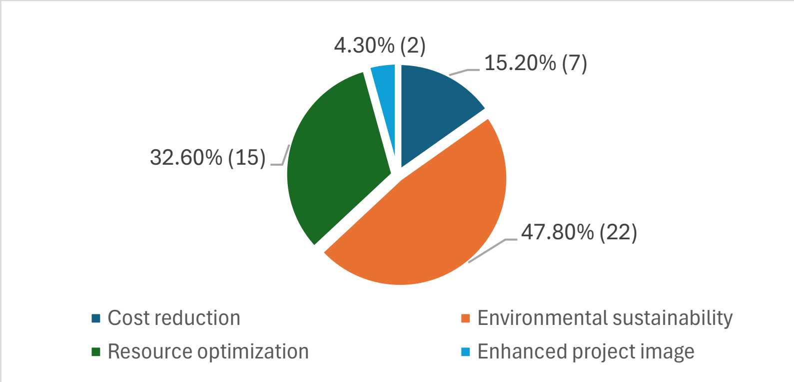

Figure 8: Greatest opportunity for CE in design
Source: Data Analysis of the Questionnaire Survey

Figure 9 shows the impact of the early design stage on the long-term sustainability of refurbishment projects.

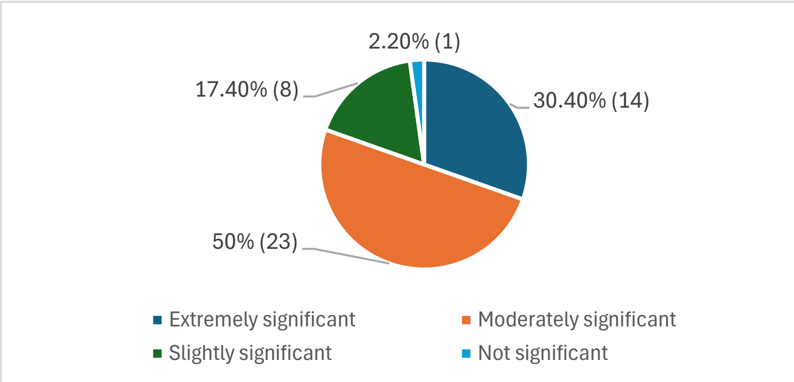

Figure 9: Impact of the early design stage on long - term sustainability
Source: Data Analysis of the Questionnaire Survey

4. CONCLUSION

This research successfully developed a detailed Circular Economy plan specifically for the design stage of refurbishment projects based on the 2D3R rules: Design for Disassembly, Design for Adaptability, Reduce, Reuse and Recycle. It considers using sustainable methods at the start of design, so that materials can be reused and buildings adapted to live longer with less waste. Data obtained through expert interviews and survey responses revealed several key challenges and opportunities. Participants emphasized the critical importance of early-stage integration of CE strategies, including Design for Disassembly, material reuse, and lifecycle-based design approaches. Identified barriers to implementation included low stakeholder awareness, inadequate policy enforcement, limited training opportunities, and underutilization of digital tools such as Building Information Modelling (BIM). To overcome these constraints, respondents recommended targeted awareness-raising initiatives, the development of clear regulatory frameworks, the incorporation of CE practices in the initial stages of design, the advancement of digital competencies, and stronger collaboration among industry stakeholders. The findings underscore that effective CE integration in refurbishment projects, particularly in developing contexts such as Sri Lanka, requires a comprehensive approach involving technological adaptation, stakeholder engagement, and the formulation of context-sensitive regulations. In general, it guides users to include CE in rebuilding designs which supports the move from linear to circular construction. Figure 10 below shows the 2D3R framework.

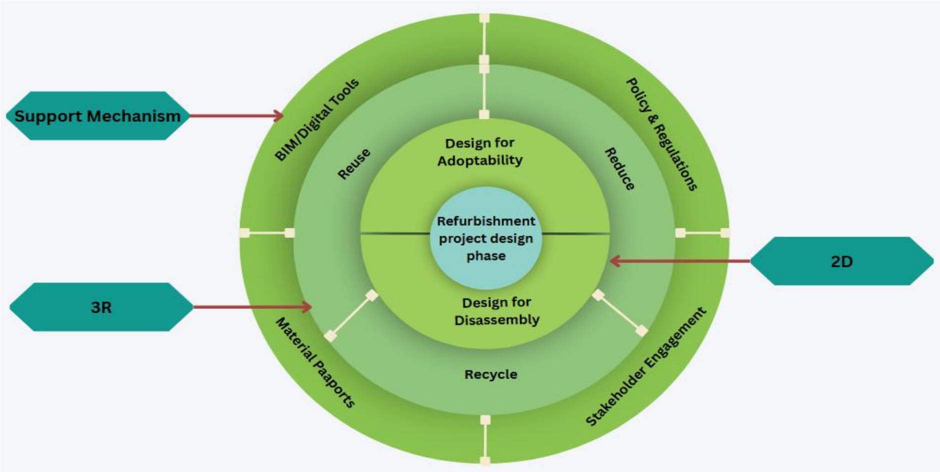

Figure 10: 2D3R Framework
Source: Data Analysis of the Questionnaire Survey

5. ACKNOWLEDGEMENTS

The Authors wish to acknowledge Liverpool John Moores University (LJMU) and Sri Lanka Institute of Information Technology (SLIIT) for the facilitation of this study by providing university resources throughout this research. A sincere thanks to all professionals involved in the interview and questionnaire survey. Their time and knowledge were critical in this study, and we really do appreciate them sharing their experiences.

REFERENCES

AlJaber, A., Alasmari, E., Martinez-Vazquez, P., & Baniotopoulos, C. (2023). Life Cycle Cost in Circular Economy of Buildings by Applying Building Information Modeling (BIM): A State of the Art. *Buildings*, *13*(7). https://doi.org/10.3390/buildings13071858

AlJaber, A., Martinez-Vazquez, P., & Baniotopoulos, C. (2023). Barriers and Enablers to the Adoption of Circular Economy Concept in the Building Sector: A Systematic Literature Review. *Buildings*, *13*(11), 1–21. https://doi.org/10.3390/buildings13112778

Athapaththu, K., Karunasena, G., & Ekanayake, E. M. A. C. (2016). Sustainable Construction practices of Sri Lankan Contractors. *The 5th World Construction Symposium 2016: Greening Environment, Eco Innovations & Entrepreneurship*, *July*, 489–497.

Baarnes, S., & Liang, E. Z. (2025). A Case Study of Sustainable Resource Management Through Reuse of Building Materials. *Lecture Notes in Civil Engineering*, *237*, 941–954. https://doi.org/10.1007/978-3-031-69626-8_79

Bimsara, K. D. M., Abenayake, D. N., Lingasabesan, V., & Shanika, V. G. (2024). *Adopting circular economy practices in major building materials and elements to minimise waste in Sri Lanka*. *August*, 105–118. https://doi.org/10.31705/wcs.2024.9

Bostancı, H. B., Tanyer, A. M., & Habert, G. (2025). REVERT Framework: Stakeholder Perspective to Enable Circular Transformation of Construction Industry. *The 1st International Conference on Net-Zero Built Environment*, *09 January*, pp 1039–1049.

Charef, R., Morel, J. C., & Rakhshan, K. (2021). Barriers to implementing the circular economy in the construction industry: A critical review. *Sustainability (Switzerland)*, *13*(23), 1–18. https://doi.org/10.3390/su132312989

Csete, M. S., & Esses, D. (2022). Usage of Production Function in Linear Economy. *Periodica Polytechnica Transportation Engineering*, *50*(2), 223–226. https://doi.org/10.3311/PPtr.16616

De Silva, S., Samarakoon, S. M. S. M. K., & Haq, M. A. A. (2023a). Use of circular economy practices during the renovation of old buildings in developing countries. *Sustainable Futures*, *6*(October), 100135. https://doi.org/10.1016/j.sftr.2023.100135

Dsilva, J., Zarmukhambetova, S., & Locke, J. (2023). Assessment of building materials in the construction sector: A case study using life cycle assessment approach to achieve the circular economy. *Heliyon*, *9*(10), e20404. https://doi.org/10.1016/j.heliyon.2023.e20404

Ekanayake, B. J., Sandanayake, Y., & Ramachandra, T. (2018). Application of value management to refurbishment projects: A Sri Lankan case study. *Proceeding of the 34th Annual ARCOM Conference, ARCOM 2018*, *September*, 597–606.

Ekins, P., Domenech, T., Drummond, P., Bleischwitz, R., Hughes, N., & Lotti, L. (2019). The Circular Economy: What, Why, How and Where. In *Background paper for an OECD/EC Workshop on 5 July 2019 within the workshop series "Managing environmental and energy transitions for regions and cities*.

Fernandes, J., & Ferrão, P. (2023a). A New Framework for Circular Refurbishment of Buildings to Operationalize Circular Economy Policies. *Environments - MDPI*, *10*(3). https://doi.org/10.3390/environments10030051

Fernandes, J., & Ferrão, P. (2023b). Urban Metabolism-Based Approaches for Promoting Circular Economy in Buildings Refurbishment. *Environments*, *10*(1), 13. https://doi.org/10.3390/environments10010013

Ghisellini, P., Cialani, C., & Ulgiati, S. (2016). A review on circular economy: The expected transition to a balanced interplay of environmental and economic systems. *Journal of Cleaner Production*, *114*, 11–32. https://doi.org/10.1016/j.jclepro.2015.09.007

Leindecker, G., Askar, R., Güngör, B., Blázquez, T., Trubina, N., Gómez-Gil, M., Karanafti, A., Bragança, L., & Wolf, C. De. (2024). Material and Building Passports as Supportive Tools for Enhancing Circularity in Buildings. *Circular Economy Design and Management in the Built Environment*, 507–543. https://doi.org/10.1007/978-3-031-73490-8

Metinal, Y. B., & Gumusburun Ayalp, G. (2025). Uncovering Barriers to Circular Construction: A Global Scientometric Review and Future Research Agenda. *Sustainability (Switzerland)*, *17*(4). https://doi.org/10.3390/su17041381

Milovic, T., Laban, M., Stracev-Curcin, A., & Bulatovic, V. (2024). Circular Economy and Its barriers To Implementation In The Construction Sector. *Applied Engineering Science*, *22*(2).

Osobajo, O. A., Oke, A., Omotayo, T., & Obi, L. I. (2022). A systematic review of circular economy research in the construction industry. *Smart and Sustainable Built Environment*, *11*(1), 39–64. https://doi.org/10.1016/j.heliyon.2022.e09169

Rahla, K. M., Mateus, R., & Bragança, L. (2021). Selection Criteria for Building Materials and Components in Line with the Circular Economy Principles in the Built Environment—A Review of Current Trends. *Infrastructures*, *6*(4). https://doi.org/10.3390/infrastructures6040049

Tambovceva, T., & Titko, J. (2022). Introduction To Circular Economy. In *Ekonomikas un kulturas augstskola*. https://doi.org/10.1142/9789811241949_0002

Weerakoon, P., & Thayaparan, M. (2023). Analysis of Barriers Towards Implementing Circular Economy in Sri Lankan Built Environment. *World Construction Symposium*, *1*(July), 162–173. https://doi.org/10.31705/WCS.2023.14

Wijesinghe, E. D. A. T., Jayawickrama, T. S., Tennakoon, G. A., & Wijewickrama, M. K. C. S. (2024). 5S Principles for Sustainable Resource and Waste Management in Sri Lankan Construction Projects. *World Construction Symposium*, *August*, 1–14. https://doi.org/10.31705/WCS.2024.1

Wijewansha, A. S., Tennakoon, G. A., Waidyasekara, K. G. A. S., & Ekanayake, B. J. (2021). Implementation of circular economy principles during pre-construction stage: the case of Sri Lanka. *Built Environment Project and Asset Management*, *11*(4), 750–766. https://doi.org/10.1108/BEPAM-04-2020-0072

Improving Post-Harvest Rice Drying Efficiency through a Low-Cost Halogen Dryer Design for Rural Communities

Supun Sadeepa and Roshan Thilakarathna*
Department Mechanical and Manufacturing Technology, Faculty of Technology, Wayamba University of Sri Lanka.
fot209185@kul.wyb.ac.lk, roshant@wyb.ac.lk

ABSTRACT

Small-scale rice farmers in Sri Lanka often depend on traditional sun-drying methods, which are inefficient, weather-dependent, and contribute to significant post-harvest losses. This research focuses on the conceptual design and evaluation of a low-cost wet rice dryer using halogen lamps as the heat source, aimed at improving drying efficiency before milling. Field surveys were conducted to identify the common challenges faced by rural farmers, including uneven drying, weather interruptions, and grain rejection by millers due to high moisture content. Based on the survey results, key user requirements were identified, including low operating cost, simple structure, and potential for multi-crop drying. Based on the survey results, key user requirements were identified, including low operating costs, a simple structure, and the potential for multi-crop drying. A conceptual design was developed accordingly, with a drying chamber and tray system optimized for 1 cm thick rice layers. The full assembly was modeled in 3D using CAD software, allowing for virtual evaluation of airflow, heat source positioning, and accessibility.

Finite Element Analysis (FEA) was applied to simulate the mechanical response of the tray under typical loads, confirming its structural soundness. Preliminary thermal experiments were conducted using a controlled test box setup to evaluate the heating performance of a 1000W halogen lamp. The system successfully achieved drying temperatures up to 82°C, which are suitable for surface moisture reduction. Temperature trends were recorded over time, and manual quality checks showed promising results for further development. These findings indicate the technical feasibility of the design and its potential to improve post-harvest efficiency in rural settings. The study provides a foundation for future stages of prototype fabrication, sensor integration, and field validation.

KEYWORDS: *halogen lamp dryer, low-cost design, post-harvest technology, prototype development, rice moisture reduction, small-scale rice processing, wet rice drying*

1 INTRODUCTION

Rice *(Oryza sativa)* plays a vital role in the diets of millions of people worldwide. It is especially important in Sri Lanka as the staple food and a source of livelihood for many farming communities. From cultivation to consumption, rice undergoes several stages of processing, and drying is one of the most critical. Proper drying preserves rice quality, prevents spoilage, and prepares the grain for milling (Thakur *et al*., 2024). However, for many small-scale farmers, especially in rural areas, access to reliable and efficient drying methods remains a challenge.

In Sri Lanka, it is still common to see farmers rely on open sun drying, where rice is spread on the ground in open areas. This method is highly dependent on weather conditions and often results in uneven drying, contamination, and grain loss due to insects, birds, or rainfall. When rice is not dried adequately, it cannot be milled effectively, as high moisture content can lead to mechanical issues in milling machines, such as clogging, blade damage, or system failure. According to Chua *et al*. (2003), many millers refuse to process wet rice, forcing farmers to bear significant post-harvest losses.

Recognizing this problem, this research aims to design and develop a low-cost wet rice dryer that can be fabricated using locally available materials and operated by small-scale farmers. The proposed dryer is intended to reduce moisture content in rice before milling, using a controlled heating system powered by halogen lamps. The project also explores ways to improve drying performance by enhancing airflow and properly insulating the chamber (Wang *et al*., 2025).

By offering a practical and affordable solution, this research seeks to support rural agricultural communities by minimizing grain loss and improving the overall efficiency of the rice milling process. The work combines design, fabrication, and experimental testing to create a prototype dryer that is both accessible and effective.

2 METHODOLOGY

The methodology of this research followed a structured process, beginning with a field survey and data collection from local farmers to identify challenges related to drying wet rice under small-scale conditions (Xangsayasane *et al*., 2019). Based on the insights gathered, design considerations were defined, focusing on energy efficiency, low cost, and user-friendly operation as mentioned (Nath *et al*., 2024). A conceptual layout of the dryer was then developed to guide structural planning and heat source arrangement. This was followed by detailed 3D modelling using CAD software, in which each component, such as the frame, heating unit, and tray system, was designed and assembled digitally for compatibility and precision (Mihret *et al*., 2023). Each design and development stage was aligned with practical constraints and existing literature on small-scale post-harvest technologies.

2.1 Survey and Data Collection

To initiate the research process, a field survey was conducted targeting small-scale rice farmers and local mill operators. A total of eight (08) subjects participated in the survey to gather relevant insights. The below Table 3 shows the sample of the field survey. The primary aim of this research was to understand the practical difficulties faced during the post-harvest phase, particularly in drying of wet rice before milling. Data was collected through informal interviews and direct observations in rural farming areas, where many farmers rely on open sun drying methods, which are weather-dependent and often ineffective (Dissanayaka *et al*., 2020).

Most respondents reported that wet rice often leads to machine damage during milling or to complete rejection by mill owners, resulting in financial loss and waste, as explained in this (Introduction of Rubber Roller Milling Machine for Improving the Domestic Milled Rice Quality, n.d). The survey also revealed that the average daily quantity of rice processed ranges from 40 to 50 kg, but, individual milling instances are typically around 5 kg per batch. This information was critical in determining the design capacity and layout of the proposed drying system. The feedback collected directly shaped the direction of the conceptual and structural design to ensure the final solution would be practical, affordable, and well-suited to the local context.

Table 1: Survey Data Collection Sample

Question point	Description
Subject 01	
1. Rice flour amount per day	20kg - 30kg
2. Price for 1kg of rice flour	80/= - 100/=
3. Method of drying	Dry on a cloth
4. Time for drying the wet rice	30min
5. Challenges faced when drying the wet rice	Weather issues, uneven drying
6. Problems faced while milling wet rice?	Grain breaking, machine clogging
7. How does wet rice threshing affect machine breakdowns during rice threshing?	When milling the wet rice flour
8. If designing a dryer, what features should it include?	Multi-food drying, that is, drying other foods using this dryer.
9. Are you willing to spend money on a dryer?	15000/= - 20000/=
10. How will it affect your business if rice is dried by a machine rather than the rice drying method you are using?	The drying time of wet rice is usually 30 minutes, so its milling efficiency can be increased. If so, this method is a very suitable solution for that.
11. Would you consider using this machine if it could dry other crops or foods other than rice?	That is a good idea for this mechanism.
12. How do you measure the moisture content of the rice you take for drying?	Wet rice is heavier than normal. Also, if you touch wet rice with your hand, the rice will stick to your hand. They use that method to measure moisture.
13. What is the average moisture content of the rice before you dry it?	No
14. Do you monitor the moisture content of the rice after drying it? If yes, how?	Yes, He touched the rice. If you keep the rice in your hand while taking it out of the rice. Then he decides that the rice is dry. Otherwise, the rice is not dry.
15. Who are you primarily producing rice flour for?	For business

2.2 Design consideration and Conceptual design

The wet rice dryer was designed with a focus on efficiency, low cost, and ease of use. Controlled heat sources like halogen lamps were selected to ensure even drying, while a moisture monitoring system is planned to avoid over-drying, as explained in this (Chua *et al*., 2003). Food-grade and durable materials were chosen to improve safety and lifespan (Kim, 2013). The overall structure was kept simple to allow easy maintenance and local fabrication, according to review (Bunyawanichakul, 2006) . The below figures 1(a) and 1(b) illustrate the conceptual design and some main components of the machine, providing a clear understanding of its structure and overall drying process.

2.3 3D model designing

A 3D model of the wet rice dryer was developed to visualize and validate the design before fabrication. Each component, such as the frame, trays, and heating unit, was modelled separately and assembled to ensure proper fit and function. This process helped identify design improvements early, particularly in airflow and heat distribution, according to reviewed this (Bennamoun *et al*., 2003). The final model supports both construction and future optimization.

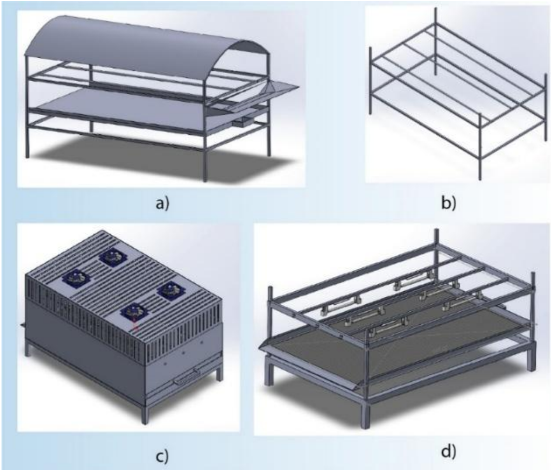

Figure 1.Conceptual sketch and 3D design of the proposed machine.

(a) Conceptual design of the dryer; (b) conceptual design of the halogen light bar; (c) 3D design of the final proposed dryer; (d) base part of the dryer with tray and light bars.

According to Figure 1(a) and (b), all major components of the dryer were designed and assembled. The 3D model of the rice dryer was fully completed, with each part, such as the frame, trays, and lamp holders, designed individually to ensure accuracy and compatibility. Once all components were finalized, they were assembled into a complete model to visualize the overall structure and functionality. The design was refined based on insights gained from earlier experiments, allowing for practical improvements in airflow and lamp positioning. Halogen lamps were selected as the heating source due to their high heat output, fast response, and cost-effectiveness, making them suitable for small-scale drying. A power rating of 1000 W per lamp was chosen to achieve rapid heating to the target temperature range while maintaining efficient energy use.

3 RESULTS & DISCUSSION

3.1 Calculation of design

In this study, BG 352 rice was selected as the preferred variety for rice flour production due to its suitability for industrial milling applications (Pathiraje et al., 2010). When evaluating material properties, two key density values were considered: bulk density and true density. The bulk density of rice typically ranges from 0.77 to 0.87 g/cm³, while the true density, which refers to the mass per unit volume of the rice grain itself (excluding air spaces), ranges from 1.17 to 1.41 g/cm³. In contrast, bulk density accounts for the air gaps between grains when stored or handled in bulk. For design calculations in this research, the bulk density value was selected and converted to 800 kg/m³ to suit volume and mass estimations within the drying chamber.

New Tray Area Calculation

1. Volume Needed

$$V = \frac{5kg}{800kg/\text{m3}} \quad (1)$$

$$= 0.00625\,m3$$

2. Tray Area Calculation (for 1.2 cm layer thickness)

$$A = \frac{V}{Layer\ thickness} \quad (2)$$

$$A = \frac{0.00625\,m3}{0.012}$$

$$= 0.520\,m2$$

Possible Tray Dimensions m^3

- 70 cm × 88 cm (0.7 m × 0.9 m)
- 103.6 cm ×0.593 cm (1.036× 0.593 m)

The selected tray is 104 cm × 595 cm (1.04 mm 0.595 mm)

According to Eqs. (1) and (2) calculation was carried out. Accordingly, the total area is = 0.614 m^2. This area is considered as sufficient for the rice in the tray.

3.2 Survey result

To ensure the proposed dryer meets the real needs of end users, a field survey was carried out among small-scale rice farmers and mill operators. The objective was to gather practical insights on current drying methods, common challenges, and typical processing capacities. The data collected from this survey served as the foundation for shaping the design requirements and functional goals of the dryer.

Based on the field survey findings, several important factors related to small-scale rice drying and milling were identified. The typical drying thickness used by farmers was around 1 cm or less, and the average drying time using traditional sun drying methods was approximately 30 minutes. Respondents reported that the average quantity of rice milled per day was around 50 kg, with an individual consumption of about 5 kg per person per session. Additionally, the average temperature of rice before milling was approximately 30°C. When discussing affordability, the survey indicated that the average acceptable cost for a locally built drying machine was around LKR 27,000, making low-cost solutions like the proposed dryer both feasible and relevant for the target users. According to the survey, Authors were able to record different temperature from dry rice samples and the below figure 2 illustrates the survey results of temperatures for four selected subjects.

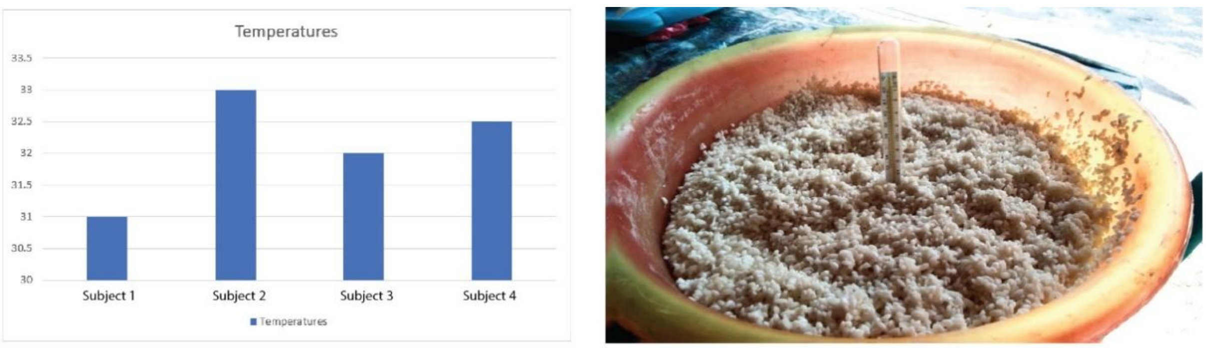

a) b)

Figure 2. Survey results of temperatures for four selected subjects. (a) Different rice sample temperature levels; (b) method of wet rice temperature measurement.

During the survey, temperature data of wet rice samples were collected from four different locations. It was observed that the temperature varied slightly across areas, ranging from 30°C and 33°C. As shown in Figure 2 (b), the recorded temperatures were used to create a graphical representation, which highlights a maximum temperature of **33°C** and a minimum of 31°C. The measurements were taken using a standard thermometer, as illustrated in Figure 2. (b).

3.3 Experiments and testing

The paragraphs below describe the experiments conducted by the authors to evaluate the performance of halogen lamps in achieving the required drying temperature.

Experiment 01

An experimental setup was prepared to evaluate the heating efficiency of the halogen lamps used in the drying system according to below figure 3(a). In the first experiment, a 1000W halogen lamp was tested, and the setup successfully achieved a maximum temperature of 82°C. These initial results demonstrated the lamp's ability to generate sufficient heat within a short period. Based on this outcome, further experiments are planned to optimize the heating conditions and determine the optimal parameters for efficient, uniform rice drying.

Experiment 02

An experimental setup was developed to evaluate the heating efficiency of the halogen lamps used in the dryer design according to Figure 3. (a). In the initial trial, a 1000W halogen lamp was tested, and the system successfully reached a maximum temperature of 80.7°C, indicating strong heat generation potential according to Figure 3. (b). For this experiment, the ambient room temperature was recorded at 32.5°C according to Figure 3. (d). To simulate actual drying conditions, as shown in figure 3(c), a 100g rice sample was prepared by soaking it in water for 40 minutes, after which the excess water was drained before placing the sample into the insulated test chamber. These preliminary results will guide future experiments focused on optimizing lamp performance and determining the optimal conditions for moisture removal during the drying process.

During heating, temperature measurements were taken at regular intervals to monitor the drying performance. The experiment began by placing the prepared rice sample evenly inside an insulated box, maintaining a uniform thickness of 1 cm across the surface according to figure 3(e). A 1000W halogen lamp was then activated as the heat source. The initial temperature of the box was recorded at 32.5°C, and over the course of 5 minutes, as shown in figure 4(b). The temperature gradually increased. By the end of the heating period, the final temperature reached 68.3°C, indicating a significant and consistent rise in thermal energy within the chamber suitable for the rice drying process.

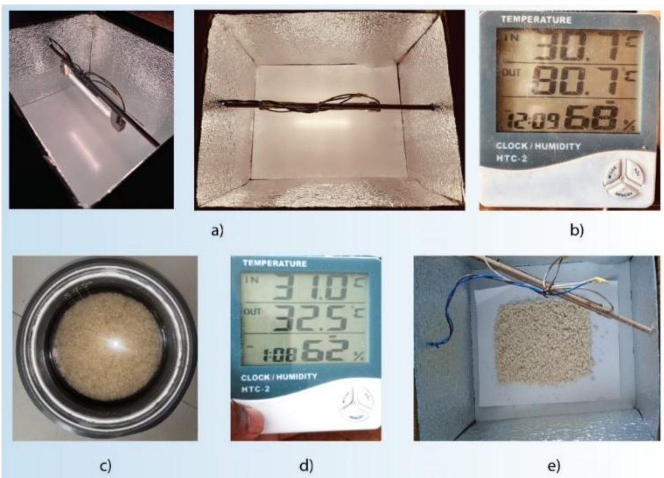

Figure 3. Results of Experiments 1 and 2 (a) Testing the experimental dryer box with different light intensities; (b) experimental box reaching maximum temperature; (c) rice soaking; (d) rice soaking temperature; (e) 1 cm thickness of rice sample during the drying process.

Quality Check

After turning off the halogen lamp, the dried rice sample was manually inspected, as shown in Figure 4. (a) The rice was found to be neither sticky nor wet to the touch, indicating that effective surface drying had been achieved. Based on this manual evaluation, the drying quality was considered satisfactory for the intended application.

Observations & Results

During the experiment, a steady increase in temperature was observed within the first five minutes of operation. The halogen lamp effectively provided sufficient heat for removing surface moisture from the rice sample. No signs of overheating or burning were detected, indicating that the drying process was controlled and safe under the tested conditions.

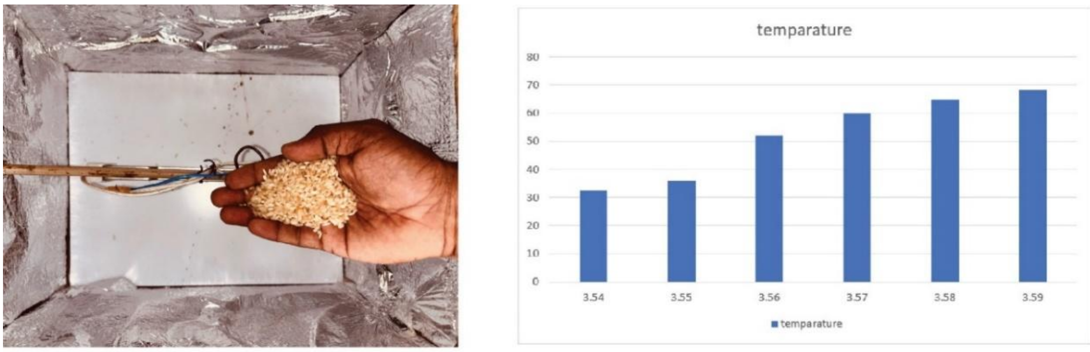

a) b)

Figure 4.Temperature monitoring results. (a) Inspection of the rice sample after the drying process; (b) temperature changes over time.

3.4 Phototype and Testing

In this experiment, the rice sample was soaked as shown in **Error! Reference source not found.**(c). After soaking, the sample was placed in the experimental box at a thickness of 1 cm, as illustrated in **Error! Reference source not found.**. The halogen lamp was then switched on, and the drying process was initiated while monitoring the temperature using a measuring instrument, as shown in Figure 2(b). Temperature and time readings were recorded and presented in Figure 4(b). After 5 minutes of drying, the condition of the rice sample was examined, as depicted in Figure *4*(a).

Phototype Testing 01

This was the first performance test conducted after the prototype was developed. The aim of this first performance test was to evaluate the dryer's ability to reduce the moisture content of soaked rice efficiently while monitoring temperature and moisture trends. A 100 g rice sample was soaked in water for 1 hour, resulting in an initial moisture content of approximately 40%. The sample, with an initial temperature of 29 °C, was evenly spread on the drying tray Figure *5*(e). Halogen lamps served as the heat source, and temperature and moisture content were continuously measured using a thermocouple and moisture sensor connected to an Arduino Nano. Data were logged in real time to Excel for analysis.

The drying process lasted 18 minutes, during which the temperature increased steadily to 60 °C and the moisture content decreased to an expected 14%. Manual quality checks confirmed that the rice was dry and free from surface moisture Figure *5*(b), and the final moisture content was recorded

Figure 5(c). The complete prototype used in this test is shown in Figure 5(d). The graphical data demonstrated a consistent temperature rise accompanied by a corresponding decrease in moisture, confirming the dryer's effective performance.

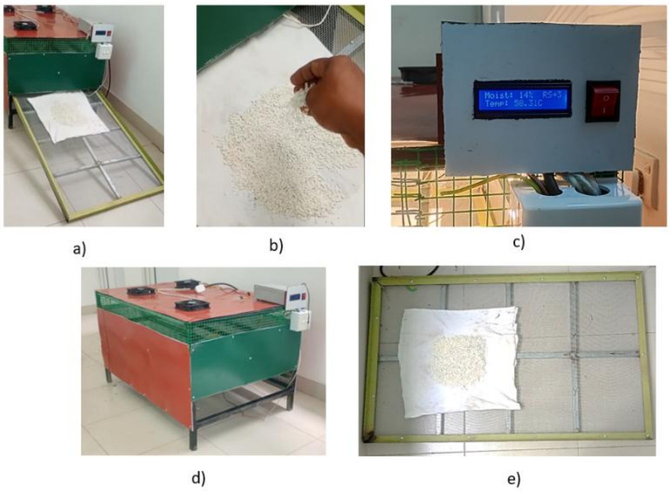

Figure 5.Testing the rice sample on the phototype dryer. *(a) Rice sample on the drying chamber; (b) Quality checking the rice sample;(c) Final moisture content level after drying; (d) Final phototype of dryer; (e) spreading rice sample on dryer*

Phototype Testing 02

Following the initial prototype evaluation, a second performance test was carried out to assess the dryer's operation under full-load conditions. In this test, a 5 kg rice sample was soaked in water for 2 hours **Error! Reference source not found.**(d). After soaking, the water was drained, and the rice was evenly distributed on the drying tray **Error! Reference source not found.**(c). The initial temperature and moisture content were recorded as 29 °C and 42%, respectively. The drying process was initiated using four halogen lamps as the heat source. Temperature and moisture content were continuously monitored using a thermocouple and a moisture sensor connected to the Arduino Nano, with real-time data logging to Excel. The process continued until the moisture content reached the target range of 14%.

The total drying time recorded was 42 minutes, during which the temperature rose steadily while the moisture content decreased, as shown in ***Error! Reference source not found.***(b). A manual quality check was conducted at the end of the process, **Error! Reference source not found.**(a), confirming that the rice was dry, non-sticky, and suitable for milling. This test demonstrated that the dryer maintained effective performance and drying uniformity even under maximum load conditions.

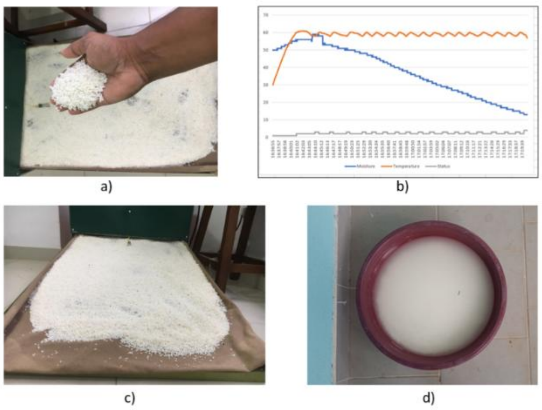

Figure 6: Testing the rice sample of maximum capacity (a) checking the drying quality of rice sample; (b) Temperature vs moisture content graph; (c) Place the rice on drying tray; (d) soaking rice sample

3.5 Simulation of Drying Tray

To ensure the structural integrity of the drying tray, a simulation was carried out using SolidWorks simulation tools. The tray was modelled using steel material, with a 50 N force applied to simulate the load during drying, and fixed supports at the rail positions to reflect actual mounting conditions. As illustrated in Figure 7(a), the setup accurately represented the tray's behavior under stress. The simulation yielded a maximum stress of 98,530 N/m², well below the steel's yield strength, confirming the structural safety of the design. The maximum displacement observed was 0.275 mm, and the strain was minimal. The detailed results are shown in the displacement diagram Figure 7(b), strain distribution diagram Figure 7(c), and stress diagram Figure 7(d). These results confirm that the tray design is both stable and mechanically suitable for use in the drying system.

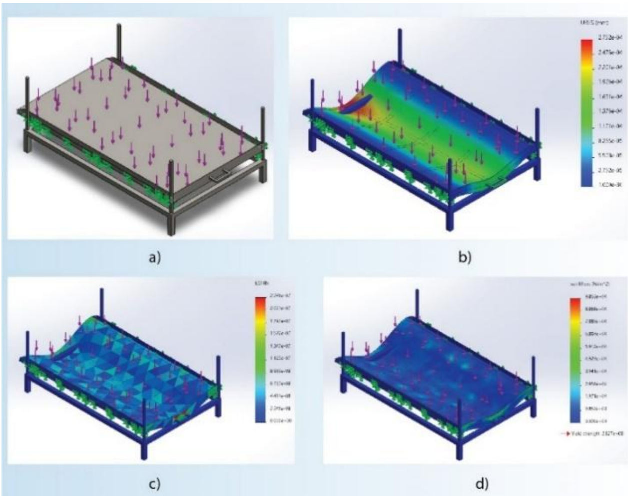

Figure 7. Finite Element Analysis (FEA) of the dryer tray. (a) Force distribution on the tray; (b) displacement results; (c) strain results; (d) stress results.

4 CONCLUSION & FUTURE WORK

This study presented the design and development of a cost-effective wet rice dryer to address the practical issues faced by small-scale rice processors. The system was designed with simplicity, affordability, and functionality in mind. It uses halogen lamps as the heat source and features a manually accessible tray system for ease of use. Field surveys confirmed the need for such a device, especially in rural areas where weather-dependent drying methods often lead to grain loss and reduced milling efficiency.

Initial experiments showed that the prototype could reach the required drying temperatures in a short time, and the drying quality met acceptable standards during manual evaluation. Based on these outcomes, further enhancements are planned, including optimizing drying efficiency and increasing drying capacity to meet larger processing demands. Additionally, the current quality assessment method after drying relies on manual evaluation; future work will focus on developing an objective, measurable quality detection system. Other improvements will include adding controlled airflow using exhaust fans and integrating moisture sensors to automate the drying process more precisely. Additional testing with larger samples will also be carried out to evaluate performance and long-term reliability. Overall, this system shows promise as a practical and affordable solution for improving post-harvest rice handling at the small-scale level.

5 ACKNOWLEDGEMENTS

The authors gratefully acknowledge the support of all lecturers and laboratory technicians of the Department of Mechanical and Manufacturing Technology, Faculty of Technology, Wayamba University of Sri Lanka, in completing this work. Furthermore, the authors express their sincere gratitude to the editors and anonymous reviewers for their insightful suggestions and constructive comments, which have greatly improved the quality of this research paper.

REFERENCES

Bennamoun, L., & Belhamri, A. (2003). Design and simulation of a solar dryer for agriculture products. *Journal of Food Engineering*, *59*(2–3), 259–266. doi: 10.1016/S0260-8774(02)00466-1

Bunyawanichakul, P. (2006). *DEVELOPMENT OF A CYCLONE RICE DRYER*.

Chua, K. J., & Chou, S. K. (2003). Low-cost drying methods for developing countries. In Trends in Food Science and Technology (Vol. 14, Issue 12, pp. 519–528). Elsevier Ltd. doi: 10.1016/j.tifs.2003.07.003

Dissanayaka, D. M. S. K., & Wijayaratne, L. K. W. (2020). Common Agricultural Practices and Post-Harvest Losses in Trincomalee, Sri Lanka. In Journal of Tropical Forestry and Environment (Vol. 10, Issue 02).

Introduction of Rubber Roller Milling Machine for Improving the Domestic Milled Rice Quality. (n.d.). Retrieved from https://www.researchgate.net/publication/380929315

Kim, M. H. (2013). Review on Rice Flour Manufacturing and Utilization. *Journal of Biosystems Engineering*, *38*(2), 103–112. doi: 10.5307/jbe.2013.38.2.103

Mihret, Y. C., Delele, M. A., & Hailemesikel, S. T. (2023). Design, development, and testing of rice-husk fueled mixed-flow rice dryer for small-scale rice producer farmers. *Heliyon*, *9*(7). doi: 10.1016/j.heliyon.2023.e18077

Nath, B., Chen, G., O'Sullivan, C. M., & Zare, D. (2024). Research and Technologies to Reduce Grain Postharvest Losses: A Review. In Foods (Vol. 13, Issue 12). Multidisciplinary Digital Publishing Institute (MDPI). doi: 10.3390/foods13121875

Pathiraje, P. M. H. D., Madhujith, W. M. T., Chandrasekara, A., & Nissanka, S. P. (2010). The Effect of Rice Variety and Parboiling on in vivo Glycemic Response. In Tropical Agricultural Research (Vol. 22, Issue 1).

Thakur, A., Singh, A., & Bharat, N. K. (2024). Conservation and development of rice germplasm for natural farming. In Climate-Smart Rice Breeding (pp. 45–61). Springer Nature. doi: 10.1007/978-981-97-7098-4_3

Wang, Y. J., Li, Y. F., Pan, S., Qin, M. Y., Yuan, Y. D., Yuan, W. J., & Li, C. (2025). Rice drying quality using gas-catalytic infrared equipment: an experimental study. *IOP Conference Series: Earth and Environmental Science*, *1500*(1), 012047. doi: 10.1088/1755-1315/1500/1/012047

Xangsayasane, P., Vongxayya, K., Phongchanmisai, S., Mitchell, J., & Fukai, S. (2019). Rice milling quality as affected by drying method and harvesting time during ripening in wet and dry seasons. *Plant Production Science*, *22*(1), 98–106. doi: 10.1080/1343943X.2018.1544463

Analysis and optimization of OLSR and AODV routing protocols for highly mobile autonomous aerial vehicle networks: experimental performance evaluation in various application scenarios

Nguyen Duc Tu, Luybov Gorbacheva, Ammar Muthanna
The Bonch-Bruevich Saint-Petersburg State University of Telecommunications, St. Petersburg, 193232, Russian Federation

ABSTRACT

Driven by the rapid evolution of Autonomous Aerial Vehicle (AAV) technology, ad-hoc AAV networks are becoming increasingly significant in diverse domains such as telecommunications, security surveillance, search-and-rescue operations, emergency management, precision agriculture, and cargo transportation. Owing to their flexible deployment and tight coordination capabilities, AAVs enable real-time data exchange, unlocking considerable potential for tasks that demand high accuracy and swift response. Nevertheless, their three-dimensional mobility and continuously changing topology impose substantial challenges on the design of suitable routing solutions, because conventional protocols originally developed for Mobile Ad-hoc Networks (MANETs) are seldom optimized for aerial characteristics. This discrepancy underscores the necessity for a comprehensive analysis and optimal configuration that satisfy the stringent requirements of low latency, high throughput, and reliability in mission-critical AAV applications. Against this backdrop, the present study focuses on the analysis and modelling of two widely adopted routing protocols—Optimized Link State Routing (OLSR) and Ad hoc On-Demand Distance Vector (AODV)—in various deployment contexts of ad-hoc AAV networks. By evaluating the performance of these protocols, we identify their advantages, limitations, and possible enhancement directions, and subsequently propose configuration guidelines that deliver improved link quality.

1 INTRODUCTION

Against the backdrop of swift advances in telecommunication technologies, AAVs are attracting growing research attention and seeing ever-wider practical adoption. Unlike traditional communication approaches that rely on terrestrial infrastructure, AAVs extend network coverage into the airspace, enabling optimized service areas, reduced deployment costs, and flexible adaptation to contemporary connectivity demands. Establishing telecommunications infrastructure based on AAVs, however, poses several challenges, most notably in routing capability, real-time data exchange, and Quality-of-Service (QoS) assurance. This section analyses the broader context and importance of AAVs with a particular emphasis on telecommunications, while also identifying design obstacles that are specific to AAV networks.

Context and significance of Autonomous Aerial Vehicles

Leveraging breakthroughs in electronics, wireless communication, artificial intelligence (AI), and battery technology, AAVs are recognized as a crucial platform for next-generation telecommunications infrastructure. Moreover, the convergence of Edge-Computing solutions [1], 5G-to-6G technologies, and the Internet-of-Things (IoT) trend empowers AAVs not only to collect information but also to process, relay, and even provide connectivity services to external entities [2].

At present, Autonomous Aerial Vehicles (AAVs) are being integrated into numerous practical telecommunication scenarios, including but not limited to the following:

- Temporary mobile broadcasting nodes—During mass gatherings or in disaster-stricken areas, AAVs equipped with on-board gNodeB (5G) or eNodeB (4G) units can promptly augment network capacity and temporarily extend coverage without the costly construction of cumbersome terrestrial infrastructure [2].
- Last-mile connectivity solutions—In mountainous terrain or regions with under-developed infrastructure, AAVs operate as relay entities between end-user equipment and ground base stations, thereby markedly enhancing link quality and service continuity.

- Monitoring and data acquisition—Owing to their agile maneuverability, AAVs can continuously refresh imagery, video streams, or environmental information and forward these data sets to a processing center, supporting urban management, precision agriculture, and climate-change surveillance [3].

The harmonious convergence of AAV platforms with cutting-edge telecommunication technologies has accelerated the digitalization of diverse socioeconomic activities, yielding improved operational efficiency, cost reduction, and the emergence of novel business models.

In the context of burgeoning applications such as telepresence, virtual reality (VR), smart healthcare, and 5G/6G services, AAVs have further substantiated their role as a flexible, cost-effective, and high-performance solution for monitoring and emergency support [4]. By virtue of sustained radio transmission, real-time data processing, and high mobility, AAVs can rapidly establish communication bridges in regions where the existing infrastructure is impaired or inaccessible. Consequently, rescue teams and command centers can exchange information, high-definition live video, and geospatial data to track evolving situations, localize victims, and implement timely interventions. In telemedicine applications, for instance, AAVs not only facilitate the transport of critical medical data and enable live consultations but also deliver equipment or biological specimens to isolated areas, thereby shortening response times and elevating treatment efficacy. Moreover, the deployment of AAVs obviates the need for extensive terrestrial infrastructure—such as fixed towers or fiber-optic backhaul—conserving financial resources, manpower, and deployment time when compared with conventional solutions. Hence, AAVs constitute a pivotal element within the intelligent-telecommunications ecosystem, underpinning emergency monitoring, enlarging coverage areas, and providing a platform for advanced services—including telepresence, VR, and smart healthcare—in scenarios that demand immediacy and stringent reliability.

Communication and Routing Challenges in AAV-Centric Networking Environments Despite their disruptive potential, AAV systems confront an array of technical hurdles, particularly as requirements for bandwidth, latency, and reliability continue to escalate. These obstacles become increasingly pronounced when AAVs operate in three-dimensional space, exhibit constant mobility, and must uphold stable connectivity.

- Highly dynamic topology in three-dimensional space—Because AAVs move at high velocity while continually changing altitude, radio links are inherently unstable. Conventional MANET-oriented routing protocols struggle to react in a timely manner to sudden link disruptions, necessitating either the fine-tuning of existing algorithms or the development of novel routing schemes that can adapt swiftly to topological perturbations.
- Energy and radio-resource constraints—Beyond sustaining flight, an AAV must uphold uninterrupted data exchange over radio channels characterized by finite capacity. To maximize mission endurance, the system must balance transmission efficiency against power consumption, a trade-off rendered more acute by high-bit-rate requirements such as HD video or real-time services.
- Channel interference and attenuation—Operating at altitude and in open space exposes AAVs to numerous external influences (weather, terrain, obstacles, signal reflections, etc.). The resulting channel instability calls for highly adaptive mechanisms in power control, modulation–coding selection, and routing strategy. Without optimization, fading and interference severely degrade link maintenance capabilities, culminating in elevated packet-loss ratios.
- QoS, low-latency, and security requirements—Many AAV applications, notably in monitoring and emergency support, demand data transmission with exceptional reliability and ultra-low latency. Routing protocols that are not tailored to meet these criteria may incur congestion, violate delay thresholds, or introduce security vulnerabilities.

Against this backdrop, the investigation and assessment of routing protocols for AAV networks are essential for identifying solutions that satisfy responsiveness, connectivity, and resource-efficiency objectives. In this article, we model and analyze two protocols—OLSR and AODV—under varying operational conditions, including AAV velocity, mobility model, fleet size, and mission-area dimension. By measuring throughput, latency, packet-loss ratio, and energy expenditure, we delineate each protocol's merits and limitations and propose configuration-optimization guidelines. The resulting insights facilitate the selection of an appropriate routing paradigm capable of achieving stringent QoS, reliability, and flexibility targets in modern AAV networking environments.

I. Classification of Routing Protocols in Autonomous Aerial Vehicle Networks

In recent years Autonomous Aerial Vehicle (AAV) networks have attracted growing attention, largely because three-dimensional operational space and high vehicle velocities make sustaining a stable communication channel particularly challenging. To address this issue numerous routing strategies have been proposed, all geared toward the agile maintenance and timely update of link information. In general, routing protocols for AAV networks can be grouped into five major families: proactive [5], reactive [6], hybrid [7], geographic [8], and swarm-intelligence/reinforcement-learning-based [9].

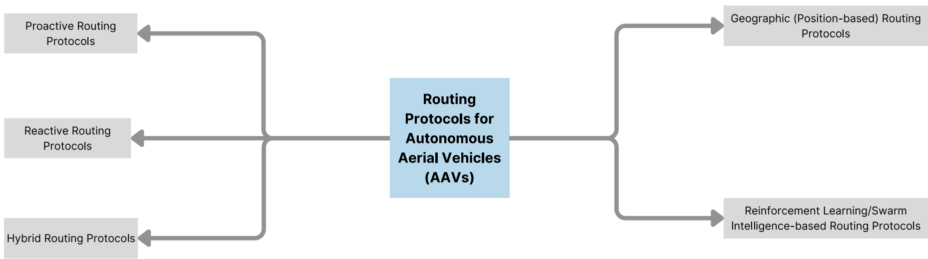

Fig. 1. Classification of routing protocols for Autonomous Aerial Vehicle networks.

1.1 Proactive Routing Protocols

Proactive schemes continuously maintain up-to-date routes to every node by periodically refreshing link-state information or routing tables. Because destination entries already reside in memory, route-establishment latency at data-transmission onset is minimized. Within fast-moving AAV networks these protocols are often favored for their ability to react promptly to incremental topological variations while supplying a global view that simplifies management and monitoring. Nevertheless, when AAVs maneuver incessantly and topology fluctuates rapidly, proactive solutions can consume substantial bandwidth and energy to keep routes current, a drawback that becomes pronounced as network scale increases. Representative examples include OLSR (Optimized Link State Routing), which employs a Multi-Point Relay (MPR) mechanism to curtail broadcast traffic, and DSDV (Destination-Sequenced Distance Vector), which couples classic distance-vector rules with sequence numbers to preserve routing consistency [5], [10].

1.2 Reactive Routing Protocols

In contrast, reactive schemes discover routes only when a data session is initiated, thereby reducing control overhead because topology information is not perpetually maintained. For AAV networks exhibiting bursty traffic or idle periods, this on-demand paradigm affords greater flexibility and conserves both bandwidth and energy. A notable drawback, however, is that initial route discovery can incur additional delay when packets must be dispatched suddenly. Furthermore, at very high AAV speeds the discovery process may be invoked repeatedly, causing network congestion or repeated re-establishment cycles. Widely used reactive protocols include AODV (Ad hoc On-Demand Distance Vector), which leverages sequence numbers to avoid loops, and DSR (Dynamic Source Routing), which relies on a route cache at the source node to reuse previously learned paths [6], [11].

1.3 Hybrid Routing Protocols

To combine the strengths of proactive and reactive approaches, hybrid protocols partition the network into zones or clusters. Within each zone the protocol behaves proactively for immediate responsiveness; between zones it adopts a reactive method to limit unnecessary large-scale broadcasts. For AAV networks this dual strategy mitigates routing-table exchange overhead while retaining prompt local reaction. Nevertheless, maintaining zone boundaries and managing clusters becomes complex when AAVs move continuously or as network size expands. A canonical example is the Zone Routing Protocol (ZRP), originally investigated for MANETs and later proposed for AAV scenarios [12].

1.4 Geographic Routing Protocols

Advances in positioning technologies such as GPS and high-precision inertial sensors have made location-based routing a promising solution for AAV systems. Instead of storing exhaustive link-state data, nodes keep only their current coordinates and those of the destination, forwarding packets via a greedy strategy. This method sharply lowers routing-table maintenance cost, as each node requires knowledge of only its immediate neighborhood rather than an entire multi-hop path. Geographic protocols still face challenges when position information is inaccurate or when voids arise in the three-dimensional space that hinder signal reachability. GPSR (Greedy Perimeter Stateless Routing) is a renowned member of this family, blending greedy forwarding with perimeter traversal to circumvent voids and adapt to diverse AAV scenarios [13], [14].

1.5 Swarm-Intelligence/Reinforcement-Learning-Based Routing

Beyond conventional designs, the application of swarm intelligence (SI) and reinforcement learning (RL) opens new avenues in AAV routing. Rather than relying solely on static routing tables, AAV nodes can learn mobility patterns and channel conditions, autonomously refining forwarding decisions over time. Inspired by the evolutionary behavior of insects or bird swarms, SI/RL schemes allow AAV networks to adapt gracefully to abrupt topological changes and channel dynamics. Yet computational complexity and the need to synchronize learned information across nodes can impose significant overhead—especially in resource-constrained environments. Ant Colony Optimization (ACO) and bee-inspired protocols use virtual pheromones to guide packet delivery, whereas Q-learning applies reward–penalty mechanisms to optimize objectives such as throughput or latency.

2 OPERATIONAL PRINCIPLES OF THE OLSR PROTOCOL

The Optimized Link State Routing (OLSR) protocol is grounded in the classical link-state paradigm but achieves greater efficiency through its Multipoint Relay (MPR) mechanism. Every node periodically exchanges link-state and routing information with its neighbors, thereby building a global routing table without waiting for a data-forwarding request. This proactive behavior enables swift packet delivery both in conventional ad-hoc networks and—more critically—in Autonomous Aerial Vehicle (AAV) environments. The key innovation lies in OLSR's selective use of MPRs: each node chooses a minimal subset of neighbors as relays such that every node in the network is reachable through at least one MPR, thus eliminating redundant broadcast transmissions. MPR selection is driven by link-quality and coverage criteria that markedly reduce control-traffic overhead.

OLSR defines three core control messages. HELLO packets discover and refresh neighbor relations; TC (Topology Control) packets advertise selected MPR links; and MID (Multiple Interface Declaration) packets list additional addresses when a node owns multiple interfaces. Parameters such as HELLO_INTERVAL and TC_INTERVAL specify the periodicity of HELLO and TC messages and hence directly influence link-state freshness versus bandwidth consumption. The WILLINGNESS parameter quantifies a node's readiness to forward traffic and thereby shapes MPR selection and the resulting global topology. For highly dynamic AAV applications, careful tuning of these parameters' balances control-update granularity against spectral efficiency. Numerous OLSR enhancements tailored to AAVs have been proposed, concentrating on adaptive MPR selection as node density or velocity grows and on dynamic adjustment of HELLO/TC rates to accommodate three-dimensional mobility while meeting stringent reliability and throughput demands. These efforts collectively aim to minimize delay and energy cost while preserving adaptability under incessant topology changes.

3 OPERATIONAL PRINCIPLES OF THE AODV

Protocol Ad hoc On-Demand Distance Vector (AODV) routing emphasizes bandwidth and resource conservation in highly mobile scenarios through its reactive (on-demand) philosophy. When a source must transmit but lacks a route, it broadcasts a Route Request (RREQ); any intermediate node possessing a fresh route may respond with a Route Reply (RREP). To preclude loops and guarantee route freshness, AODV incorporates monotonically increasing sequence numbers. Route maintenance is likewise meticulous: upon detecting a link break, the responsible node issues a Route Error (RERR) to affected sources, prompting them to invalidate the stale path. Frequently, AODV invokes local repair to re-establish connectivity near the failure point, thereby curtailing delay relative to network-wide RREQ re-broadcast. Parameters such as ACTIVE_ROUTE_TIMEOUT and ALLOWED_HELLO_LOSS govern route-lifetime thresholds and tolerated HELLO losses, allowing AODV to adapt to frequent AAV maneuvers and tight throughput/latency budgets. Owing to these design choices, AODV remains a viable option for many AAV missions in which routing performance is pivotal to overall system reliability.

II. **Performance Evaluation Parameters**

To evaluate the performance of OLSR and AODV routing protocols in Autonomous Aerial Vehicle networks, this study uses the following key evaluation parameters:

1. Packet Delivery Ratio (PDR).

PDR quantifies reliability as the fraction of packets that reach their destinations:

$$\mathrm{PDR}_{\mathrm{avg}} = \frac{1}{n}\sum_{i=1}^{n}\frac{\left|P_{\mathrm{recv}}^{i}\right|}{\left|P_{\mathrm{sent}}^{i}\right|}\times 100\%$$

Where:

- n is the number of traffic sessions,
- $|P_{\mathrm{sent}}^{i}|$ is the number of packets issued in session i,
- $|P_{\mathrm{recv}}^{i}|$ is the number successfully received.

PDR reflects the level of reliability and efficiency of the routing protocol in ensuring packet transmission from source to destination. The higher the PDR value, the better the protocol performance. In the AAV network environment, PDR is a critical parameter when evaluating routing protocol performance due to high mobility and rapid topology changes that increase the probability of packet loss.

2. End-to-End Delay (EED).

EED measures temporal efficiency:

$$\mathrm{EED}_{\mathrm{avg}} = \frac{\sum_{p\in P_{\mathrm{recv}}}\left(T_{\mathrm{arr}}(p) - T_{\mathrm{dep}}(p)\right)}{|P_{\mathrm{recv}}|},$$

Where:

- P_{recv} is the set of received packets,
- $T_{\mathrm{dep}}(p)$ the departure time,
- $T_{\mathrm{arr}}(p)$ the arrival time of packet p.

These metric aggregates routing, queuing, MAC, and transmission delays.

3. Average Throughput.

Throughput reflects data-transfer capacity:

$$\mathrm{Throughput}_{\mathrm{avg}} = \frac{\sum_{i=1}^{n}|P_{\mathrm{recv}}^{i}|S}{T}\cdot\frac{8}{1000}\ \text{(kbit/s)},$$

Where:

- S the packet size (bytes),
- T the active transmission duration (s).

Jitter (Delay Variation). Jitter captures fluctuation in inter-packet delay and is recursively estimated per RFC 3550:

$$J_i = J_{i-1} + \frac{|D_i - D_{i-1}| - J_{i-1}}{16},$$

Where: D_i and D_{i-1} are successive packet delays and the $1/16$ factor smooths short-term variations.

Collectively, these metrics enable a comprehensive appraisal of routing-protocol effectiveness for AAV networks, balancing reliability, responsiveness, bandwidth utilization, and temporal stability.

III. **Performance Evaluation of Routing Protocols for Autonomous Aerial Vehicle Networks**

The performance of Autonomous Aerial Vehicle networks is determined by factors such as routing protocol, movement speed, node density, and movement model. In this study, we evaluate two popular routing protocols (OLSR and AODV) in various scenarios to find the optimal solution for the operation of Autonomous Aerial Vehicle networks.

We use the Network Simulator 3 (NS-3.34) to simulate the operation of Autonomous Aerial Vehicle networks in four different scenarios: analysis by number of nodes, analysis by movement speed, analysis by movement model, and analysis by coverage area.

Table 1 General simulation parameters

Parameter	**Value**	**Parameter**	**Value**
Wi-Fi standard	IEEE 802.11g	CCA threshold	–90 dBm
PHY mode	ErpOfdm	Packet size	512 bytes
Data rate	6 Mbit s^{-1}	Application rate	128 kbit s^{-1}
Tx power	18 dBm	Propagation model	LogDistance (exponent = 2.0)
Receiver sensitivity	–85 dBm	Simulation time	200 s

In these simulations, we use the LogDistance attenuation model with parameter Exponent=2.0 to model signal attenuation in the radio transmission environment of Autonomous Aerial Vehicle networks. The value Exponent=2.0 corresponds to the Free Space Path Loss attenuation model, which is suitable for radio wave propagation conditions of aerial base stations in open space, where there are few obstacles and complex reflection and refraction phenomena. The LogDistance model is a common channel attenuation model based on experimental observation that signal intensity decreases as a logarithmic function of distance, calculated using the formula:

$$PL(d) = PL(d_0) + 10 \times n \times \log_{10}\left(\frac{d}{d_0}\right)$$

Where:

$PL(d)$ - signal attenuation (path loss) at distance d,
$PL(d_0)$ - signal attenuation at reference distance d_0,
n - attenuation exponent, in our simulation taken as 2.0,
d - distance between transmitter and receiver.

2. Performance Analysis Based on Number of Nodes

In this simulation, we analyze the performance of OLSR and AODV protocols when changing the number of Autonomous Aerial Vehicle nodes from 5 to 60. The movement model used is GaussMarkov with a speed of 10 m/s.

Table 2. Simulation Parameters Based on Number of Nodes

Parameter	Value
Number of Nodes	5–60
Speed	10 m/s
Mobility model	GaussMarkov
Flight Area	800 m × 800 m × 100 m

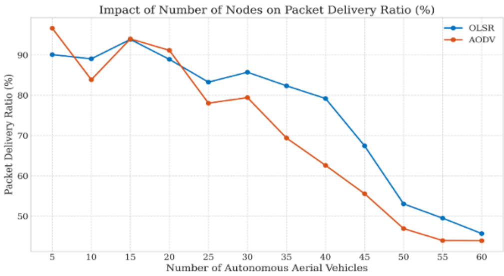

Fig. 2. Impact of Number of Nodes on Packet Delivery Ratio

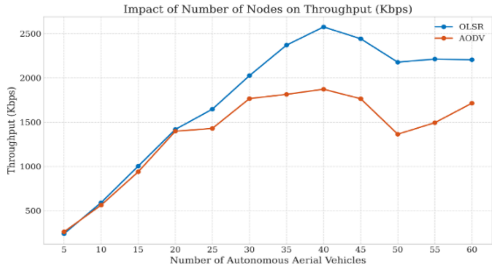

Fig. 3. Impact of Number of Nodes on Throughput

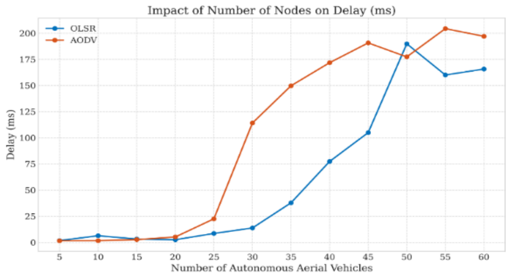

Fig. 4. Impact of Number of Nodes on Delay

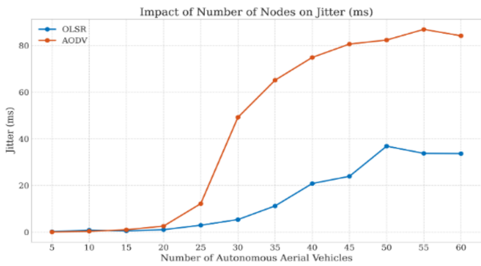

Fig. 5. Impact of Number of Nodes on Jitter

Initially, we compared the performance of protocols for Autonomous Aerial Vehicle networks, AODV and OLSR, in terms of Packet Delivery Ratio (PDR) to determine the appropriate choice for reconnaissance scenarios. In the Autonomous Aerial Vehicle network model, node density is typically sparse, which complicates maintaining connections between nodes. Therefore, we evaluated the performance of AODV and OLSR by gradually increasing the number of nodes during the simulation, thereby determining the impact of node density on network performance.

Fig. 2 illustrates the PDR for each protocol, where the horizontal axis represents the number of nodes, and the vertical axis represents the PDR. The results show that at low node density, AODV achieves a higher packet delivery ratio. In a reconnaissance scenario, the network topology changes rapidly and frequently, allowing AODV (a reactive protocol) to optimize route discovery, when necessary, thereby maintaining a relatively good PDR at small scales. In contrast, OLSR stores a routing table for all nodes, resulting in higher costs to maintain the routing table, reducing PDR in an environment with a small number of nodes.

We also tested the hypothesis that the PDR of Autonomous Aerial Vehicle network protocols would increase with the growth in the number of nodes. In practice, both AODV and OLSR show an increase in PDR up to a certain maximum, followed by a decline. For example, AODV reaches a PDR of about 94% with 15 nodes, after which a decrease is observed; similarly, OLSR reaches 93.87% also with 15 nodes and decreases starting from 20 nodes. This indicates that the optimal node density for both protocols in our simulation environment is around 15 nodes. Regarding throughput, both AODV and OLSR tend to increase with the number of nodes up to a certain threshold before declining. OLSR reaches a peak throughput of about 2575.86 Kbps with 40 nodes, while AODV reaches approximately 1871.53 Kbps. This result shows that at medium and high node densities, OLSR is capable of processing data more efficiently. Considering delay, both protocols show a notable increase in delay as the network expands. AODV maintains lower delay at low node densities but grows faster compared to OLSR with a large number of nodes. At 40 nodes, OLSR registers about 77.39 ms, while AODV reaches 171.82 ms. This demonstrates the advantage of OLSR in terms of delay in networks with many nodes. Finally, the jitter value also increases proportionally to the network size, and AODV typically has higher jitter than OLSR. The reason lies in the "reactive" nature of AODV, which must frequently search for new routes when the topology is constantly changing.

Findings: In a reconnaissance scenario with low node density, AODV proves to be more suitable. At the same time, OLSR works more efficiently at medium and high node densities. Additionally, the PDR performance of Autonomous Aerial Vehicle network protocols does not increase continuously with the growth in the number of nodes but begins to decline after a certain threshold due to increased costs for exchanging routing information.

3. Performance Analysis Based on Autonomous Aerial Vehicle Velocity

In this section, we evaluate the impact of node movement velocity on the performance of AODV and OLSR routing protocols. In Autonomous Aerial Vehicle networks, nodes move at medium to high velocities, leading to rapid and frequent changes in network structure. Therefore, we conduct simulations varying node velocities from 5 m/s to 60 m/s to assess the protocols' ability to adapt to changes in network structure.

Table 3. Simulation Parameters Based on Node Velocity

Parameter	**Value**
Number of Nodes	20
Velocity	5–60 m/s
Mobility model	GaussMarkov
Flight Area	800 m × 800 m × 100 m

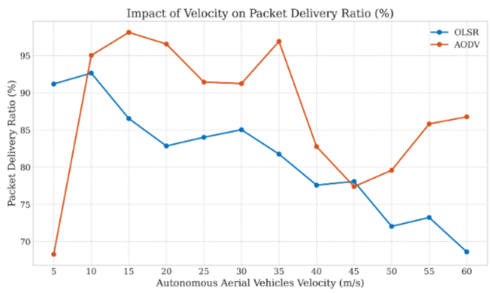

Fig. 6. Impact of Velocity on Packet Delivery

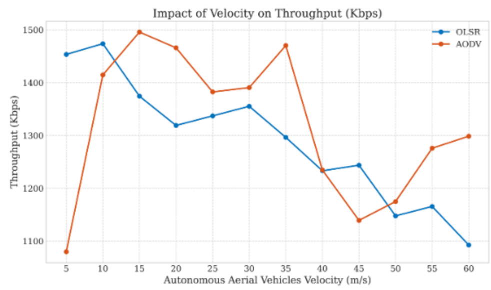

Fig. 7. Impact of Velocity on Throughput

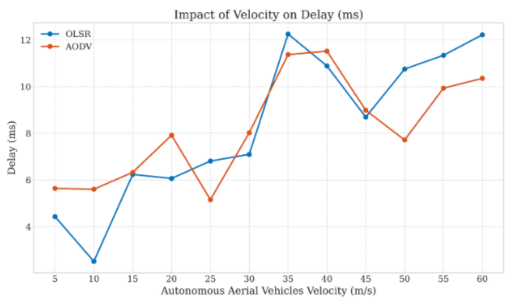

Fig. 8. Impact of Velocity on Delay

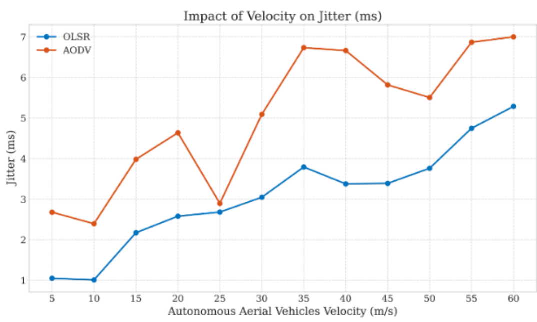

Fig. 9. Impact of Velocity on Jitter

Fig. 6 shows the Packet Delivery Ratio (PDR) as node velocity changes. In the figure, the x-axis represents node velocity (m/s), and the y-axis represents the PDR. From Fig. 6, we observe that the PDR performance of OLSR gradually decreases with increasing node velocity. Specifically, the PDR of the OLSR protocol decreases from 91.18% at a velocity of 5 m/s to 68.63% at a velocity of 60 m/s. This shows that OLSR, a proactive routing protocol, experiences difficulties maintaining an up-to-date routing table at high node velocities. In contrast, AODV demonstrates better adaptability to high node velocities. The PDR of the AODV protocol remains above 95% at velocities of 15 m/s and 20 m/s, and decreases only to approximately 86.77% at a velocity of 60 m/s. This proves that AODV, a reactive routing protocol, can effectively establish routes on demand, even when the network topology changes rapidly.

Regarding throughput, AODV maintains higher throughput than OLSR at most node velocities. At a velocity of 20 m/s, AODV achieves a throughput of about 1465.91 Kbps, while OLSR reaches 1318.86 Kbps. When the velocity increases to 60 m/s, AODV's throughput decreases to 1298.48 Kbps, while OLSR significantly drops to 1092.45 Kbps. In terms of delay, we found that AODV has higher delay than OLSR at most velocities. At a velocity of 20 m/s, AODV has a delay of about 7.91 ms, while OLSR has 6.06 ms. When the velocity increases to 60 m/s, AODV's delay increases to 10.35 ms, while OLSR increases to 12.21 ms. This shows that at high velocities, the cost of maintaining OLSR's routing table increases significantly, leading to higher delay. The jitter of both protocols increases with node velocity, but AODV demonstrates higher jitter than OLSR in most cases. At a velocity of 60 m/s, AODV's jitter is about 7.00 ms, while OLSR's is 5.28 ms. This is due to the reactive nature of AODV, which requires more frequent establishment of new routes in an environment with constantly changing topology.

Findings: The AODV routing protocol demonstrates better adaptability to high node velocities in Autonomous Aerial Vehicle networks. AODV's PDR performance remains at a higher level than OLSR's as node velocity increases, showing that AODV is more suitable for high-mobility reconnaissance scenarios. However, AODV has higher delay and jitter, which may affect delay-sensitive real-time applications.

4. Performance Analysis Based on Mobility Model

In this simulation, we analyze the performance of OLSR and AODV protocols with four different mobility models: GaussMarkov, Random Waypoint, Random Direction, and RandomWalk3d. The number of nodes is fixed at 20, and the velocity is 25 m/s.

Table 4. Simulation Parameters Based on Mobility Model

Parameter	Value
Number of Nodes	20
Velocity	25 m/s
Mobility Model	GaussMarkov, Random Waypoint, Random Direction, RandomWalk3d
Flight Area	800 m × 800 m × 100 m

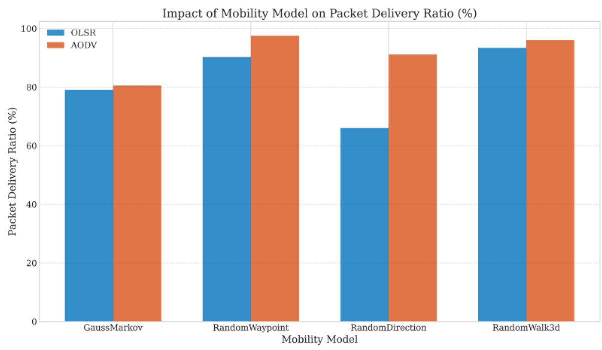

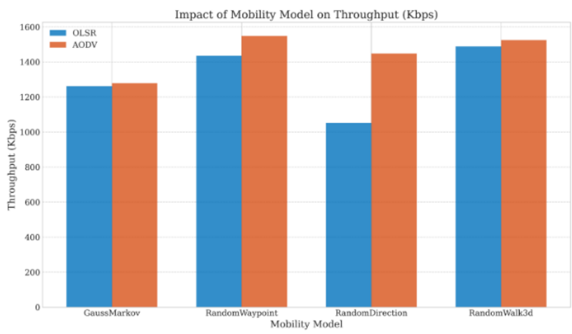

Fig. 10. Impact of Mobility Model on Packet Delivery Ratio

Fig. 11. Impact of Mobility Model on Throughput

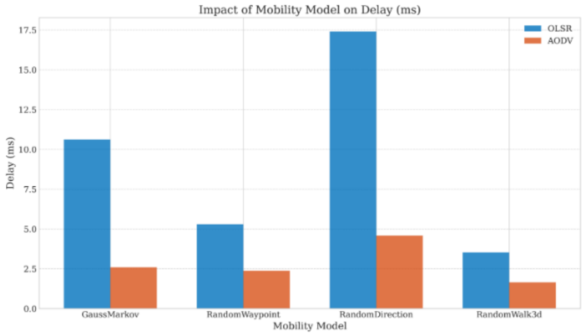

Fig. 12. Impact of Mobility Model on Delay

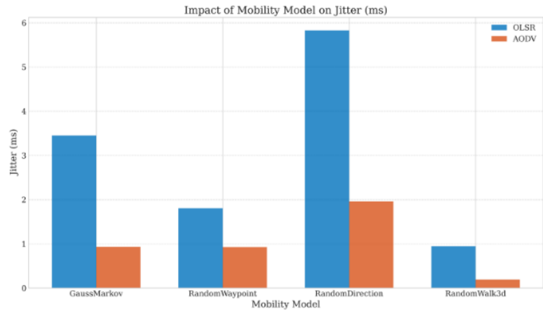

Fig. 13. Impact of Mobility Model on Jitter

From the simulation data, it is evident that the PDR of the OLSR protocol ranges from 66.05% to 93.39% depending on the mobility model. The RandomWalk3d model provides the highest PDR for OLSR (93.39%), followed by Random Waypoint (90.26%), GaussMarkov (79.12%), and the lowest performance with Random Direction (66.05%).

For AODV, PDR values vary from 91.21% to 97.52%, with Random Waypoint providing the highest performance (97.52%), followed by RandomWalk3d (96.00%), Random Direction (91.21%), and GaussMarkov (80.50%). Regarding throughput, both OLSR and AODV achieve their highest values with the Random Waypoint model, 1435.17 Kbps and 1548.92 Kbps respectively. The Random Direction model gives the lowest throughput for OLSR (1052.12 Kbps), while GaussMarkov gives the lowest throughput for AODV (1278.63 Kbps). Delay also varies significantly depending on the mobility model. AODV has the lowest delay with RandomWalk3d (1.65 ms) and the highest with Random Direction (4.59 ms). OLSR has the lowest delay with RandomWalk3d (3.53 ms) and the highest with Random Direction (17.40 ms).

Findings: These results show that the mobility model has a strong influence on the performance of routing protocols in Autonomous Aerial Vehicle networks. Random Waypoint and RandomWalk3d models generally provide better performance for both OLSR and AODV, while Random Direction creates more serious challenges due to frequent and unpredictable changes in network topology.

5. Performance Analysis Based on Coverage Area

In this simulation, we analyze the performance of OLSR and AODV protocols when changing network density, maintaining a constant number of nodes (25), but varying the simulation area size from 500 m × 500 m to 2000 m × 2000 m. This is equivalent to changing node density from 100 nodes/km² to 6.25 nodes/km². The purpose of this simulation is to investigate the effect of node density on routing protocol performance. By varying the flight area size from 500×500 m² to 2000×2000 m² with a fixed number of nodes, we create environments with different node densities, from dense (100 nodes/km²) to sparse (6.25 nodes/km²).

Table 5. Simulation Parameters Based on Area Dimensions

Parameter	Value
Number of Nodes	25
Velocity	10 m/s
Mobility Model	GaussMarkov
Flight Area	500×500, 800×800, 1200×1200, 1600×1600, 2000×2000 m²

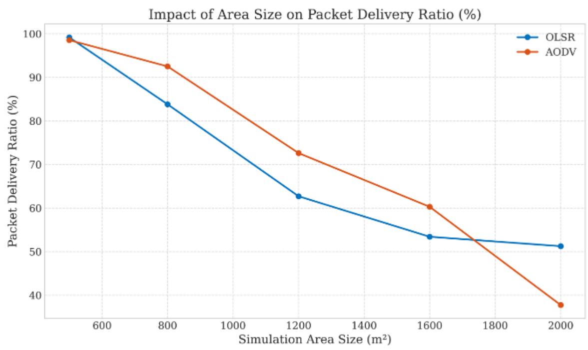

Fig. 14. Impact of Simulation Area Size on Packet Delivery Ratio

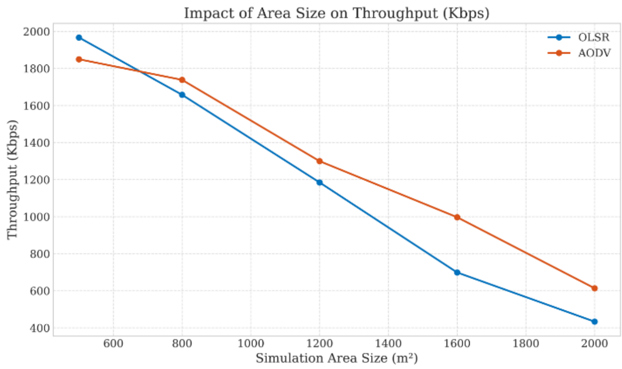

Fig. 15. Impact of Simulation Area Size on Throughput

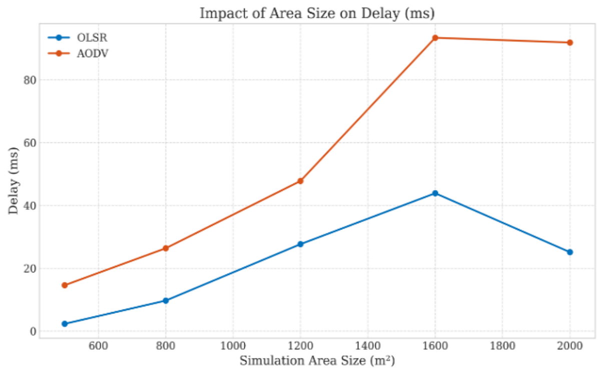

Fig. 16. Impact of Simulation Area Size on Delay

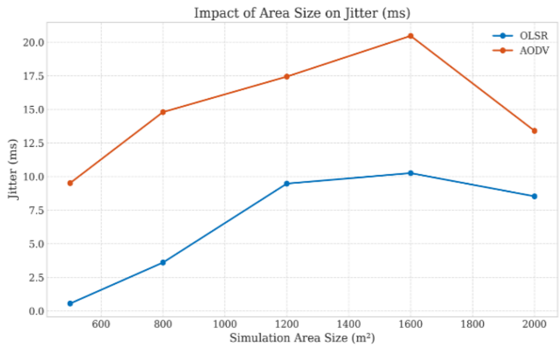

Fig. 17. Impact of Simulation Area Size on Jitter

The purpose of this simulation is to study the effect of node density on routing protocol efficiency. By varying the flight area size from 500×500 m² to 2000×2000 m² with a fixed number of nodes, we create different conditions with varying node densities - from high (100 nodes/km²) to extremely low (6.25 nodes/km²). The results show that the Packet Delivery Ratio (PDR) in both OLSR and AODV protocols decreases as node density decreases. At the highest density (100 nodes/km²), PDR in OLSR reaches 99.18%, and in AODV - 98.55%. However, at the lowest density level (6.25 nodes/km²), PDR in OLSR decreases to 51.24%, and in AODV - to 37.73%. Throughput also significantly drops as node density decreases. In OLSR, the maximum value is 1967.18 Kbps at 100 nodes/km² and decreases to 433.18 Kbps at 6.25 nodes/km². Similarly, in AODV, throughput reaches 1849.75 Kbps at maximum density and decreases to 613.46 Kbps at low density.

Regarding delay, an interesting trend is observed: as node density decreases from high to medium, delay increases, but then decreases at extremely low density. In OLSR, delay increases from 2.30 ms (at 100 nodes/km²) to 43.88 ms (at 9.77 nodes/km²) and then decreases to 25.12 ms (at 6.25 nodes/km²). A similar trend is found in AODV: from 14.59 ms (maximum density) to 93.38 ms (9.77 nodes/km²) and a further decrease to 91.87 ms (6.25 nodes/km²). This phenomenon can be explained by the specifics of routing protocols. At high density, nodes have multiple alternative routes, ensuring low delay. However, as density decreases, the number of available paths decreases, and routes need to be rebuilt more frequently, increasing delay. At extremely low density, many packets do not reach their destination at all due to lack of connectivity, and the average delay only considers successfully delivered packets, usually with a short transmission path. Comparing OLSR and AODV shows that OLSR generally demonstrates better results at most density levels, especially in terms of PDR and delay at low density. This may be related to the proactive nature of OLSR, allowing it to maintain more stable routing information even in conditions of weak connectivity.

Findings: Node density significantly affects the efficiency of routing protocols in Autonomous Aerial Vehicle networks. As node density decreases, PDR and throughput significantly decrease. OLSR proves to be more adaptive to low node density compared to AODV. In reconnaissance scenarios over a large area with a limited number of Autonomous Aerial Vehicles, optimization of node placement or implementation of intermediate relays may be required to maintain the required level of network performance.

IV. **Practical Applications**

Based on comprehensive analysis, we found that neither protocol completely outperforms the other in all situations. AODV and OLSR each have their advantages depending on the deployment scenario. The choice of an appropriate protocol should be based on the specifics of the application, the expected number of deployed Autonomous Aerial Vehicles, mobility velocity, and QoS requirements. Based on simulation results, we propose the following suitable applications for OLSR and AODV in real-world Autonomous Aerial Vehicle scenarios:
Applications Suitable for OLSR:

1. Large-scale Infrastructure Monitoring: In tasks requiring the deployment of multiple Autonomous Aerial Vehicles for monitoring power lines, pipelines, or transportation systems, OLSR demonstrates an advantage in handling a large number of nodes with high performance. The ability to maintain stable throughput above 1500 Kbps at densities of 25-40 nodes makes OLSR suitable for transmitting high-quality images and real-time video.
2. Autonomous Aerial Vehicle Networks with Static or Slow Movement: For long-term monitoring scenarios such as environmental monitoring, precision agriculture, or wildlife research, where Autonomous Aerial Vehicles move at low velocities (5-15 m/s) or fly along fixed trajectories, OLSR provides low delay and reasonable routing information forwarding costs.
3. Deployment in Concentrated Coverage Areas: OLSR is most effective when Autonomous Aerial Vehicles operate in high-density areas such as urban areas, large events, or concentrated combat zones. With PDR above 99% at a density of 100 nodes/km^2, OLSR ensures reliable data exchange between Autonomous Aerial Vehicles and ground stations.
4. Applications for 3D Mapping and Spatial Modeling: When deploying Autonomous Aerial Vehicles to create 3D models of structures or complex terrain, OLSR with the RandomWalk3d mobility model provides high PDR (93.39%) and low delay (3.53 ms), suitable for continuous transmission of sensor data.

Applications Suitable for AODV:

1. Reconnaissance Missions and Moving Target Tracking: With the ability to maintain high PDR (above 95%) at velocities up to 35 m/s, AODV is suitable for rapid reconnaissance missions, tracking moving targets, or search and rescue operations where Autonomous Aerial Vehicles need to move quickly and flexibly.
2. Deployment in Vast Areas with Low Density: AODV shows greater flexibility when Autonomous Aerial Vehicles operate dispersed in vast areas, especially with the Random Waypoint model (PDR 97.52%). This is an appropriate choice for missions exploring border territories, forested mountains, or islands.

V. **Conclusion and Directions for Future Research**

In this study, we conducted a comprehensive performance evaluation of two representative routing protocols (OLSR and AODV) in Autonomous Aerial Vehicle network environments through four highly practical simulation scenarios. The results show that no protocol has absolute superiority, but each protocol has its advantages depending on deployment conditions. OLSR demonstrates high performance in high-density and low-velocity environments, while AODV is more suitable for scenarios with high velocity and rapidly changing topology.

Based on the analysis, we proposed several potential improvements for both protocols, as well as a hybrid protocol to overcome existing limitations. In particular, the integration of parameters such as velocity, energy, and link quality into the routing process, as well as the application of reinforcement learning, promise to significantly enhance the performance of Autonomous Aerial Vehicle networks in practical applications.

Directions for future research will focus on implementing and evaluating the proposed improvements through more detailed simulations and practical tests. We plan to:

1. Develop and implement improved versions of OLSR and AODV on the NS-3 platform, evaluating their performance compared to the original protocols.
2. Expand simulations to include more realistic factors such as energy disruptions, environmental interference, and visibility limitations.
3. Study the impact of encryption and security protocols on routing performance in Autonomous Aerial Vehicle networks.
4. Develop analytical models based on machine learning to predict network performance in complex scenarios.
5. Test hybrid routing architecture in real deployment scenarios such as disaster monitoring and support for rescue operations.

Through these efforts, we aim to create optimal routing solutions for Autonomous Aerial Vehicle networks, contributing to the application of Autonomous Aerial Vehicles in many important areas of modern society.

4 REFERENCES

[1] A. Rovira-Sugranes, A. Razi, F. Afghah, and J. Chakareski, “A Review of AI-enabled Routing Protocols for UAV Networks: Trends, Challenges, and Future Outlook,” Nov. 08, 2021, arXiv: arXiv:2104.01283. doi: 10.48550/arXiv.2104.01283.

[2] Y. Yamazaki, M. Tamaki, C. Premachandra, C. J. Perera, S. Sumathipala, and B. H. Sudantha, “Victim Detection Using UAV with On-board Voice Recognition System,” in 2019 Third IEEE International Conference on Robotic Computing (IRC), Feb. 2019, pp. 555–559. doi: 10.1109/IRC.2019.00114.

[3] N. Ya’acob, M. Zolkapli, J. Johari, A. L. Yusof, S. S. Sarnin, and A. Z. Asmadinar, “UAV environment monitoring system,” in 2017 International Conference on Electrical, Electronics and System Engineering (ICEESE), Nov. 2017, pp. 105–109. doi: 10.1109/ICEESE.2017.8298395.

[4] M. A. Khan et al., “Swarm of UAVs for Network Management in 6G: A Technical Review,” IEEE Trans. Netw. Serv. Manag., vol. 20, no. 1, pp. 741–761, Mar. 2023, doi: 10.1109/TNSM.2022.3213370.

[5] T. H. Clausen and P. Jacquet, “Optimized Link State Routing Protocol (OLSR),” Internet Engineering Task Force, Request for Comments RFC 3626, Oct. 2003. doi: 10.17487/RFC3626.

[6] I. D. Chakeres and E. M. Belding-Royer, “AODV routing protocol implementation design,” in 24th International Conference on Distributed Computing Systems Workshops, 2004. Proceedings., Hachioji, Tokyo, Japan: IEEE, 2004, pp. 698–703. doi: 10.1109/ICDCSW.2004.1284108.

[7] L. Wang and S. Olariu, “A two-zone hybrid routing protocol for mobile ad hoc networks,” IEEE Trans. Parallel Distrib. Syst., vol. 15, no. 12, pp. 1105–1116, Dec. 2004, doi: 10.1109/TPDS.2004.73.

[8] Q. Usman, O. Chughtai, N. Nawaz, Z. Kaleem, K. A. Khaliq, and L. D. Nguyen, “A Reliable Link-adaptive Position-based Routing Protocol for Flying Ad hoc Network,” Oct. 12, 2020, arXiv: arXiv:2010.06005. doi: 10.48550/arXiv.2010.06005.

[9] C. Liu, Y. Wang, and Q. Wang, “PARouting: Prediction-supported adaptive routing protocol for FANETs with deep reinforcement learning,” Int. J. Intell. Netw., vol. 4, pp. 113–121, 2023, doi: 10.1016/j.ijin.2023.05.002.

[10] C. E. Perkins and P. Bhagwat, “Highly dynamic Destination-Sequenced Distance-Vector routing (DSDV) for mobile computers,” ACM SIGCOMM Comput. Commun. Rev., vol. 24, no. 4, pp. 234–244, Oct. 1994, doi: 10.1145/190809.190336.
[11] D. B. Johnson, D. A. Maltz, and J. Broch, “DSR: The Dynamic Source Routing Protocol for Multi-Hop Wireless Ad Hoc Networks”.
[12] M. R. Pearlman and Z. J. Haas, “Determining the optimal configuration for the zone routing protocol,” IEEE J. Sel. Areas Commun., vol. 17, no. 8, pp. 1395–1414, Aug. 1999, doi: 10.1109/49.779922.
[13] B. Karp and H. T. Kung, “GPSR: greedy perimeter stateless routing for wireless networks,” in Proceedings of the 6th annual international conference on Mobile computing and networking, Boston Massachusetts USA: ACM, Aug. 2000, pp. 243–254. doi: 10.1145/345910.345953.
[14] J. Zhou, Y. Chen, B. Leong, and P. S. Sundaramoorthy, “Practical 3D geographic routing for wireless sensor networks,” in Proceedings of the 8th ACM Conference on Embedded Networked Sensor Systems, Zürich Switzerland: ACM, Nov. 2010, pp. 337–350. doi: 10.1145/1869983.1870016.

Fog computing power for telepresence suit as user terminal for Metaverse

Vladislav Mogilatov, Valeria Kaijalainen, Artem Volkov, Ammar Muthanna, Andrey Koucheryavy
The Bonch-Bruevich St Petersburg State University of Telecommunications

ABSTRACT

Fog computing represents an emerging paradigm in information and communication technologies that is becoming pivotal for meeting the growing performance requirements of modern computing systems, particularly in the context of the Internet of Things (IoT) and real-time services. One of the most promising 2030-network service classes enabled by fog is telepresence. This paper investigates both the theoretical and practical aspects of deploying fog-computing solutions in telepresence networks to minimize latency and enhance overall system performance. The study combines analytical modelling with discrete-event simulations carried out in Any Logic.

1 INTRODUCTION

The accelerating pace with which new technologies are conceived and deployed in the telecommunications domain has created an imperative for continuous adaptation. While fifth-generation (5G) networks are still maturing—and many layers, from standardisation through production, remain in flux—the rapid advancement of enabling technologies has already brought the notion of 2030 communication networks, commonly referred to as 6G, to the research forefront [1], [2], [3], [4]. This transition is not merely an incremental upgrade; it calls for the creation of genuinely new service categories that will define the coming decade of connectivity.

A. Envisioned Capabilities of 6G Networks

Although detailed specifications and standards for 6G are yet to be ratified, the community broadly converges on several key development vectors:

- Ultra-high data rates: 100 Gbit/s – 1 Tbit/s
- Extreme low latency: ≈ 0.1 ms
- Massive device density: ≈ 100 devices per m^3
- Extended spectrum utilization: 1 – 10 THz
- Native integration of artificial intelligence for traffic prediction, resource allocation, and network self-optimization
- Support for novel service verticals such as holographic telepresence, tactile Internet, and immersive extended reality

One paradigm that can satisfy these unprecedented requirements is fog computing. Conceptually a further evolution of cloud computing, fog shifts processing and storage resources closer to the network edge, thereby curbing the latency incurred when data must traverse to centralized clouds and back.

B. Fog Computing for IoT and Real-Time Services

Fog computing enables data processing on edge devices—computers, mobile handsets, sensors, or smart nodes—rather than exclusively in distant data centers. By handling computations at or near the "last mile," fog mitigates cloud-roundtrip delays and supports instantaneous interactions. It also allows a substantial share of operations to be executed locally, reducing backhaul congestion. Adoption is expected to accelerate owing to three converging factors:

1. Rising computational power of terminal equipment
2. Mature cloud-storage and processing ecosystems that complement, rather than replace, edge resources

Practical solutions to the scalability and latency bottlenecks inherent in largescale IoT deployments

C. Reference Architecture Considerations

In 2015, the Open Fog Consortium introduced a reference architecture specification that crystallizes the foundational traits of fog computing. While comprehensive, the Open Fog framework does not explicitly target data-storage locality; it is primarily designed to execute computations near clients to minimize latency, transport costs, and other network-bound constraints while meeting bandwidth requirements. Control elements—including configuration, access management, and network monitoring—are likewise deployed near the edge rather than orchestrated from a central gateway. The architecture further supports local analytics, with results securely synchronized to the cloud for deeper processing or long-term use [5], [6].

Open Fog's architecture emphasizes horizontal scalability and system interoperability, while maintaining high standards of security, elasticity, and flexibility (see Fig. 1.1).

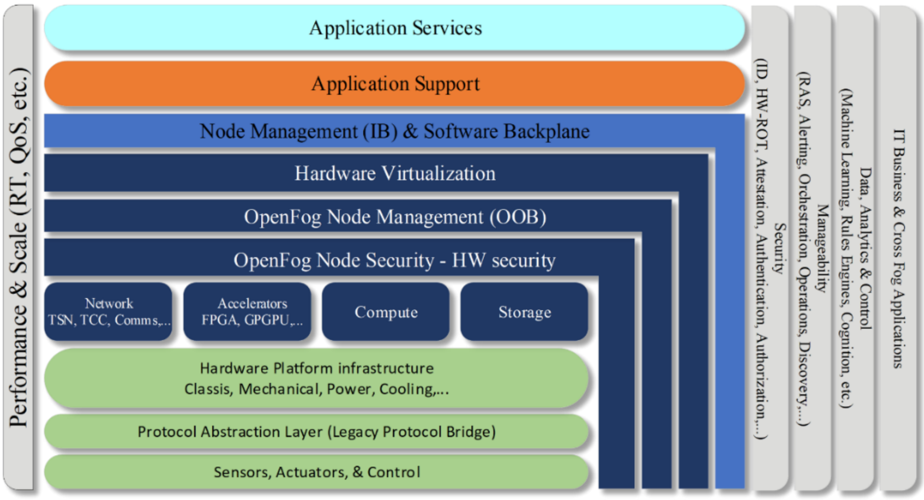

Figure 1.1 OpenFog Architecture

The reference architecture comprises the following key components [7]:

1. Physical Layer – encompasses all physical devices such as sensors, actuators, and edge-computing nodes.
2. Connectivity Layer – provides communication between physical-layer devices and the rest of the network, including access technologies, protocols, and interfaces.
3. Control Layer – manages resources, tasks, and security within the fog-computing environment; it offers mechanisms for performance monitoring, orchestration, and access control.
4. Processing Layer – dedicated to processing and analyzing data received from the physical layer, including real-time analytics, machine learning, and artificial-intelligence workloads.
5. Application Layer – hosts applications that consume data gathered and processed by the lower layers (e.g., monitoring, management, and optimization services).
6. Data-Management Layer – ensures efficient data handling across all layers, covering acquisition, storage, processing, and analysis.
7. Security Layer – a cross-cutting plane that shields data and devices at every tier from unauthorized access and cyber-attacks.

Fog computing embodies a distributed architecture that accelerates data processing, lowers latency, and locates computational resources close to end-users. By deploying compute nodes at the network edge, data can be processed nearer to its source. The Open Fog framework thus provides the foundation for scalable, flexible, and secure systems capable of real-time operation. In this sense, fog computing is not merely an alternative to cloud platforms but a necessary complement for the next wave of ultra-low-latency technologies. A broad body of literature addresses various facets of fog evolution and implementation.

2 RELATED WORKS

Table 1.1 Surveyed Contributions in Fog and Cloud Computing

Author(s)	Year	Contribution
S. Delfin; N. P. Sivasanker; Nishant Raj; Ashish Anand	2019	Fog Computing: A New Era of Cloud Computing [8] – analyses the conceptual foundations of fog computing
Asma N. Elmoghrapi; Ahmed Bleblo; Younis A. Younis	2022	Fog Computing or Cloud Computing: A Survey [9] – compares advantages and drawbacks of the two paradigms
Pooyan Habibi; Mohammad Farhoudi; Sepehr Kazemian; Siavash Khorsandi; Alberto Leon-Garcia	2020	Fog Computing: A Comprehensive Architectural Survey [10] – offers an exhaustive overview from an architectural viewpoint
Muneer Bani Yassein; Ismail Hmeidi; Farah Shatnawi; Saif Rawasheh	2020	Fog Computing: Characteristics, Challenges, and Issues [11] – focuses on fog-computing security concerns
Manoj Muniswamaiah; Tilak Agerwala; Charles C. Tappert	2021	Modern Computing and the Internet of Things (IoT): A Survey [12] – explores IoT integration with cloud and fog computing
Ahmed Salem; Marc St-Hilaire; Muhammad Sajjad Khan	2023	Mathematical Models for SLA-Aware Task Allocation in Fog Computing [13] – proposes analytical models for load balancing and energy efficiency
Mani Sharifi; Abdolreza Abhari; Sharareh Taghipour	2021	Real-Time Application-Processor Scheduling in Fog Computing [14] – presents a MILP-based scheduling model
Engr. Urooj Yousuf Khan; Tariq Rahim Soomro	2023	A Review of iFogSim: A Simulation Tool for Future Fog Networks [15]– evaluates the iFogSim simulation software

Delfin et al. [8] trace the origins of fog computing, highlight its principal advantages, catalogue representative use-case families, and discuss pathways for integrating fog with established cloud-centric solutions as the paradigm continues to mature.

Elmoghrapi et al. [9] expand the discussion by juxtaposing cloud and edge-local computing models. Their comprehensive survey assesses how each technology affects day-to-day digital interactions, clarifying that cloud and fog serve complementary—rather than interchangeable—roles in advanced network ecosystems. Habibi et al. [10] provide an exhaustive architectural panorama, comparing contemporary reference frameworks with application-specific designs. The review dissects algorithmic and technological facets, then maps the distinguishing features of cloud, edge, mobile-edge, and fog paradigms.

Security emerges as a recurrent theme. Bani Yassein et al. [11] analyze fog from a layered perspective, underscoring privacy and protection challenges that must be addressed before large-scale adoption is feasible. Because IoT workloads generate prodigious sensor data that demand near-instant analytics, Muniswamaiah et al. [12] investigate how tightly coupling fog resources with IoT platforms can unlock performance gains across heterogeneous devices.

Salem et al. [13] contribute formal task-allocation models for service-level-agreement (SLA) compliance in fog clusters. One formulation target load-balancing efficiency, whereas another emphasizes eco-sustainability by minimizing energy consumption. Sharifi et al. [14] advance this line of inquiry with a mixed-integer linear-programming (MILP) scheduler that delivers optimal dispatching decisions; they benchmark its efficacy against a FIFO baseline under two representative scenarios. Finally, Yousuf Khan and Soomro [15] evaluate iFogSim, a widely used discrete-event simulator that offers modular templates and class libraries for modelling next-generation fog topologies and application flows.

3 MODEL NETWORK

The integration of fog computing into the design of telepresence traffic-handling devices provides an effective approach to mitigating several critical challenges, including limited onboard computational capacity, rapid battery depletion, data acquisition constraints and scalability issues, as well as insufficient transmission speeds. By leveraging distributed processing at the network edge, fog-enabled telepresence systems can achieve higher efficiency, more compact form factors, and enhanced user experience due to reduced latency and optimized resource utilization.

Building on a rigorous analysis of traffic offloading mathematical models, we have developed a discrete-event simulation model that emulates data transmission from a telepresence suit to metaverse infrastructures. This simulation enables comprehensive performance evaluation, including delay metrics and load distribution across fog nodes, providing a framework for fine-tuning real-time applications.

The figures included in this study illustrate the prototype architecture and operational workflow of the proposed model, highlighting how fog-assisted offloading can effectively reduce end-to-end delays while improving throughput and energy efficiency in telepresence environments.

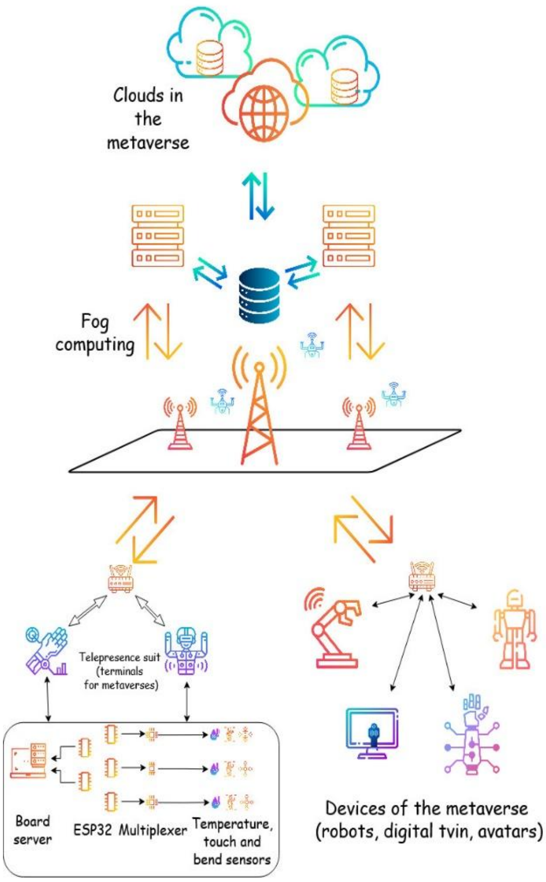

Figure 1.2 Model Architecture

Mathematical Model

We consider a mobile-computation offloading scheme that comprises a single fog-computing node and a remote cloud-computing facility. The telepresence suit equipped with M processing boards is treated as a multi-server queuing system capable of diverting traffic to both fog and cloud resources. *Figure 1.2* illustrates an exemplary network in which

- M low-power devices represent the on-board processors,
- node $M + 1$ denotes the fog-computing element, and
- node $M + 2$ corresponds to the cloud-computing element.

During operation, the suit's boards consume substantial computing cycles and electrical power. According to the proposed model, a portion of the data-processing workload is offloaded to the fog node. Should the fog segment become saturated, overflow tasks are forwarded to the remote cloud to prevent congestion. Our design goal is to reduce the number of boards, minimize energy consumption, and utilize network resources efficiently while maintaining strict end-to-end latency constraints.

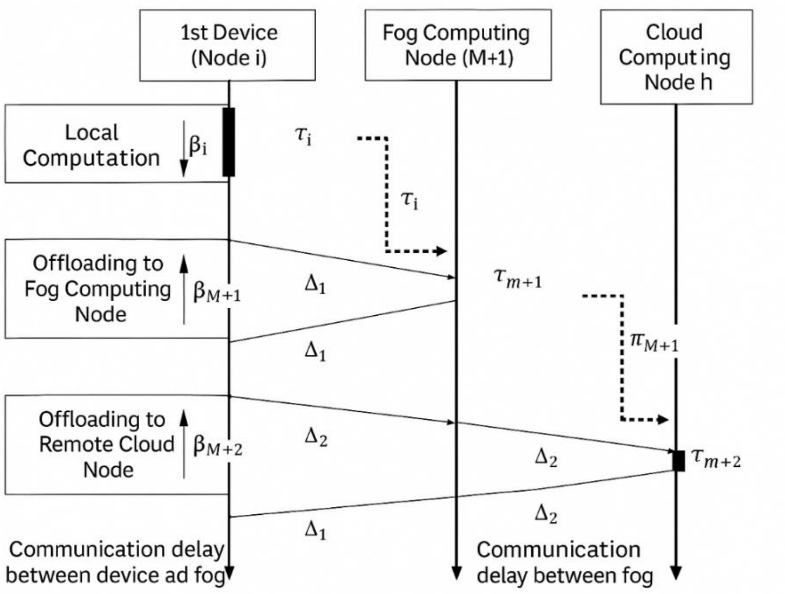

Figure 1.3 Network-Based Computation-Offloading Model

Let β_i denote the random variable representing the response time of a task originating from board i.

- Upper branch — Local execution. The task is processed entirely on board i; hence the board sustains the greatest computational load, but the response time is minimal and equals the local processing duration:

$$\beta_i = t_i.$$

- Middle branch — Fog-level execution. The task is offloaded via a wireless link to the fog node. Although transmission incurs delay, this option conserves the board's processing cycles and energy. The response time is the sum of the round-trip transmission delay $2\Delta_1$ and the fog-processing time t_{M+1}:

$$\beta_i = 2\Delta_1 + t_{M+1}.$$

- Lower branch — Cloud-level execution. When the fog node is unable to handle the task, it forwards the job to the remote cloud, thereby relieving fog congestion at the expense of additional latency. The response time now includes the round-trip delay to the cloud $2\Delta_2$:

$$\beta_i = 2\Delta_1 + 2\Delta_2 + t_{M+2}.$$

The expressions in (1) capture the latency trade-offs among local, fog, and cloud processing paths, forming the basis for the performance analysis presented in [16].

This computation-offloading scheme can be formalized in terms of queueing networks. Let M denote the number of processing boards—equivalently, the local-computation nodes—within the coverage area of the fog node. A board that acquires and forwards sensor data is indexed as node i, where $1 \le i \le M$. Each such node generates a Poisson stream of requests with rate λ_i [requests s^{-1}]. Every task requires a specific computational workload, measured in operations or floating-point operations. Let $w_i, \quad 1 \le i \le M$, be the non-negative random variable representing the workload of a task originating on board i, with cumulative distribution function $W_i(x) = \Pr\{w_i \le x\}$. Denote by μ_i the constant service rate of board i in instructions per second. A task is offloaded to the fog node whenever $w_i > w^*$, where w^* is the workload threshold; otherwise, it is executed locally on the mobile device. The offloading probability for board i is therefore $\pi_i = 1 - W_i(w^*)$. With the foregoing notation, the complete mathematical model of the system is depicted schematically in *Figure 1.3* [14].

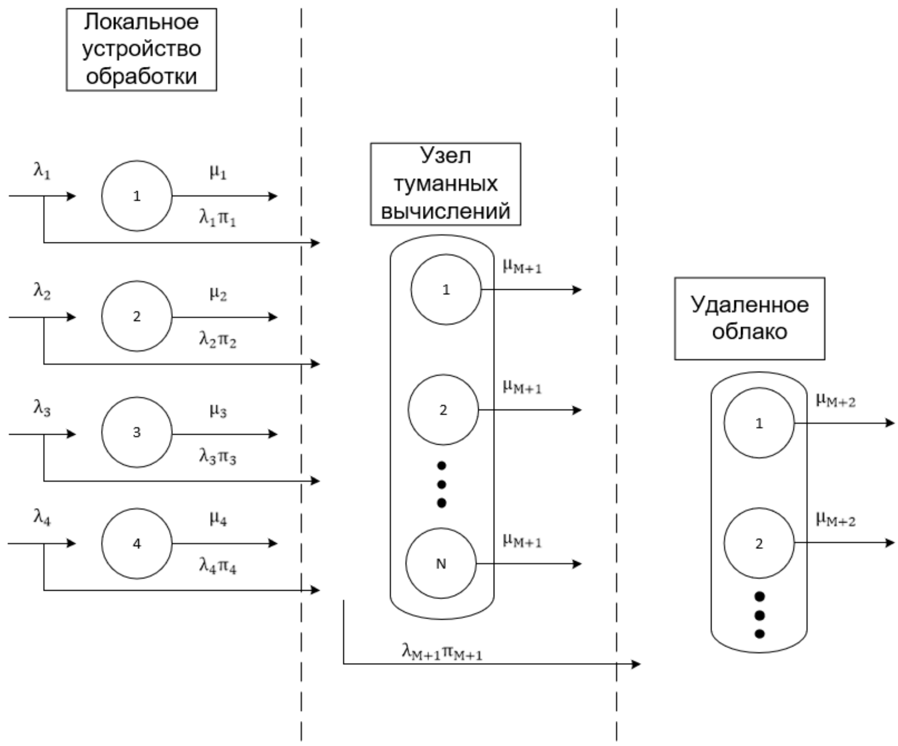

Figure 1.4 Queueing-System Model for Telepresence-Suit Traffic Offloading

Table 1.2 Probability Distribution of the Response-Time Random Variable β_i

β_i value	t_i	$2\Delta_1 + t_{M+1}$	$2\Delta_1 + 2\Delta_2 + t_{M+2}$
Probability P	$1 - \pi_i$	$\pi_i(1 - \pi_{M+1})$	$\pi_i \, \pi_{M+1}$

Simulation Model

Building on the mathematical framework outlined above, we developed a discrete-event simulation in AnyLogic and conducted a series of experiments to validate the analytical results. The simulator implements both fog-assisted and non-fog data-transmission scenarios, allowing direct comparison of end-to-end performance.

The accompanying figure depicts the experimental test-bed layout, while the corresponding table lists the parameter values used in the simulations. This model enables network planners to:

- Forecast system behavior when telepresence traffic is integrated with fog computing,
- Dimension fog clusters appropriately, and
- Estimate the user-side network resources required to sustain real-time service delivery.

These capabilities are instrumental for designing scalable, low-latency telepresence architectures in next-generation networks [17] [18].

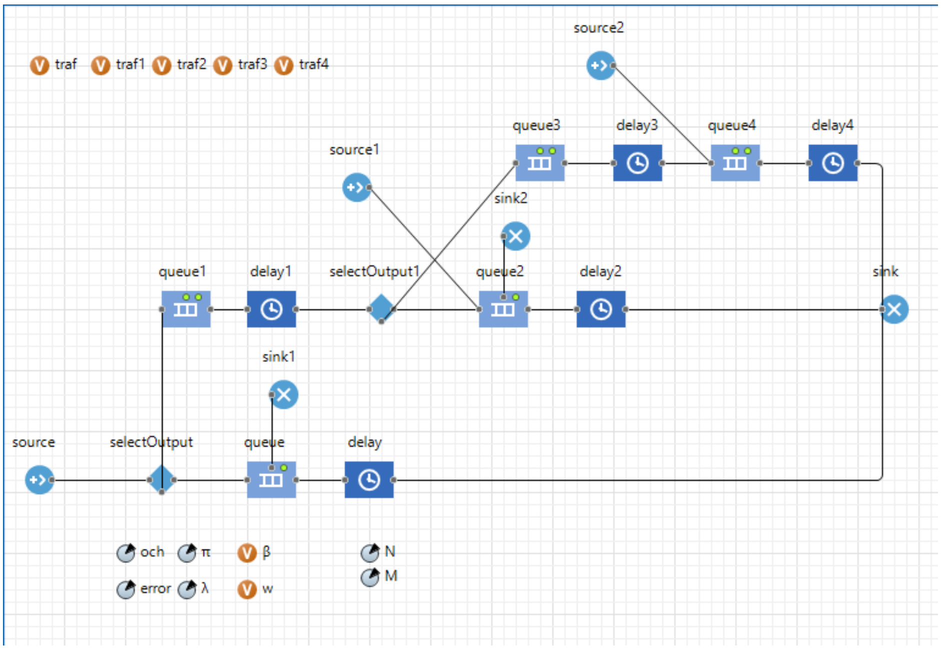

Figure 1.5 Discrete-Event Simulation Model of the Queueing System

Table 1.3 Model Parameters Used in the Experiments

Parameter (Name)	Symbol
Flow arrival rate per board	λ_i
Offloading probability	π
Offloaded-workload threshold	w^*
Local processing rate	μ_i
Fog-node processing rate	μ_{M+1}
Cloud processing rate	μ_{M+2}
One-way fog-transmission delay	Δ_1
Additional cloud-transmission delay	Δ_2
Mean response time	β_i
Overload events (error)	$error$
Queue length	och
Number of processing boards	M
Devices in the fog cluster	N

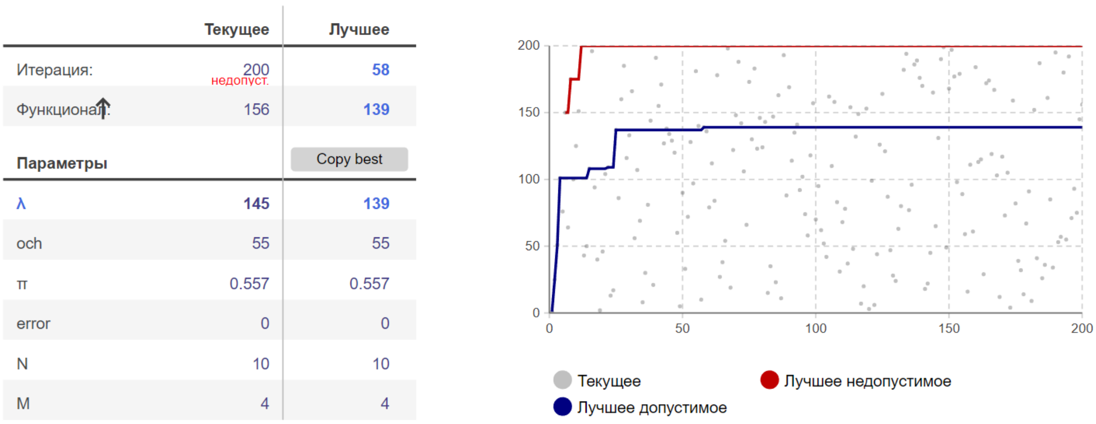

Figure 1.6 Optimisation-Model Outcome

In the first experiment, we determined the optimal values of the offloading probability and the queue length that minimize the mean system sojourn time. Because timely delivery of every packet is critical for telepresence traffic, the configuration must guarantee zero overload events.
The optimization yielded an offloading probability of $\pi = 0.557$, which is fully consistent with the analytical model, along with the corresponding minimal queue length. This configuration balances the volumes offloaded to fog, processed locally, and forwarded to the cloud, ensuring uniform workload distribution across the boards.

The second and third experiments employed parameter sets derived from the actual telepresence-suit hardware specification and refined through the simulation framework. We established,

- the maximum data volume that the boards can collect and process without fog support, and
- the performance gains—in terms of throughput and latency—achieved through fog-computing integration.

Table 1.4 Experimental Results

Metric	**Baseline**	**Prototype**	**Fog Deployment**
Number of processing boards	20	4	4
Offloading probability	$\pi = 0.559$	$\pi = 0$	$\pi = 0.557$
Mean response time β [s]	0.012	0.021	0.007
Aggregate arrival rate λ [tasks s^{-1}]	80	48	139
Normalized β	1.00	1.75	0.58
Normalized λ	1.00	0.60	1.74

The introduction of fog computing into telepresence service architecture addresses critical challenges including limited on-board computational power, rapid battery depletion, data-acquisition bottlenecks, scalability constraints, and insufficient transmission throughput. As demonstrated, the fog-enabled configuration triples the data-collection and transfer capacity without adding extra hardware to the suit. Consequently, system efficiency is markedly improved while complexity and cost remain unchanged, enabling a lean yet high-performance telepresence solution suitable for next-generation 6G networks.

4 CONCLUSION

The application of analytical modelling and discrete-event simulation in AnyLogic has produced several quantitative outcomes: (i) a pronounced reduction in system response time, significantly exceeding the data-processing rates of current solutions; (ii) lower energy consumption owing to task execution at fog nodes; and (iii) a decrease in the amount of required on-board hardware. By integrating fog computing, the traffic intensity can be maximized without a three-fold increase in the number of processing boards, thereby demonstrating substantial economic efficiency.

The simulation model has experimentally validated the theoretical insights obtained from the mathematical analysis. This validation not only confirms the accuracy of the theoretical calculations but also identifies optimal operating parameters for the system under a variety of conditions, providing a reliable basis for further research on fog-cluster sizing.

The experiments clearly indicate the significant advantages of employing fog computing in telepresence devices, including a three-fold improvement in system performance and a corresponding reduction in response time. These findings confirm that the integration of fog technologies is a promising avenue for the advancement of telepresence systems, delivering higher efficiency and greater user convenience for end users.

REFENRENCE:

[1] C.-X. Wang, J. Huang, H. Wang, X. Gao, X. You, and Y. Hao, “6G Wireless Channel Measurements and Models: Trends and Challenges,” *IEEE Veh. Technol. Mag.*, vol. 15, no. 4, pp. 22–32, Dec. 2020, doi: 10.1109/MVT.2020.3018436.

[2] H. Tataria, M. Shafi, A. F. Molisch, M. Dohler, H. Sjöland, and F. Tufvesson, "6G Wireless Systems: Vision, Requirements, Challenges, Insights, and Opportunities," *Proc. IEEE*, vol. 109, no. 7, pp. 1166–1199, July 2021, doi: 10.1109/JPROC.2021.3061701.

[3] A. Shi, F. Sun, and M. Li, "An Exploration of Holographic Scenarios in 6G Networks," in *2022 10th International Conference on Information Systems and Computing Technology (ISCTech)*, Dec. 2022, pp. 450–456. doi: 10.1109/ISCTech58360.2022.00076.

[4] A. Volkov, A. Muthanna, and A. Koucheryavy, "Fifth generation communication networks: on the way to networks 2030," *Telecom IT*, vol. 8, no. 2, June 2020, doi: 10.31854/2307-1303-2020-8-2-32-43.

[5] abid, "Introducing the Industrial Internet Consortium, Now Incorporating OpenFog!," Industry IoT Consortium. Accessed: July 21, 2025. [Online]. Available: https://www.iiconsortium.org/2019/02/introducing-the-industrial-internet-consortium-now-incorporating-openfog/

[6] "3. OpenFog Consortium Architecture Working Group, OpenFog architecture overview, OpenFog Consortium, - Google Search." Accessed: July 21, 2025. [Online]. Available: https://www.iiconsortium.org/pdf/OpenFog_Reference_Architecture_2_09_17.pdf

[7] Thang, D. V., Volkov, A., Muthanna, A., Koucheryavy, A., Ateya, A. A., & Jayakody, D. N. K. (2025). Future of Telepresence Services in the Evolving Fog Computing Environment: A Survey on Research and Use Cases. Sensors, 25(11), 3488.

[8] S. Delfin, N. P. Sivasanker., N. Raj, and A. Anand, "Fog Computing: A New Era of Cloud Computing," in *2019 3rd International Conference on Computing Methodologies and Communication (ICCMC)*, Mar. 2019, pp. 1106–1111. doi: 10.1109/ICCMC.2019.8819633.

[9] A. N. Elmoghrapi, A. Bleblo, and Y. A. Younis, "Fog Computing or Cloud Computing: a Study," in *2022 International Conference on Engineering & MIS (ICEMIS)*, July 2022, pp. 1–6. doi: 10.1109/ICEMIS56295.2022.9914131.

[10] P. Habibi, M. Farhoudi, S. Kazemian, S. Khorsandi, and A. Leon-Garcia, "Fog Computing: A Comprehensive Architectural Survey," *IEEE Access*, vol. 8, pp. 69105–69133, 2020, doi: 10.1109/ACCESS.2020.2983253.

[11] M. B. Yassein, I. Hmeidi, F. Shatnawi, and S. Rawasheh, "Fog Computing: Characteristics, Challenges and Issues," in *2020 International Conference on Mathematics and Computers in Science and Engineering (MACISE)*, Jan. 2020, pp. 240–245. doi: 10.1109/MACISE49704.2020.00051.

[12] M. Muniswamaiah, T. Agerwala, and C. C. Tappert, "Fog Computing and the Internet of Things (IoT): A Review," in *2021 8th IEEE International Conference on Cyber Security and Cloud Computing (CSCloud)/2021 7th IEEE International Conference on Edge Computing and Scalable Cloud (EdgeCom)*, June 2021, pp. 10–12. doi: 10.1109/CSCloud-EdgeCom52276.2021.00012.

[13] A. Salem, M. St-Hilaire, and M. S. Khan, "Mathematical Models for Task Assignment with Service Level Agreement in Fog Computing," in *2022 International Conference on Smart Applications, Communications and Networking (SmartNets)*, Nov. 2022, pp. 1–8. doi: 10.1109/SmartNets55823.2022.9993983.

[14] M. Sharifi, A. Abhari, and S. Taghipour, "Modeling Real-Time Application Processor Scheduling for Fog Computing," in *2021 Annual Modeling and Simulation Conference (ANNSIM)*, July 2021, pp. 1–12. doi: 10.23919/ANNSIM52504.2021.9552113.

[15] Engr. U. Yousuf Khan and T. Rahim Soomro, "Overview of iFogSim: A Tool for Simulating Fog Networks of the Future," in *2022 14th International Conference on Mathematics, Actuarial Science, Computer Science and Statistics (MACS)*, Nov. 2022, pp. 1–4. doi: 10.1109/MACS56771.2022.10023395.

[16] Zhao, L. H., Zhang, J., Bah, M. J., Li, Z., Ying, J. J. C., Muthanna, A., & Elgendy, I. A. (2025). Energy-Efficient Task Offloading in Multi-server Mobile Edge Computing Networks: A Deep Reinforcement Learning Approach. Arabian Journal for Science and Engineering, 1-22.

[17] Vorobyova D. et al. IoT network model with multimodal node distribution and data-collecting mechanism using mobile clustering nodes //Electronics. – 2023. – Т. 12. – №. 6. – С. 1410..

[18] van Thang, D., Volkov, A., Muthanna, A., Elgendy, I. A., Alkanhel, R., Jayakody, D. N. K., & Koucheryavy, A. (2025). A Framework Integrating Federated Learning and Fog Computing

Based on Client Sampling and Dynamic Thresholding Techniques. IEEE Access, 13, 95019-95033.

FACULTY OF ENGINEERING

SLIIT UNI

THE KNOWLEDGE UNIVERSITY